CHARACTERIZING *SALMONELLA* PATHOGENICITY ISLAND 2 EFFECTOR INTERACTIONS IMPLICATED IN HOST ENDOMEMBRANE REORGANIZATION

by

Katelyn Janzen

B.Sc. Honours, The University of the Fraser Valley, 2013

A THESIS SUBMITTED IN PARTIAL FULFILLMENT OF

THE REQUIREMENTS FOR THE DEGREE OF

DOCTOR OF PHILOSOPHY

in

THE FACULTY OF GRADUATE AND POSTDOCTORAL STUDIES

(Microbiology and Immunology)

THE UNIVERSITY OF BRITISH COLUMBIA

(Vancouver)

April 2021

The following individuals certify that they have read, and recommend to the Faculty of Graduate and Postdoctoral Studies for acceptance, the dissertation entitled:

Characterizing *Salmonella* pathogenicity island 2 effector interactions implicated in host endomembrane reorganization

submitted by Katelyn Dawn Janzen in partial fulfillment of the requirements for

the degree of Doctor of Philosophy

in Microbiology and Immunology

Examining Committee:

B. Brett Finlay, Professor, Microbiology and Immunology, UBC
Supervisor

Michael Murphy, Professor, Microbiology and Immunology, UBC
Supervisory Committee Member

James Kronstad, Professor, Microbiology and Immunology, UBC
University Examiner

Deanna Gibson, Associate Professor, Biology, UBCO
University Examiner

Additional Supervisory Committee Members:

Wayne Vogl, Professor, Cellular and Physiological Sciences, UBC
Supervisory Committee Member

Julian Guttman, Professor, Biological Sciences, SFU
Supervisory Committee Member

Abstract

The success of *Salmonella* Typhimurium as a pathogen relies on its ability to invade and survive within intestinal epithelial cells. *S.* Typhimurium thrives as an intracellular pathogen through the activity of a type III secretion system (T3SS2) whose secreted effectors create a unique intracellular replicative niche for *S.* Typhimurium through regulation of host immune pathways, host cell cytoskeleton rearrangement, regulating host cell ubiquitination events, and hijacking the host endosomal system. Significant efforts to elucidate T3SS2 effector molecular mechanisms through single effector studies have thus far been unable to fully explain the events leading to establishment of the *S.* Typhimurium intracellular niche.

We undertook a systematic study to delineate the contribution of each effector associated with manipulation of the host endosomal system—namely SifA, SopD2, PipB2, SteA, SseJ, and SseFG by creating a deletion mutant library containing single-effector and multiple effector deletion mutants. It was shown that each of *Salmonella*-induced filament biogenesis, intracellular localization of the *Salmonella*-containing vacuole, intramacrophage replication, colonization, and virulence depends on the activities of multiple effectors. We demonstrate the complex interplay between effectors and highlight the necessity to study T3SS2-secreted effectors as groups, rather than as individual effectors

A T3SS2 overexpression mutant ($T3SS2^{+}$) was created to increase the abundance of secreted T3SS2 proteins and tagged effectors implicated to manipulate the host endosomal system. To identify novel host targets for these effectors while maintaining natural effector delivery throughout infection, a global mass spectrometry screen was performed using the SILAC (stable isotopic labelling with amino acids in cell culture)-labelling method to label host cells and infected them with $T3SS2^{+}$ mutants. Using this method, the host protein annexin A2

was identified as a target for both SopD2 and PipB2. A shared host target for two effectors may explain the complex and nuanced phenotypes observed during *S.* Typhimurium infection. Together, the work presented here demonstrates that T3SS2-secreted effectors are dependant on each other's activities during infection and shows binding of two effectors to a single host protein. This work contributes to our understanding of the intracellular lifestyle of *S.* Typhimurium and sets a new paradigm for future research.

Lay Summary

Salmonella Typhimurium is a common foodborne pathogen, yet we do not fully understand how it causes disease. *S.* Typhimurium invades intestinal epithelial cells where it creates a unique niche for itself and secretes a multitude of its own proteins (effectors) into the host cell. To better understand how *S.* Typhimurium creates its intracellular niche, we studied the contribution of each effector to certain phenotypes and found that multiple effectors were required for any given phenotype. To unravel the complex effector interactions during infection we created a strain of *Salmonella* that specifically secretes an increased abundance of all effectors of interest. Using this *Salmonella* strain, and a method to profile all host and bacterial proteins within a cell, we identified a common host target for two effectors. Together, the work presented here contributes to our understanding of the intracellular lifestyle of *S.* Typhimurium and sets a new paradigm for future research.

Preface

Chapter 1: A version of Chapter 1 has been published. **Knuff K**, Finlay BB. What the SIF is happening—the role of intracellular *Salmonella*-induced filaments. Frontiers in cellular and infection microbiology. 2017 Jul 25;7:335. I wrote this review with important input and editing from B.B. Finlay.

Chapter 2: A version of Chapter 2 has been published. **Knuff-Janzen K**, Tupin A, Yurist-Doutsch S, Rowland JL, Finlay BB. Multiple *Salmonella*-pathogenicity island 2 effectors are required to facilitate bacterial establishment of its intracellular niche and virulence. PLOS One. 2020 Jun 25;15(6):e0235020. A. Tupin and I collected all data and analyzed all the experiments. S. Yurist-Doutsch performed the mouse experiments and collected data. JL Rowland developed methodology and provided valuable input to the editing of this manuscript. I was responsible for writing the manuscript. B.B. Finlay provided important input and contributed to the editing of the manuscript.

Chapter 3: A version of Chapter 3 (along with Chapter 4) is currently being prepared for submission. I was responsible for experimental design, performing experiments, collecting data, analyzing data, figure preparation, and writing of the manuscript with intellectual input from B.B. Finlay.

Chapter 4: A version of Chapter 4 (along with Chapter 3) is currently being prepared for submission. **Knuff-Janzen, K**, McCoy, J. Moon, K, Foster, L.J. Finlay, B.B. Quantitative proteomic screen identifies Annexin A2 as a target for the effectors SopD2 and PipB2. *In*

preparation. Co-authors for this manuscript contributed as follows: Dr. J. McCoy assisted in experimental design, performing experiments, and data analysis. KM Moon performed in-gel digests and mass spectrometry analysis under the supervision of L.J. Foster.

Chapter 5: Chapter 5 is original and unpublished.

The mouse work presented in this dissertation were performed according to protocol number A13-0265 approved by the University of British Columbia's Animal Care Committee and in direct accordance with the Canadian Council of Animal Care (CACC) guidelines.

Table of Contents

List of Tables

List of Figures

List of Abbreviations

A/T	Adenine/Thymine
ACBD3	Acyl-CoA binding domain containing 3
ADP	Adenosine diphosphate
AHNAK	AHNAK nucleoprotein; Desmoyokin
AnxA2	Annexin A2
Arl8b	ADP-ribosylation factor-like protein 8B
ATPase	Adenosine triphosphate hydrolase
BCA	Bicinchoninic acid
BCV	Bacteria-containing vacuole
BSA	Bovine serum albumin
C57BL/6	C57 black 6
CDC42	Cell division cycle 42
CFU	Colony forming units
DAP	DL-2,6-Diaminopimelic acid
DAPI	4′,6-diamidino-2-phenylindole
DMEM	Dulbecco's modified essential medium
DNA	Deoxyribonucleic acid
DPBS	Dulbecco's phosphate-buffered saline
ECL	Enhanced chemiluminescence
EEA1	Early endosome antigen 1
ELISA	Enzyme-linked immunosorbent assay

EM	Electron microscope
F-actin	Filamentous actin
FBS	Fetal bovine serum
FYCO1	FYVE and coiled-coil domain containing protein 1
G-actin	Globular actin
GEFs	Guanine nucleotide exchange factors
GTP	Guanosine triphosphate
GTPase	Guanosine triphosphate hydrolase
h.p.i.	Hours post-infection
HA	Hemagglutinin
HeLa	Immortalized cervical epithelial cell line isolated from Henrietta Lacks
His	Histidine
H-NS	Histone-like nucleoid-structuring
HRP	Horseradish peroxidase
IB	Immunoblot
IFNγ	Interferon gamma
IFs	Intermediate filaments
IHF	Integration host factor
IP	Immunoprecipitation
IP-MS	Immunoprecipitation coupled with mass spectrometry
kDa	Kilodalton
LAMP1	Lysosomal associated membrane protein 1

$LAMP1^+$	LAMP1-positive
LB	Luria-Bertani
LBPA	Lysobisphosphatidic acid
LC-MS/MS	Liquid chromatography-tandem mass spectrometry
LNTs	LAMP1-negative tubules
LPM	Low phosphate and magnesium
M Cells	Microfold cells
m/z	Mass to charge ratio
M6PR	Mannose-6-phosphate receptor
MOI	Multiplicity of infection
mRNA	Messenger ribonucleic acid
MTOC	Microtubule organizing center
NADPH	Dihydronicotinamide-adenine dinucleotide phosphate
NGS	Normal goat serum
Ni	Nickel
NTS	Non-typhoidal salmonellosis
OD	Optical density
P	Pellet
p.i.	Post invasion
PCR	Polymerase chain reaction
PH	Pleckstrin homolog
PI(3)P	Phosphatidylinositol-3-phosphate

PI3-kinase	Phosphoinositide 3-kinase
PLEKHM1	Pleckstrin homology and RUN containing member 1
PLEKHM2	Pleckstrin homology and RUN containing member 2
RAW 264.7	Immortalized mouse macrophages originating from Abelson leukemia virus transformed cells derived from BALB/c mice
RhoA	Ras homolog family member A
RILP	Rab-interacting lysosomal protein
RIPA	Radioimmunoprecipitation assay
RPMI	Roswell Park Memorial Institute
S	Secreted
SCAMP3	Secretory carrier membrane protein 3
SCV	*Salmonella*-containing vacuole
SDS	Sodium dodecyl sulphate
SDS-PAGE	Sodium dodecyl sulphate-polyacrylamide gel electrophoresis
SH3	SRC homology 3
SIF	*Salmonella*-induced filaments
SILAC	Stable isotope labelling of amino acids in cell culture
SISTs	*Salmonella*-induced SCAMP3 tubules
SITs	*Salmonella*-induced tubules
SKIP	SifA-and-kinesin interacting protein
SNARE	SNAP receptor
SNX1	Sorting nexin-1
SNX3	Sorting nexin-3

SPI-1	*Salmonella* pathogenicity island-1
SPI-2	*Salmonella* pathogenicity island-2
SVATs	Spacious vacuole-associated tubules
T3SS	Type III secretion system
T3SS1	Type III secretion system encoded on *Salmonella* pathogenicity island-1
T3SS2	Type III secretion system encoded on *Salmonella* pathogenicity island-2
$T3SS2^{+}$	Hyper-secreting SPI-2 encoded type III secretion system mutant
TBS-T	Tris-buffered saline containing Tween-20
TCA	Trichloroacetic acid
TfnR	Transferrin receptor
THP-1	Human-leukemic cell line; immortalized monocyte-like cells
VAMP8	Vesicle-associated membrane protein 8
VAP	Vacuole-associated actin polymerization
vATPase	Vacuolar-type ATPase
Vps34	Vacuolar protein sorting 34
v-SNARE	Vesicle-associated SNARE
WT	Wild type

Acknowledgements

A PhD can often feel like a long and lonely experience, but reflection quickly reveals an army of people supporting me the entire time. First, I would like to thank my supervisor Brett for his unwavering support and guidance throughout the entire process. Thank you for allowing me to choose my own research project and letting me take it wherever I wanted to. I cannot thank you enough for letting me do my PhD in your lab and supporting my passion for teaching.

I would like to express my gratitude to the members of my supervisory committee, Drs Michael Murphy, Wayne Vogl, and Julian Guttman, for generously offering their time, support, and guidance throughout my PhD.

I would like to thank the large and diverse group of graduate students, postdoctoral fellows, and research associates in the Michael Smith Laboratories who have provided support, guidance, and mentorship during my time in the Finlay Lab. First, I want to thank Deng who has always been there to answer any and all questions, who celebrated my successes and commiserated my failures alongside me and provided invaluable support. I would not have been able to do this without you. Second, I want to thank Jennifer Rowland who taught me to do better science and to be a better writer. Third, I want to thank James McCoy who not only made the lab environment fun, but also helped me reach the finish line. Special thanks also go to Audrey Tupin who was my partner in crime and helped to get my project going. And of course, many others along the way: Lisa, Andrew, Nina, Mihai, Kylynda, Kelsey, Charisse, Sarah, Tahereh, Roz, Eric Antionio, Anna, Weronika, Stef, Jorge, Zakaher, Avril, Ray, and Linda. Your friendship and support have meant so much. I would not have made it without you.

Finally, I would like to thank my friends and family for their constant love and support throughout this process. My parents have encouraged me throughout my academic career and

their support has proven essential. And Robert: I could not have done this without you. You met and married me in the middle of all. Thank you for your love, positivity, and never-ending support.

Dedication

To Robert who always believes in me

Chapter 1: Introduction

1.1 *Salmonella* infections

Salmonellae are Gram-negative foodborne pathogens capable of causing enteric disease in all vertebrates [1]. Salmonallae belong to the family Enterobacteriacea and consists of two species, six sub species, and many serovars [2,3]. The medically important *Salmonella* strains are all classified as *Salmonella enterica,* a species with more than 2,500 serotypes [4]. *Salmonella enterica* serovars are associated with three distinct clinical syndromes in humans: typhoid fever, gastroenteritis (or "food poisoning"), and bacteremia [5]. Typhoid fever is a life-threatening illness caused by systemic infection by *Salmonella enterica* subsp. *enterica* serovars Typhi (*S.* Typhi) and Paratyphi [6]. Non-typhoidal salmonellosis (NTS) strains *S.* Typhimurium and *S.* Enteriditis are common etiological agents of gastroenteritis in immunocompetent individuals [1]. In immunocompromised individuals, NTS can cause bacteremia and is therefore a concern for young and old individuals and the immunosuppressed [5]. Gastroenteritis associated with NTS strains is estimated to afflict 93.8 million people worldwide and cause 155,000 deaths annually [7]. The emergence of a multi-drug resistant strain of *S.* Typhimurium ST313 in Africa necessitates new therapeutic strategies [8].

More than 95% of *Salmonella* infections arise from the consumption of contaminated food or water [4]. Ingested *S.* Typhimurium makes its way through the gastrointestinal tract where it typically invades microfold cells (M cells) to gain access to the underlying Peyer's patches, but it can also induce its own uptake into the epithelial cells of the gastrointestinal epithelium [9,10]. The ability to invade non-phagocytic cells and the ability to survive and replicate within host cells are fundamental aspects to *S.* Typhimurium infections.

1.2 *Salmonella*-pathogenicity islands, type III secretion systems, and effectors

S. Typhimurium pathogenesis is largely mediated by two distinct type III secretion systems (T3SSs) encoded on *Salmonella* pathogenicity islands 1 and 2 (T3SS1 and T3SS2 respectively) [11]. These type III secretion systems transport bacterial effector proteins into the cytoplasm of the host cell where they specifically target host cell processes to promote both invasion and intracellular survival of *S.* Typhimurium [12]. The coordinated action of T3SS1 effectors during infection have been extensively studied over the years and are well understood. In comparison, the coordinated activities of T3SS2 effectors have received less attention and remain largely enigmatic.

1.2.1 *Salmonella*-pathogenicity island 1

The *Salmonella* pathogenicity island-1 (SPI-1) gene cluster is comprised of 39 genes encoding the T3SS1 and its chaperones, transcriptional regulators, and effector proteins [13]. At least 13 effectors are secreted by the T3SS1 and are critical for invasion of non-phagocytic cells. In general, these effectors interact with host cell components to induce host cell responses and promote bacterial invasion [14]. *S.* Typhimurium induces wide-scale actin rearrangements at the site of bacterial-host cell contact to initiate invasion of the host cell [15]. *S.* Typhimurium both directly and indirectly induces actin cytoskeleton rearrangements: T3SS1-secreted effectors directly modulate actin dynamics or indirectly promotes actin rearrangements by stimulation of host signal transduction pathways [14].

1.2.1.1 Regulation of SPI-1

1.2.1.1.1 Regulation from within SPI-1

Regulation of SPI-1 gene expression during infection requires both environmental stimuli and genetic regulators. There have been multiple identified positive and negative regulators of

SPI-1 expression. Here we discuss a select few, see Altier 2005 [16] for a comprehensive review. The central positive regulator of SPI-1 expression is HilA which activates the *sip* operon, *inv/spa* operon, and *prg* operon. The *sip* operon encodes secreted proteins while the *inv/spa* and *prg* operons encode components of the T3SS1 secretion apparatus [17–21]. HilA also activates another transcriptional regulator, InvF, which induces the expression of the *sip* operon encoded secreted proteins [16,18]. While HilA regulates the expression of T3SS1 secretion apparatus machinery, InvF regulates the expression of T3SS1-secreted proteins encoded outside of SPI-1. The secreted proteins encoded within SPI-1 are controlled by both HilA and InvF [19].

Given the central role HilA plays during infection, *hilA* expression is tightly regulated at multiple levels. Encoded within SPI-1 are the transcriptional regulators HilC and HilD in addition to HilA and InvF [16]. HilA is repressed by the histone-like nucleoid-structuring (H-NS) DNA binding protein [22,23]. H-NS silencing of *hilA* expression is counteracted by HilC and HilD which directly bind the *hilA* promoter region, and independent of each other derepress *hilA* expression [24–26].

1.2.1.1.2 Regulation from outside SPI-1

SPI-1 gene expression is also controlled by the global transcriptional regulator SirA which is the response regulator component of the SirA/BarA two-component system [27–29]. SirA/BarA regulates the Csr post-transcriptional regulatory system which in turn regulates both SPI-1 and SPI-2 gene expression [30]. CsrA is a post-transcriptional regulatory protein that promotes mRNA degradation by binding to certain sequences overlapping with the Shine Delgarno sequence in target mRNAs, thereby preventing ribosome binding and subsequent translation [31–33]. The proteins CsrB and CsrC both sequester CsrA to impede its ability to repress translation [32–35]. CsrA has a binding site within the *hilD* mRNA transcript, thus

preventing translation of *hilD*. SirA activates expression of both *csrB* and *csrC*, enabling counteraction of CsrA-mediated post-transcriptional repression, thus permitting translation of *hilD* and other proteins. In turn, HilD activates *hilA* expression and *ssrAB* expression (discussed below) which are central regulators of SPI-1 and SPI-2, respectively [30].

Unnecessary expression of invasion-related genes is costly to pathogens. As such, the environment surrounding *S.* Typhimurium can both repress and activate invasion. Oxygen tension is one of the key environmental regulators of SPI-1 expression. Oxygen concentration differs between the lumen of the intestine (anerobic) and the brush border of the small intestine (microaerophilic). The transition from the anerobic to microaerophilic environment triggers SPI-1 expression through HilA [16,36–38]. It is also thought that the high osmolarity of the small intestine induces *hilA* expression and induces changes to DNA supercoiling affecting transcription of invasion associated genes.

1.2.1.2 T3SS1-dependent invasion

S. Typhimurium modifies the actin cytoskeleton enabling invasion by initiating the activity of the Rho family GTPases CDC42 and Rac through the activity of T3SS1-secreted effectors SopE, SopE2, and SopB. SopE and SopE2 function as guanine nucleotide exchange factors (GEFs) that directly activate both CDC42 and Rac to induce membrane ruffling [39–42]. Activation of CDC42 and Rac triggers a cascade of signal transduction events ultimately leading to actin cytoskeleton rearrangement enabling invasion [43]. SopB directly interacts with CDC42 [44] and indirectly activates RhoG through activation of a SH3-containing guanine exchange factor [41] to mediate actin remodelling. SopB also functions as an inositol phosphatase that hydrolyzes a variety of substrates [45,46]. SopB-generated phosphatidyloinsitol-3-phosphate

binds host VAMP8, a v-SNARE protein, at the site of invasion to promote efficient invasion [47,48].

Rearrangement of the actin cytoskeleton requires actin binding proteins in addition to the activity of Rho GTPases. *S.* Typhimurium uses the T3SS1-secreted effectors SipA and SipC to bind actin [49–51]. SipA is thought to initiate actin polymerization at the invasion site to increase the stability of actin bundles, allowing the host cell membrane to form ruffles that ultimately engulf *S.* Typhimurium [14]. SipC has been shown to have multiple activities including actin nucleation, bundling of filamentous (F)-actin, and translocation of T3SS1-secreted effectors. Specific domains within SipC have been attributed to each of these functions [52]. In all, the T3SS1-secreted effectors hijack host processes to allow efficient invasion of *S.* Typhimurium into host cells.

1.2.1.3 SCV formation

S. Typhimurium resides within a unique compartment termed the *Salmonella*-containing vacuole (SCV) immediately following host cell invasion. Entry into a bacteria-containing vacuole (BCV) is seen with various intracellular pathogens including *Legionella pneumophila, Shigella flexneri, Francisella tularensis, Mycobacterium tuberculosis, and Edwardsiella* species. Like *Salmonella*, *Legionella* and *M. tuberculosis* largely remain and replicate within a BCV, while *Shigella*, *Fransciella*, and *Edwardsiella* escape their vacuoles and replicate within the host cell's cytoplasm [53,54].

The early stages of SCV formation and maturation ("early SCVs") in HeLa cells resembles early endosomes with markers for endocytic sorting and recycling pathways and subsequent maturation pathways, partially owing to the activities of T3SS-secreted effectors. The T3SS1-secreted effector SopB maintains high levels of SCV membrane-associated

phosphatidylinositol-3-phosphate (PI(3)P) during the initial stages of SCV maturation [48]. SopB recruits the small GTPase Rab5, which in turn recruits the PI3-kinase Vps34 which phosphorylates phosphatidylinositol to PI(3)P [59]. Increased levels of PI(3)P facilitates recruitment of early endosome antigen 1 (EEA1) and lysosomal associated membrane protein (LAMP) 1 to the SCV membrane [1,60]. Rab5 promotes docking and fusion of early endosomes to various targets, and regulates the conversion of early to late endosomes [61,62]. Early SCVs are also characterized by the endocytic markers transferrin receptor (TfnR), Rab4, and Rab11 [63,64]. Rab4 regulates early sorting events in endosomes while Rab11 recycles membrane components between the plasma membrane and the Golgi [65,66].

SCV maturation, like endosome maturation, is marked by the rapid loss of early-, sorting-, and recycling-membrane markers, and acquisition of the late endosomal markers Rab7, LAMPs 1, 2, and 3, and vATPase (see Figure 1.1 for comparison of SCV and endosome maturation) [63,67–70]. SCVs acquire the late endosome markers Rab7 and Rab9, but are not enriched for the characteristic late endosomal/lysosomal markers cathepsin D, lysobisphosphatidic acid (LBPA), and mannose-6-phosphate receptor (M6PR) [68,71,72]. This altered maturation program results from the activities of several T3SS2-secreted effectors and delayed interactions with late endocytic compartments.

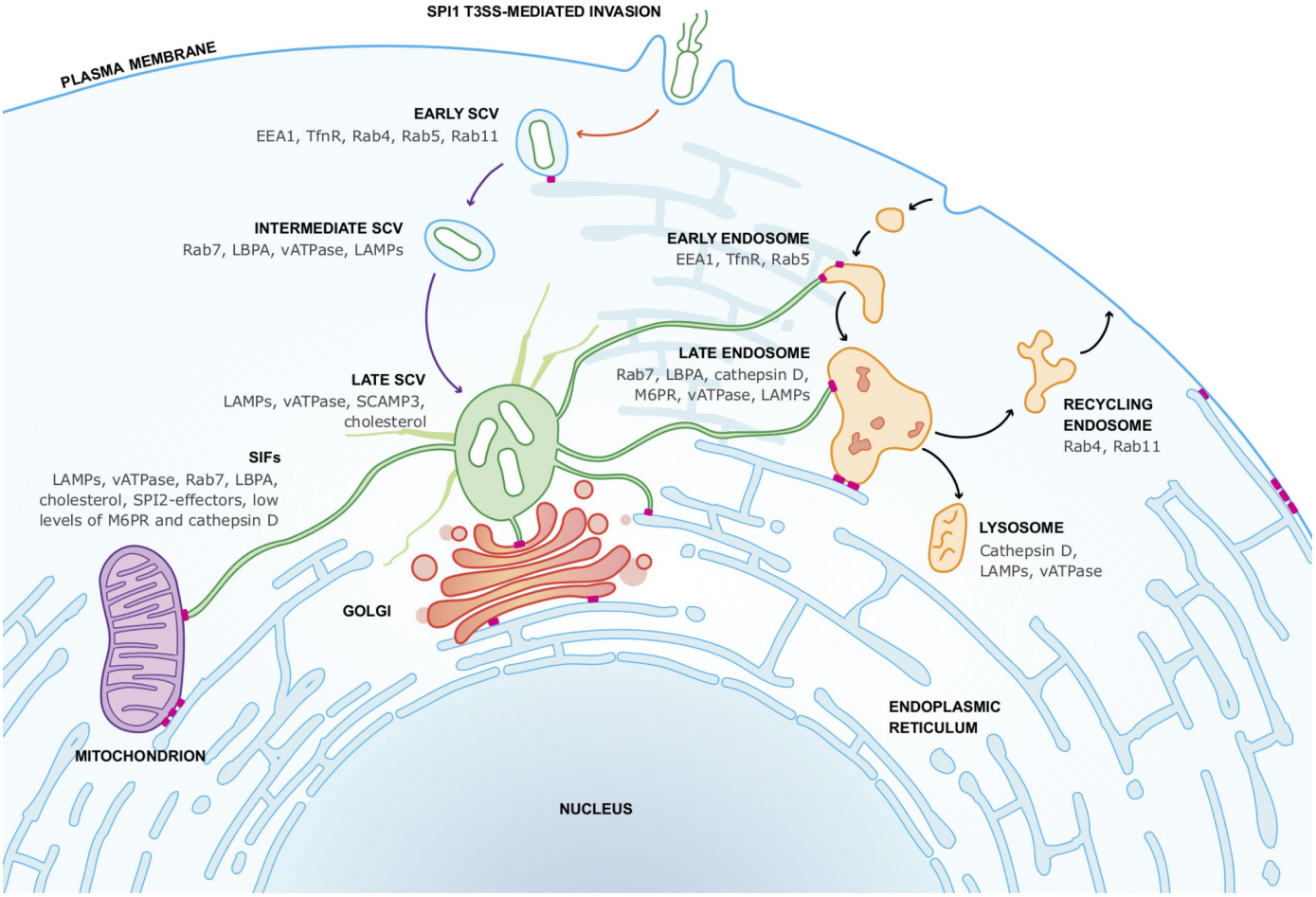

Figure 1.1 - SCV maturation and SIF biogenesis in epithelial cells. *S.* Typhimurium invades epithelial cells in a T3SS1-depenant manner and specifically resides within the SCV within the host cell. Studies primarily in HeLa cells have revealed that formation of the early SCV is dependent on T3SS1-secreted effectors (orange arrow) and occurs within 15 min post-infection (p.i.). SCV maturation is dependent on T3SS2-secreted effectors (purple arrows). The late SCV is formed by 3-4 hours post infection (h.p.i.). SCV maturation closely resembles but is distinct from endosome maturation (black arrows). The SCV is located next to the Golgi by 8 h.p.i., coinciding with the formation of SIFs (green tubules). SIFs from an extensive network throughout the host cell facilitating interactions with host organelles. The tubular endoplasmic reticulum (blue tubules) forms multiple contact sites (pink bars) with organelles, the plasma membrane, and the early SCV. Originally published in [73]

1.2.2 *Salmonella*-Pathogenicity Island 2

Salmonella-Pathogenicity Island 2 (SPI-2) is a 25 kb locus [74] containing genes necessary for *Salmonella* replication within host cells and systemic infection in mice [75]. SPI-2

contains 31 genes organized in four operons [76,77] and includes genes encoding structural components of a T3SS, genes encoding translocation proteins, chaperone proteins, and the SsrA/B two-component regulatory system [78]. Many of the genes encoding T3SS2-secreted effectors reside outside of SPI-2. Identification of T3SS2-secreted effectors has been hindered by a lack of a conserved motives or signatures within the coding region of effectors [79]. So far, there has been at least 28 T3SS2-secreted effectors identified [80].

1.2.2.1 Regulation of SPI-2

Like regulation of SPI-1, the regulation of SPI-2 is complex, occuring on multiple levels including both environmental and genetic levels. SPI-2 is primarily expressed upon host cell invasion and internalization within the SCV [81], though some evidence suggests that SPI-2 is expressed in the ileum lumen before *S.* Typhimurium has had the chance to invade the intestinal epithelium [82]. The regulation of SPI-2 is tightly controlled and involves several two-component systems.

1.2.2.1.1 SsrA/SsrB two-component system

The two-component regulatory system SsrA/SsrB encoded within SPI-2 is a major regulator of virulence associated events linked to SPI-2. The response regulator SsrB binds to all promoters within SPI-2 and is indispensable for expression of the T3SS2 secretion apparatus and its associated effectors encoded within SPI-2, as well as effectors encoded outside SPI-2 [76,83–85]. SsrA (also commonly referred to as SpiR) functions as the membrane-bound cognate sensor kinase for SsrB. Unlike most two component systems, *ssrA* and *ssrB* each have their own promoters, such that regulation of *ssrA* is separate and distinct from the regulation of *ssrB* [86]

1.2.2.1.2 H-NS regulation of SPI-2

Characteristic of genes acquired by horizontal gene transfer, the DNA comprising SPI-2 is A/T rich [76,85] and is therefore subject to transcriptional silencing mediated by H-NS [87–89]. H-NS is a nucleoid-associated protein that prevents uncontrolled expression of genes acquired by horizontal gene transfer [75] (reviewed in [90]). H-NS binds directly to the *ssrA* promoter to silence *ssrA* transcription [91]. *S.* Typhimurium readily expresses SPI-2 virulence genes during infection indicating that *S.* Typhimurium has evolved to overcome H-NS silencing. SsrB likely antagonizes H-NS silencing of SPI-2 genes as it binds to all SPI-2 promoters and is indispensable for SPI-2 expression [75,83,92]. Under certain SPI-2 inducing conditions (specifically during stationary phase in Luria-Bertani (LB) medium) the SPI-1 protein HilD removes H-NS silencing of the SsrA/B two-component system resulting in expression of SPI-2 associated proteins. It is important to note that the HilD-dependent activation of SsrA/B occurs only under certain *in vitro* conditions, and not conditions recapitulating the intracellular environment that *S.* Typhimurium typically inhabits [30,91].

1.2.2.1.3 Regulation of SsrA/B by two-component systems

The SsrA/B two-component system is regulated by two additional two-component systems: OmpR/EnvZ and PhoP/PhoQ. The OmpR/EnvZ two-component system is comprised of the response regulator EnvZ which phosphorylates the response regulator OmpR in response to changes in osmolarity and pH [86]. Shortly after *S*. Typhimurium enters the macrophage environment phosphorylated OmpR binds the *ssrA* promoter and initiates transcription of *ssrA* [93]. Phosphorylated OmpR also binds to the promoter region of *ssrB* to initiate transcription of *ssrB* [86]. In this way, the OmpR/EnvZ two-component system participates in SPI-2 regulation.

The SsrA/B two component system is also regulated by the two-component system PhoP/Q. PhoP/Q is required for *S.* Typhimurium virulence [94] and survival within the toxic

environment of macrophages [95]. There is strong evidence supporting regulation of SPI-2 gene expression by PhoP/Q. First, PhoP-regulated genes are expressed by intracellular *S.* Typhimurium [81,96,97]. Second, SPI-2 expression requires the activity of PhoP when *S.* Typhimurium is grown in conditions of low Mg^{2+} and low pH [93,98] which are conditions that SCV-bound *S.* Typhimurium experience within the macrophage. PhoP regulates the SsrA/B two-component system through direct binding to the *ssrB* promoter to regulate transcription, and regulates SsrA post-transcriptionally through binding to a region in the 5' untranslated region of the *ssrA* mRNA transcript [75,99].

1.3 The intracellular replicative niche

Being inside the host cell is a dangerous place for *S.* Typhimurium: both the cytosol and the vacuolar environments are inhospitable. *S.* Typhimurium has mechanisms in place to both maintain the vacuolar membrane and to subvert the lysosomal degradation pathway [69,100]. *S.* Typhimurium resides within the SCV following invasion as the cytosolic environment of phagocytic cells limits *S.* Typhimurium replication through detection by caspase-1 and caspase-11 thus resulting in cell death via pyroptosis [80,102]. In non-phagocytic cells, autophagy can limit cytosolic growth of *S.* Typhimurium that rupture the SCV membranes [101]. However, a small portion of *S.* Typhimurium (around 10%) manage to escape the SCV, evade the host autophagic machinery, and enter a hyper-replicative state within the cytosol of epithelial cells [55–58].

Host cells can also combat intracellular pathogens by making use of reactive oxygen species and reactive nitrogen intermediates. Macrophages are equipped with NADPH oxidase and inducible nitric oxide synthase, both of which are deployed in response to *S.* Typhimurium

infection [103,104]. *S.* Typhimurium counteracts these host defenses by inhibiting both the expression of these enzymes and their delivery to the SCV [105–108]. Data suggests that inhibition of delivery of both of NADPH oxidase and inducible nitric oxide synthase is T3SS2-dependant, though no T3SS2-secreted effectors have been identified to specifically play a role in this process.

S. Typhimurium avoids these defenses by remaining within the vacuole; however, remaining within the vacuole presents its own set of challenges. Intravacuolar S. Typhimurium is susceptible to the activities of the endolysosomal system wherein late endosomes, lysosome/late endosome hybrids, autophagosomes, and phagosomes are subject to lysosomal hydrolase mediated proteolysis. The activities of the T3SS2-secreted effectors allow *S.* Typhimurium to form a replicative niche permissive to replication and to avoid host defenses.

1.3.1 Intracellular SCV positioning

The SCV migrates from the periphery of the host cell to the microtubule organizing center (MTOC) 1-2 hours post invasion in cultured epithelial cells. SCV migration is mediated by the dynein-dynactin microtubule motor complex which is linked to the SCV by RILP (Rab-interacting lysosomal protein) [109]. By 4-6 hours post-infection (h.p.i.), the SCV is situated in the juxtanuclear region and *S.* Typhimurium begins to replicate within the SCV. The precise position of the SCV at later time points during infection results from a balancing act amongst T3SS2-secreted effectors.

It was originally thought that the T3SS2-secreted effectors SifA and SseG were responsible for the subcellular localization of the SCV during infection. SifA binds the host protein SifA-and-Kinesin-Interacting-Protein (SKIP, also known as PLEKHM2) to down-regulate kinesin-1 recruitment at the SCV membrane [110]. SseG was found have a Golgi-

targeting domain and co-localized with markers for the *trans*-Golgi network. Furthermore, association between the SCV and the Golgi depended on SseG [111]. Additional effectors have since been identified to play a role in SCV positioning.

In addition to SifA and SseG, the T3SS2-secreted effectors SseF, PipB2, and SteA have all been shown to participate in SCV positioning. SseF and SseG are thought to interact to promote SCV positioning near the Golgi apparatus and nucleus around 8 h.p.i. by interacting both with each other, and with the host protein ACBD3 (a multifunctional cytosolic Golgi network-associated protein) [112,113]. PipB2 acts as a linker between the SCV and the kinesin light chain, enabling kinesin-1-driven anterograde transport along microtubules [114]. It was recently shown that PipB2 and SifA bind to both each other and kinesin-1, and both regulate the activity of kinesin-1 [115]. SteA is also thought to contribute to SCV positioning during infection. SteA was found to be functionally linked to SseF and SseG and may participate in regulation of microtubules motors on the surface of the SCV. The mechanism underpinning SteA's involvement in SCV positioning remains unclear.

1.3.2 SCV maturation

The activities of the T3SS2-secreted effectors change the early SCV into a unique compartment permissive for bacterial replication, termed the "late SCV". The T3SS2-secreted effectors SifA, SopD2, and SseJ are partly responsible for the SCV's unique maturation program. In addition to regulating kinesin-1 activity at the SCV membrane, the SifA-SKIP complex binds and sequesters Rab9, inhibiting Rab9-dependent recruitment of M6PR to the SCV membrane. Decreased M6PR recruitment to the SCV membrane decreases recruitment of lysosomal enzymes to the SCV, thereby protecting intracellular *S.* Typhimurium from host defenses [100]. SopD2 further alters SCV maturation by directly impairing Rab7-dependent recruitment of the

host trafficking-related effectors FYCO1 (FYVE and coiled-coil domain containing protein 1) and RILP. In uninfected cells, FYCO1 and RILP mediate plus- and minus- end-directed movement of vesicular cargo along microtubules, respectively, by linking vesicular cargo to their respective microtubule motors [109,116,117]. Inhibition of RILP- and FYCO1-mediated microtubule-based trafficking by SopD2 in infected cells thereby prevents delivery of lysosomes to the SCV [118]. SseJ has two activities: phospholipase A activity, and glycerophospholipid:cholesterol acyltransferase activity [119]. Given these two enzymatic activities, SseJ may alter SCV lipid composition, thus altering the localization of lipid-bound proteins to the SCV [120,121] and consequently mediating interactions with the host's endocytic pathway. In this way, *S.* Typhimurium alters the normal endosome maturation program to transform the late SCV into a unique niche within the host cell.

1.4 *S.* Typhimurium-mediated cytoskeletal rearrangements

Central to *S.* Typhimurium take-over of the host cell is its ability to redirect host microtubule motors to hijack the host's endosomal system and to promote centrifugal extension of SIFs from the SCV (discussed below in Section 1.5). The microtubule network is a component of the host's cytoskeleton which also includes actin and intermediate filaments. Together, these three cytoskeletal components control the shape and mechanics of the cell, with each component playing its own role. Briefly, actin is dispersed throughout the cell, but is mostly concentrated at the plasma membrane to control cell shape and cell movement. Microtubules radiate throughout the cell originating from the microtubule-organizing center and primarily function to control organelle and vesicle movement within the cell; actin can also participate in this [122,123]. Intermediate filaments (IFs) provide additional mechanical support to the cell. IFs are typically

crosslinked to each other, as well to actin filaments and microtubules through proteins called plectins [124].

1.4.1 T3SS-mediated cytoskeleton reorganization

Effectors secreted into the host cell by T3SS1 enables invasion through reorganizing of the actin cytoskeleton as described in section 1.2.1.2. Effectors secreted by the T3SS2 also modulate host actin. Several hours after invasion SCV-bound *S.* Typhimurium is surrounded by an actin nest composed of filamentous (F) actin, formation of which is dependent on T3SS2-secreted effectors [59,69,125]. The formation of SCV-associated actin nest, also known as vacuole-associated actin polymerization (VAP) is mediated by the T3SS2-secreted effector SteC [125]. The T3SS2 effectors SspH2 and SpvB also localize to the SCV-associated VAP [84,126,127]. SspH2 targets the host actin-binding protein profilin to inhibit the rate of actin polymerization *in vitro* [126]. SpvB also inhibits F-actin polymerization through its activity as an ADP-ribosylation transferase. Thus, it appears that SteC promotes VAP formation the around the SCV, while SspH2 and SpvB inhibits it. Therefore, VAP formation is likely regulated by the balance of these effectors. The biological role of the VAP remains unclear, however intracellular *S.* Typhimurium that are not associated with a VAP experience decreased replication within macrophages [128].

The T3SS2-mediated process of *Salmonella*-induced filament (SIF) extension (discussed below in section 1.5.1) is microtubule-dependent and actin-independent. A recent ultrastructural analysis of SIFs revealed that SIFs are a double membraned-sheath that encloses a portion of cytoplasm and cytoskeletal elements including microtubules and F-actin [129]. The authors proposed that SIFs extend both longitudinally along microtubules and laterally resulting in the

double-membraned sheath enclosing elements of the host cytoskeleton [129,130]. Whether or not this enclosed F-actin plays a role during SIF biogenesis remains to be determined.

1.4.2 Annexins

Annexins are a multigene family of proteins expressed in almost all eukaryotic cell types. There are at least 160 unique annexin proteins present in no less than 65 different species. [131]. An annexin protein is defined by two characteristics:1) it must be able to bind in a Ca^{2+}-dependent manner to negatively charged phospholipids, and 2) it must contain a membrane binding module made of conserved annexin repeats packed into a α-helical disc [131]. The ability of annexins to bind negatively charged phospholipids in the presence of Ca^{2+} implicates annexins to membrane-related events such as: membrane organization regulation, membrane-cytoskeletal linkages, and steps in endocytosis and exocytosis [132,133]. It is thought that annexins can link two membranes by using their amphipathic variable N-terminal domain to link to one membrane, and their core domain to link to another membrane [134]

1.4.2.1 Annexin A2 and actin

Of the all the annexins to be described so far, only annexin A2 (AnxA2) has been previously shown to be involved in the intracellular lifestyle of *S.* Typhimurium (discussed below in section 1.4.2.3) [135]. AnxA2 is present in the cell in either a cytosolic monomeric form or as a heterotetrameric complex comprised of two AnxA2 molecules and two S100A10 (p11) molecules [136]. Binding of AnxA2 to endosomes, however, does not require S100A10 [132,137]. AnxA2 is an actin-binding protein and may function as an F-actin interaction platform [133]. AnxA2 interacts directly with polymerized F-actin *in vitro* but is not found associated with actin bundles or cables within cells [138]. AnxA2 thus may not be an actin bundling factor; instead AnxA2 may regulate actin assembly by binding to cytosolic G-actin and capping the ends

of F-actin filaments [132]. Supporting this, AnxA2 is associated with more dynamic actin structures such as those associated with phagocytosis, pinocytosis, and cell migration [138].

Grieve *et al.* 2012 suggest that AnxA2 functions at sites of actin association with membranes enriched in either cholesterol or phosphoinositides [139] as evidenced by AnxA2 having roles in many steps of membrane trafficking. While AnxA2 is enriched at the junction between actin and vesicles, the role that it plays there remains unclear. AnxA2 may act as a barbed-end capping protein to restrict actin polymerization near the vesicle. It may also function as a linker to physically connect actin to the vesicle membrane [140].

1.4.2.2 Annexin A2 and endosome maturation

AnxA2 plays important roles in the secretory and endocytic pathways [141–144] and is involved in endosome biogenesis [145]. AnxA2 usually associates with membranes rich in phosphatidylinositol-4,5-bisphosphate and/or rich in cholesterol [144]; binding of AnxA2 to early endosomes is Ca^{2+}-independent, cholesterol-dependent, and requires the AnxA2 variable N-terminus [143,144]. The N-terminal interaction domain of AnxA2 contains a unique endosome targeting sequence allowing it to associate with endosomal compartments [142,143,146]. AnxA2 association with endosomes likely acts as a membrane scaffold facilitating formation and maintenance of elongated endosomal tubules and biogenesis of other regions and may be involved in maturation of late endosomes and lysosomes [133,145,147].

It is well established that microtubules are involved in membrane trafficking within the endocytic pathway, but increasing evidence suggests that actin is also involved in this process [148]. Indeed, actin is involved in transport toward lysosomes but the mechanism involved is not fully understood [149]. Morel *et al*. found that early endosomes have patches of F-actin associated with their membranes that facilitated F-actin nucleation and polymerization [150].

AnxA2 is required for the association of F-actin with early endosomes to facilitate necessary membrane remodeling during endosome biogenesis [150]. Furthermore, AnxA2 has been implicated to regulate the actin that associates with both early and late endosomes [150], and specifically implicated in the maturation of late endosomes [151]. In sum, AnxA2 binds to cholesterol on endosomes and associates with actin to promote endosome biogenesis and maturation.

1.4.2.3 Annexin A2 during *Salmonella* infection

It was recently demonstrated that AnxA2 plays an important role during *S.* Typhimurium infection. This makes sense as entry of *S.* Typhimurium into host cells involves active remodeling of the host's actin cytoskeleton and entry of *S.* Typhimurium into a vacuole is initially similar to that of an early endosome [1]. The AnxA2/S100A10 heterotetramer plus host AHNAK, a giant phosphoprotein, is enriched at *S.* Typhimurium-invasion sites, and is essential for efficient T3SS1-mediated invasion. The phosphatase activity of the T3SS1-secreted effector SopB is partially responsible for recruitment of AnxA2, S100A10 and AHNAK to the site of invasion [135]. In all, this data shows that *S.* Typhimurium can target AnxA2 to facilitate interactions with host actin to promote invasion and establishment of its intracellular replicative niche. It has yet to be determined whether AnxA2 also participates in SCV maturation in the same way it participates in maturation of late endosomes and lysosomes.

1.5 *Salmonella*-induced tubules

A characteristic feature during *S.* Typhimurium infection that accompanies SCV maturation and intravacuolar replication is the formation of five distinct types of *Salmonella*-Induced Tubules (SITs). Intracellular *S.* Typhimurium first induces the T3SS1-dependant

spacious vacuole-associated tubules (SVATs) and SNX3 tubules 15-60 mins after invasion, but prior to the onset of replication. [152,153]. Bacterial replication begins 3-4 h.p.i. concomitant with the expression of T3SS2 and its associated effectors. Activation of the T3SS2 is associated with the formation of *Salmonella*-Induced Filaments (SIFs) [154–156], LAMP1-negative tubules (LNTs) [157], and *Salmonella*-induced secretory carrier membrane protein 3 (SCAMP3) tubules (SISTs) [158]. Both SIFs and LNTs are typically formed between 3-16 h.p.i. with SIF formation peaking at 8-16 h.p.i. and LNT formation peaking at 16 h.p.i.. SISTs are typically formed between 8-14 h.p.i. with peak formation occurring at 14 h.p.i. [159]. The host markers enriched in the membranes of the T3SS2-mediated SITs is what differentiates them from each other as formation of these tubules relies on similar T3SS2-secreted effectors and are susceptible to the same chemical treatments [159]. LNTs are marked by cholesterol and vATPase and a distinct lack of LAMP1 [157] while SISTs are marked by SCAMP3 [158]. SIFs, on the other hand are marked by LAMPs, vATPase, Rab7, SCAMP3, LBPA, and cholesterol [69,71,72,154,156,157, 159–162]. SVATs, SNX3 tubules, SISTs, and LNTs have thus far been described only in epithelial cells. SIFs have been observed in both epithelial cells and macrophages, though the SIF network is less extensive in macrophages as compared to epithelial cells. This dissertation focuses primarily on SIFs.

1.5.1 Biogenesis of *Salmonella*-induced filaments

The process of SCV maturation from the early- to late- SCV takes place around 5 h.p.i. in HeLa cells. *S.* Typhimurium replication coincides with full maturation of the late SCV and SIF extension. The remarkably dynamic process of SIF biogenesis results in a highly complex stabilized network of SIFs by 8 h.p.i., during which individual SIFs undergo extension,

contraction, branching, and fusion with other SIFs [156,160]. SIFs are the only type of SIT known to be marked by LAMPs [154,159].

The same T3SS2-secreted effectors associated with SCV maturation are also associated with SIF biogenesis. These effectors are SifA, SseJ, SopD2, PipB2, SseF, SseG, and SteA (see Table 1.1 for more information on each effector). All seven of these effectors collectively contribute to at least one or more of the following roles within the host cell: promoting SIF biogenesis, perinuclear positioning of the SCV, maintaining stability and/or modifying the SCV membrane, and recruiting and/or regulating microtubule motor activity required for extension of SIFs along microtubules [12,79,80,163].

Table 1.1 - T3SS2-secreted effectors associated with SCV maturation and SIF biogenesis. Originally published in [73].

Effector	Biochemical Activity	Known Host Target(s)	Host Subcellular Localization/Effects	References
SifA	RhoA GTPase	Rab7, Rab9, SKIP, RhoA, PLEKHM1	Localized to SIFs and SCV membranes, promotes SIF biogenesis, maintains SCV membrane stability, promotes kinesin-1-dependent movement along microtubules, enables continuous fusion of host vesicles to SCV membrane	[100,109,110,164–167]
SseJ	Deacylase; transferase	RhoA, phospholipids, cholesterol	Localized to SCV membrane and SIFs, regulates SCV membrane dynamics, inhibits SIF biogenesis, esterifies cholesterol on SCV membrane	[121,168–170]
PipB2	Unknown	Kinesin-1	Recruits kinesin-1 to SCV membrane, reorganizes late endosome/lysosome compartments	[72,114]
SopD2	Unknown	Rab7	Localized to SCV membrane and host cell endosomes, inhibits host endocytic trafficking, antagonist of SifA in regulation of membrane dynamics and SIF biogenesis	[118,157,171]
SseF/ SseG	Unknown	Acyl-CoA binding domain containing 3	Integral membrane proteins, co-localize with microtubule network/microtubule bundling, tethers SCV to Golgi, converts single-membraned SIFs to double-membraned SIFs	[112,113,129,162,172]
SteA	Unknown	Phosphatidylinositol 4-phosphate	Localized to membrane of SCV and SITs, control of SCV membrane dynamics	[173,174]

SifA classically has been considered to be the main driver of SIF biogenesis as Δ*sifA* mutants fail to induce SIFs in HeLa cells [175]. Extensive vacuolation of LAMP1^{+} vesicles is observed in uninfected host cells transfected with SifA [176] suggesting that SifA alone is sufficient to induce endosomal tubulation resembling SIF-like structures. During infection, LAMP1 enrichment at the SCV membrane is enhanced at the C-terminal domain of SifA [177]. While SifA may be sufficient to induce endosomal tubulation, SseJ, when activated by GTP-bound RhoA, cooperates with SifA to promote formation of SIF-like structures [1,178]. Observations that effector deletion mutants of any of the seven T3SS2-secreted effectors association with SIF biogenesis have altered SIF morphology and/or frequency *in vitro* [174,175,179,180] suggests that all seven SIF-related effectors are required to produce wild type SIFs within host cells.

Advances in fluorescence microscopy, transmission electron microscopy, and EM tomography have provided new insights into SIF biogenesis [129]. It was shown that nascent SIFs emerge as single-membrane tubules, dependent on SifA, and are thought to be of late endosomal or endolysosomal origin based on luminal content. Single-membraned SIFs are thought to be converted to double-membraned SIFs through the activities of SseF and SseG. Double-membraned compartments are commonly observed during formation of autophagosomes [181] so it is convenient to speculate that autophagy plays a role in SIF biogenesis since SIFs are double-membraned and multiple reports demonstrate autophagy controlling intracellular *S.* Typhimurium [101,182–185]. However, Krieger *et al* (2014) found that autophagic machinery does not play a role in SIF biogenesis; instead, SIFs likely originate from another T3SS2-dependant mechanism [129].

Kreiger *et al*. propose a model of SIF biogenesis wherein T3SS2-secreted effectors, SifA in particular, recruit and fuse host membrane vesicles to the SCV providing components for tubule extension. PipB2 then promotes SIF extension by linking nascent SIFs to the kinesin-1 microtubule motor promoting SIF extension outwards from the SCV along microtubules [186]. Single-membrane SIFs are then converted to double-membrane SIFs by SseF and SseG [129]. The double membrane structure of SIFs would allow *S.* Typhimurium to maintain contact with endocytosed materials (*e.g.,* nutrients), while remaining separated from the host cell cytosol (and potential host antimicrobial defenses). This model accounts for the activities of four of the seven effectors associated with SIF biogenesis, namely SifA, PipB2, SseF, and SseG. It remains unknown how the other three effectors contribute to this model.

1.5.2 SIFs link *S.* Typhimurium to the endocytic and exocytic pathways

S. Typhimurium has specifically evolved to establish the SIF network, yet the role of SIFs is only just beginning to be understood. Mounting experimental evidence indicates that intracellular *S.* Typhimurium directly interacts with the host's endocytic system. SIFs are characterized by host late endosomal membrane markers LAMPs, vATPase, Rab7, and cholesterol. Unlike late endosomes, SIF membranes are also marked by T3SS2-secreted effectors, and low concentrations of both M6PR and cathepsin D [71,72,155,158,159,187]. Multiple reports demonstrate that SIFs likely acquire late endocytic markers by sustained fusion events with the endocytic pathway [129,156,160].

SCAMP3 is also a major component of SIFs, which unlike most SIF markers is not associated with late endocytic compartments [158]. SCAMP3 is primarily localized to the *trans*-Golgi network and controls multivesicular endosome biogenesis in uninfected cells [188,189]. In line with this, *S*. Typhimurium redirects exocytic transport processes and interacts with the

secretory pathway [190,191]. This interaction, in addition to the endocytic pathway (discussed below), may allow *S*. Typhimurium to obtain nutrients for replication, collect membrane components for SCV and SIF biogenesis, or manipulate the host cell's response to infection.

1.5.3 Function of *Salmonella* induced filaments

It is hypothesized that SIFs allow *S*. Typhimurium to redirect host vesicular traffic to supply intravacuolar *S.* Typhimurium with endocytosed nutrients and membrane components to promote intravacuolar replication [118,190,191]. Fluorescently labeled endosomal cargo is detected within SIF networks of infected cells [156,160,192] providing evidence that SIFs have access to content endocytosed by the host cell. Furthermore, it was demonstrated that the T3SS2-dependent remodeling of the host cell's endosomal transport system provides a means by which intravacuolar *S*. Typhimurium can gain access to endocytosed nutrients [193]. Both membrane components and luminal content of the SIF network are connected to, and interchanging with, the SCV in a T3SS2-dependant manner [129,194] allowing *S.* Typhimurium access to endocytosed materials. Liss *et al* [194] also demonstrated that intravacuolar *S.* Typhimurium connected to the SIF network are significantly more metabolically active than *S.* Typhimurium in SCVs lacking connections to SIFs, suggesting that SIFs enable nutrient acquisition. Collectively, these findings suggest that *S*. Typhimurium uses the host endocytic system to expand its replicative niche, form the SIF network, and uses SIFs to gain access to nutrients to promote replication within the SCV.

1.6 Dissertation summary

The field of *Salmonella* pathogenesis is rapidly expanding and despite a large body of literature on the intracellular lifestyle of *S.* Typhimurium, there remains many questions

regarding the molecular mechanisms underpinning the effectors associated with hijacking the host's endosomal system. The studies presented in this dissertation set out to unravel the complex interactions between the effectors SifA, SopD2, PipB2, SteA, SseJ, and SseF as they relate to the intracellular replicative niche of *S.* Typhimurium.

The overarching theme of this work is that the nuanced complexities in the specific roles of effectors implicated in host endomembrane reorganization are not captured by single effector studies and single effector protein function studies leads to oversimplification of the complex host-pathogen interaction. The majority of previous T3SS2-secreted effector-host interaction studies were transfection-based, and consequently are unable to capture the complex interplay between effectors to mediate specific phenotypes during infection. In this work, we endeavor to delineate effector interactions during an infection wherein all T3SS2-secreted effectors are present.

In Chapter 2 we systematically evaluate the roles of the effectors in both single-effector deletion mutant studies and multiple-effector deletion mutant studies. From these studies, we show that establishment of the *S.* Typhimurium replicative niche requires the activities of multiple effectors and necessitates study of T3SS2-secreted effectors as groups rather than as individual effectors. In Chapter 3 we create a repertoire of *S.* Typhimurium strains that a) overexpress *ssrB* resulting in increased secretion of all T3SS2-secreted effectors, and b) secrete HA-tagged SifA, SopD2, PipB2, SteA, SseJ, or SseF into the host cell. In Chapter 4 we use our toolkit created in Chapter 3 to study effector-effector or effector-host interactions during infection. Understanding the roles of effectors in the context of infection will provide insight into the replicative niche of *S.* Typhimurium and may provide novel targets for development of new therapeutics.

Chapter 2: Multiple *Salmonella*-pathogenicity island 2 effectors are required to facilitate bacterial establishment of its intracellular niche and virulence

2.1 Synopsis

The pathogenesis of *Salmonella* Typhimurium depends on the bacterium's ability to survive and replicate within host cells. The formation and maintenance of a unique membrane-bound compartment, termed the *Salmonella*-containing vacuole (SCV), is essential for *S.* Typhimurium pathogenesis. SCV-bound *S.* Typhimurium induces formation of filamentous tubules that radiate outwards from the SCV, termed *Salmonella*-induced filaments (SIFs). SIF formation is concomitant with the onset of replication within host epithelial cells. SIF biogenesis, formation and maintenance of the SCV, and the intracellular positioning of the SCV within the host cell requires translocation of bacterial proteins (effectors) into the host cell. Effectors secreted by the type III secretion system encoded on *Salmonella* pathogenicity island 2 (T3SS2) interfere with host cellular processes and promote both intracellular survival and replication of *S.* Typhimurium. Seven T3SS2-secreted effectors, SifA, SopD2, PipB2, SteA, SseJ, SseF, and SseG have previously been implicated to play complementary, redundant, and/or antagonistic roles with respect to in SIF biogenesis, intracellular positioning of the SCV, and SCV membrane dynamics modulation during infection. We undertook a systematic study to delineate the contribution of each effector to these processes by (i) deleting all seven of these effectors in a single *S.* Typhimurium strain; and (ii) deleting combinations of multiple effectors based on putative effector function. Using this deletion mutant library, we show that each of SIF biogenesis, intracellular SCV localization, intramacrophage replication, colonization, and

virulence depends on the activities of multiple effectors. Together, our data demonstrates the complex interplay between these seven effectors and highlights the necessity to study T3SS2-secreted effectors as groups, rather than studies of individual effectors.

2.2 Introduction

Salmonella enterica serovar Typhimurium (*S.* Typhimurium) is a Gram-negative foodborne pathogen that commonly causes non-typhoidal salmonellosis (gastroenteritis) in humans. The success of *Salmonella* as an intracellular pathogen is largely due to its ability to evade host defense mechanisms by invading and residing within intestinal epithelial cells and phagocytic cells of the host [1,195]. Upon invasion of the host cell, *S.* Typhimurium resides within a unique compartment called the *Salmonella*-containing vacuole (SCV). Formation and maintenance of the SCV during infection is critical to survival within phagocytes and plays an important role in promoting *S.* Typhimurium replication in non-phagocytic cells [196].

The SCV, while a unique compartment distinct from host organelles, initially exhibits features similar to maturing endosomes. Upon invasion of the host cell, the nascent SCV (early SCV) carries the same membrane markers that characterize early endosomes such as EEA1 and transferrin receptor [63]. Subsequent SCV maturation occurs through a series of controlled selective sequential interactions with the host's endocytic pathway [63,64]. During maturation, the SCV—like late endosomes—accumulates lysosomal glycoproteins such as lysosomal associated membrane proteins (LAMP) 1 and 2 within the SCV membrane and the SCV lumen acidifies. However, unlike late endosomes, the SCV does not fully mature into a lysosome owing to manipulation of the host cell by intravacuolar *S.* Typhimurium [70,197–199].

S. Typhimurium possesses two distinct type III secretion systems (T3SSs) encoded on *Salmonella* pathogenicity islands 1 and 2 (T3SS1 and T3SS2 respectively). These two T3SSs, along with additional virulence factors, allow *S.* Typhimurium to invade, survive, and replicate within host cells [1]. Whereas the T3SS1-secreted effectors are primarily associated with facilitating invasion of non-phagocytic cells and initial formation of the early SCV, the T3SS2-secreted effectors generally function to promote replication within both phagocytic and non-phagocytic cells [11,12,79]. The T3SS2-secreted effectors exert a wide variety of functions during infection including, but not limited to, maintaining the SCV membrane, regulating intracellular SCV positioning, and forming the membranous filament-like extensions that radiate outwards from the SCV, termed *Salmonella*-induced filaments (SIFs) [166]. SIF biogenesis begins at 4-6 hours post-infection, concomitant with the onset of intercellular bacterial replication in human epithelial cells [154,156,179]. SIFs are thought to play a number of important roles during infection including nutrient acquisition from the host and cell-to-cell transfer [170,193,194,200].

A subset of seven T3SS2-secreted effectors play a role in SIF biogenesis, intracellular positioning of the SCV, and in controlling SCV membrane dynamics. These effectors of interest include: SifA, SseF, SseG, SteA, PipB2, SopD2, and SseJ [12,79,114,159,201]. The single deletion mutant of each of these seven effectors results in attenuation of virulence in the mouse model of systemic infection [69,114,161,166,169,202] and all but PipB2 contribute to survival in mouse macrophages [79]. These data highlight the importance of these effectors in both *in vitro* and *in vivo* infection models. The precise function of the seven effectors of interest is known for some but unclear for others, and their contribution to formation of the intracellular replication niche remains ambiguous. Each of SifA, SseF, SseG, SteA, PipB2, SopD2, and SseJ contribute

to at least one, if not several of the following roles during infection: SIF biogenesis, precise intracellular positioning of the SCV, SCV membrane stability, SCV membrane modification, microtubule recruitment, and/or regulation of microtubule motor activity at the SCV membrane. The effectors' overlapping roles during infection make it difficult to determine precise effector function when studying a single effector at a time. Increasing evidence suggests that T3SS2-secreted effectors cooperate to facilitate the interaction of *S.* Typhimurium with host cell machinery, leading to events such as SIF biogenesis and SCV movement [72,121,126,165].

In this study, we systematically constructed a *S.* Typhimurium SL1344-based strain that lacks all seven of our effectors of interest, as well as multiple effector deletion combinations. We show that LAMP1$^+$-tubule (SIF) extension is not exclusively driven by SifA, but rather, likely requires the activity of other effectors. We also demonstrate that LAMP1$^+$-tubule extension, intracellular positioning, intramacrophage replication, and replication *in vivo* all require the action of multiple effectors. One effector alone does not solely mediate a single process.

2.3 Materials and Methods

2.3.1 Ethics statement

All animal experiments were performed according to protocol number A13-0265 approved by the University of British Columbia's Animal Care Committee and in direct accordance with the Canadian Council of Animal Care (CACC) guidelines. Mice were euthanized at 3 days post-infection.

2.3.2 Bacterial strains and culture conditions

Bacterial strains used in this work are described in Table 2.1. All strains were routinely grown in Luria-Bertani (LB) medium at 37˚C with shaking. For growth of the *E. coli* MFD*pir*

strain, media was supplemented with DL-2,6-Diaminopimelic acid (DAP) at a final concentration of 0.3 mM when appropriate. Antibiotics were used at the following concentration when required: streptomycin 50 μg/mL, chloramphenicol 30 μg/mL.

Table 2.1 - Bacterial strains used in this study

***Escherichia coli* Strains**			
	Strain Designation	**Relevant Characteristics/Genotype**	**Source/ Reference**
	MC1061*λpir*	*hsdR mcrB araD139 Δ(araABC-leu)7679 ΔlacX74 gal1 galK rpsL thiλpir*	[203]
	MFD*pir*	*MG1655 RP4-2-TC::[ΔMu1::aac(3)IV-ΔaphA-Δnic35-ΔMu2::zeo] ΔdapA::(erm-pir) ΔrecA*	[204]
	DH10B	*F- araDJ39 Δ(ara, leu)7697 ΔlacX74 galU galK rpsL deoR ϕ80dlacZΔM15 endAI nupG recAl mcrA Δ(mrr hsdRMS mcrBC)*	[205]
***Salmonella* Typhimurium Strains**			
	Strain Designation	**Relevant Characteristics/Genotype**	**Source/ Reference**
	SL1344	Wild type strain, *hisG*	[206]
Single-effector deletion mutants	Δ*steA*	SL1344Δ*steA*	This study
	Δ*pipB2*	SL1344Δ*pipB2*	This study
	Δ*sopD2*	SL1344Δ*sopD2*	This study
	Δ*sseJ*	SL1344Δ*sseJ*	This study
	Δ*sifA*	SL1344Δ*sifA*	This study
	Δ*ssaR*	SL1344Δ*ssaR*	[207]
	Δ*sseFG*	SL1344Δ*sseF*Δ*sseG*	This study
Multi-effector deletion mutants — Sequential-effector deletion mutants	Δ*sseFG*Δ*steA*	SL1344Δ*sseF*Δ*sseG*Δ*steA*	This study
	Δ*sseFG*Δ*steA*Δ*pipB2*	SL1344Δ*sseF*Δ*sseG*Δ*steA*Δ*pipB2*	This study
	Δ*sseFG*Δ*steA*Δ*pipB2*Δ*sopD2*	SL1344Δ*sseF*Δ*sseG*Δ*steA*Δ*pipB2*Δ*sopD2*	This study
	Δ*sseFG*Δ*steA*Δ*pipB2*Δ*sopD2*Δ*sseJ*	SL1344Δ*sseF*Δ*sseG*Δ*steA*Δ*pipB2*Δ*sopD2*Δ*sseJ*	This study
	Δ*sseFG*Δ*steA*Δ*pipB2*Δ*sopD2*Δ*sseJ*Δ*sifA*	SL1344Δ*sseF*Δ*sseG*Δ*steA*Δ*pipB2*Δ*sopD2*Δ*sseJ*Δ*sifA*	This study
Multi-effector deletion mutants	Δ*sseFG*Δ*sseJ*	SL1344Δ*sseF*Δ*sseG*Δ*sseJ*	This study
	Δ*sseFG*Δ*sopD2*	SL1344Δ*sseF*Δ*sseG*Δ*sopD2*	This study
	Δ*sifA*Δ*sseJ*	SL1344 *sifA*Δ*sseJ*	This study
	Δ*sifA*Δ*sopD2*	SL1344Δ*sifA*Δ*sopD2*	This study
	Δ*sifA*Δ*sseJ*Δ*steA*	SL1344Δ*sifA*Δ*sseJ*Δ*steA*	This study
	Δ*sifA*Δ*sseJ*Δ*sopD2*	SL1344Δ*sifA*Δ*sseJ*Δ*sopD2*	This study

2.3.3 Bacterial growth curves

3 mL cultures of each strain were grown for 16-20 hours in LB media at 37˚C with shaking. Cultures were diluted 1:1000 in fresh media in a volume of 200 μL in a 96-well plate. Cell density was determined by incubating the plate at 37˚C in a BioTek plate reader that shook the plate for 5 minutes before each read, every 20 minutes. Absorbance was read at 600 nm.

2.3.4 Plasmid construction

Plasmids constructed and used in the study are listed in Table 2.2; primers used are described in Table 2.3. All plasmids were constructed using the Gibson Assembly method of cloning [208]. Complementation vectors and gene deletion vectors were routinely maintained in *E. Coli* DH10B and MC1061λ*pir*, respectively.

Table 2.2 - Plasmids used in this study

Plasmid Designation	Relevant Characteristics/Genotype	Source/Reference
pRE112	*cat sacB ori*V_{RGK},*ori*T_{RP4} Cm^R	[209]
pACYC184	*ori*P15A, Tet^R, Cm^R	[210]
pRE112-Δ*sseF*Δ*sseG*	Upstream region of *sseF* and downstream region of sseG from *S.* Typhimurium SL1344 in pRE112	This study
pRE112-Δ*steA*	Upstream and downstream regions of *steA* region from *S.* Typhimurium in pRE112	This study
pRE112-Δ*pipB2*	Upstream and downstream regions of *pipB2* region from *S.* Typhimurium in pRE112	This study
pRE112-Δ*sopD2*	Upstream and downstream regions of *sopD2* region from *S.* Typhimurium in pRE112	This study
pRE112-Δ*sseJ*	Upstream and downstream regions of *sseJ* region from *S.* Typhimurium in pRE112	This study
pRE112-Δ*sifA*	Upstream and downstream regions of *sifA* region from *S.* Typhimurium in pRE112	This study
pPIPB2	*pipB2* under the control of its native promoter in pACYC184	This study

Table 2.3 - Primers used in this study.

	Forward oligonucleotide (5'-3')	**Reverse oligonucleotide (5'-3')**
sseF 5' flanking	GAACTGCATGAATTCCCGGGCTGG ACAGTTTTATCCGCCG	CGGTATATACCTGAAAACGATTACATAT TTCGTTCTGTTATTTAAGCAATAAG
sseG 3' flanking	GAAATATGTAATCGTTTTCAGGTA TATACCGG	CAAGCTTCTTCTAGAGGTACCGAAATAA CAGACGCAGCGCC
steA 5' flanking	GAACTGCATGAATTCCCGGGCCAT CGCTTTGTGATACCCC	CATATCCTACTCCTTCAAATTTTGCTC
steA 3' flanking	CAAAATTTGAAGGAGTAGGATATG TAAAAAGCGTTTATGTTTAGCC	CAAGCTTCTTCTAGAGGTACCCGGGATG AGACAGAATGACC
pipB2 5' flanking	GAACTGCATGAATTCCCGGGGCTG CATCGTCATACTACGG	CATATATTTTCTCCCAGAGACAGCAAC
pipB2 3' flanking	GTCTCTGGGAGAAAATATATGTAG CCCTTTTTGACGTAAATCTG	CCAAGCTTCTTCTAGAGGTACCCCTGGT AATATTTATCAGGCG
sopD2 5' flanking	GTGAACTGCATGAATTCCCGGGGG GGTTTATGGACACATTCC	CTTTTTACATAATAACTCCCTTGATTATT TACCG
sopD2 3' flanking	GTAAATAATCAAGGGAGTTATTAT GTAAAAAGTCATTAAAAAGGCC	CAAGCTTCTTCTAGAGGTACCGTTCTGA CCATTACTTCTAACG
sseJ 5' flanking	CAAGCTTCTTCTAGAGGTACCCCC ACTCCCCACGCTATTATG	CATAGTGTCCTCCTTACTTTATTAAACAC G
sseJ 3' flanking	CGTGTTTAATAAAGTAAGGAGGAC ACTATGTAAAGTTCCATCGGCTGC GG	ATGAATTCCCGGGAGAGCTCCCTGGCAA CGGTTAAGGTGG
sifA 5' flanking	CAAGCTTCTTCTAGAGGTACCCAC CCCGAGCGCCGTTATTATC	CGTCTGATTTTACATATTAATCTCACTTA TACTGGAG
sifA 3' flanking	GAGATTAATATGTAAAATCAGACG ACGCTTTCTCAGACG	ATGAATTCCCGGGAGAGCTCGACCGTGA CGACCACAAACG
pRE112 plasmid backbone	GGTACCTCTAGAAGAAGCTTGGGA	CCCGGGAATTCATGCAGTTCAC
pACYC184 plasmid backbone	GCGGCCGCTCGATACCCATACG	CCCGAGATGCGCCGCGTGC
pipB2 complementation	GCACGCGGCGCATCTCGGGGAGTT GCAGGAAGGCGGCAAGC	GTATGGGTATCGAGCGGCCGCAATATTT TCACTATAAAATTCGTTAAAGAGTG

The pRE112 plasmid backbone used for all gene deletion constructs was produced using the pRE112 backbone primer set to amplify linear pRE112 from the KpnI to SacI unique restriction sites (final size of 5749 bp). pRE112 plasmid backbone was subsequently digested with DpnI (NEB) to remove any remaining circular template DNA. To generate complete, unmarked deletions, the upstream homologous region of target genes up to and including the start codon, and the downstream homologous region of the target gene starting with the stop codon were amplified by PCR from the chromosomal DNA of wild type SL1344.

As *sseF* and *sseG* are part of an operon [77], plasmid pRE112-Δ*sseF*Δ*sseG* was generated by amplifying the upstream region of *sseF* and the downstream region of *sseG* using primer pairs *sseF* 5' flanking and *sseG* 3' flanking, respectively. PCR products were ligated into the pRE112 vector using Gibson Assembly. Plasmids pRE112-Δ*steA*, pRE112-Δ*pipB2*, pRE112-Δ*sopD2*, pRE112-Δ*sseJ*, and pRE112-Δ*sifA* using the respective 5' flanking and 3' flanking primers pairs shown in Table 2.3.

2.3.5 Generation of mutants by allelic exchange

Unmarked complete deletion mutants were generated as previously described [202]. Briefly, MFD*pir* strains transformed with the gene deletion plasmids were conjugated with different SL1344 based-strains. The unmarked SL1344 gene deletions were constructed by inserting the pRE112 plasmid constructs into the SL1344 chromosome. Post-conjugation single crossover mutants between pRE112 constructs and the SL1344 chromosome were selected on LB agar plates containing chloramphenicol. Sucrose counter-selection was performed as previously described [209] to select for the second crossover event, thus effectively deleting the gene of choice, leaving only the start and stop codons.

The unmarked SL1344 mutant strain Δ*sseFG* was constructed by inserting the homologous regions from the pRE112-Δ*sseF*Δ*sseG* plasmid into the wild type chromosome. The unmarked SL1344 mutant strain Δ*sseFG*Δ*steA* was constructed by inserting the homologous regions from the pRE112-Δ*steA* into the Δ*sseFG* mutant chromosome. The unmarked SL1344 mutant strain Δ*sseFG*Δ*steA*Δ*pipB2* was constructed by inserting the homologous regions from the pRE112-Δ*pipB2* into the Δ*sseFG*Δ*steA* mutant chromosome. The unmarked SL1344 mutant strain Δ*sseFG*Δ*steA*Δ*pipB2*Δ*sopD2* was constructed by inserting the homologous regions from

the pRE112-Δ*sopD2* into the Δ*sseFG*Δ*steA*Δ*pipB2* mutant chromosome. The unmarked SL1344 mutant strain Δ*sseFG*Δ*steA*Δ*pipB2*Δ*sopD2*Δ*sseJ* was constructed by inserting the homologous regions from the pRE112-Δ*sseJ* into the Δ*sseFG*Δ*steA*Δ*pipB2*Δ*sopD2* mutant chromosome. The unmarked SL1344 mutant strain Δ*sseFG*Δ*steA*Δ*pipB2*Δ*sopD2*Δ*sseJ*Δ*sifA* was constructed by inserting the homologous regions from the pRE112-Δ*sifA* into the Δ*sseFG*Δ*steA*Δ*pipB2*Δ*sopD2*Δ*sseJ* mutant chromosome. Homologous regions from plasmid pRE112-Δ*sseJ* was introduced into the chromosomes of SL1344 mutant strain Δ*sseFG* and Δ*sifA*, creating strains Δ*sseFG*Δ*sseJ* and Δ*sifA*Δ*sseJ*, respectively. Homologous regions from the plasmid pRE112-Δ*sopD2* was introduced into the chromosomes of SL1344 mutant strains Δ*sseFG* and Δ*sifA*, creating strains Δ*sseFG*Δ*sopD2* and Δ*sifA*Δ*sopD2*, respectively. The strains Δ*sifA*Δ*sseJ*Δ*steA* and Δ*sifA*Δ*sseJ*Δ*sopD2* were generated by incorporating the homologous regions of the plasmids pRE112-Δ*steA* and pRE112-Δ*sopD2*, respectively into the Δ*sifA*Δ*sseJ* mutant chromosome. Successful gene deletions were verified by PCR and DNA sequencing (Genewiz).

2.3.6 Cell lines

HeLa (ATCC® CCL-2™), RAW 264.7 (ATCC® TIB-71™), and THP-1 (ATCC® TIB-202™) cells were directly obtained from ATCC. All cell lines were routinely maintained at 37˚C in a 5% CO_2 atmosphere. HeLa and RAW 264.7 cells were cultured in Dulbecco's Modified Essential Medium (DMEM) (Hyclone) containing 10% (v/v) heat-inactivated fetal bovine serum (FBS) (Gibco), 1% (v/v) Glutamax (Gibco), and 1% (v/v) nonessential amino acids (Gibco). HeLa and RAW 264.7 cells were used until passage 15. THP-1 cells were routinely maintained at a density of 2 x 10^5 to 1 x 10^6 cells/mL in Roswell Park Memorial Institute (RPMI) 1640

Medium (Gibco) supplemented with 10% (v/v) heat inactivated FBS, and 1% (v/v) nonessential amino acids. THP-1 cells were used until passage 10.

2.3.7 HeLa cell infections

HeLa cells were seeded on 12 mm diameter glass coverslips in 24-well plates (Corning) at a density of 5 x 10^4 cells/well, 16-24 hours prior to infection. Overnight bacterial cultures were diluted 1:33 in LB without antibiotic and incubated for 3 hours at 37˚C with shaking (late log-phase cultures). 1 mL of bacterial cultures were pelleted and resuspended in Dulbecco's Phosphate-Buffered Saline (DPBS) (Hyclone), subsequently diluted in DMEM and added to the HeLa cells at a multiplicity of infection (MOI) of ≈ 100:1. The infection proceeded for 15 minutes at 37˚C in 5% CO_2. Non-internalized bacteria were removed by three washes in DPBS and cells incubated in growth media containing 100 μg/mL until 2 hours post-infection, followed by growth media containing 10 μg/mL gentamicin for the remainder of the experiment. HeLa cells were infected for a total of 8 hours.

2.3.8 RAW 264.7 cell infections

RAW 264.7 cells were seeded in 24-well plates at a density of 1 x 10^5 cells/well 16-24 hours prior to infection. Overnight bacterial cultures (stationary phase) were pelleted and resuspended in DPBS, and subsequently opsonized in DPBS containing 10% normal mouse serum for 20 min at 37˚C. Opsonized bacteria were diluted in DMEM and added to cell monolayers at a MOI of ≈ 10:1, centrifuged at 170 *g* for 5 min at room temperature and incubated for 25 min at 37˚C in 5% CO_2. Non-internalized bacteria were removed by three washes in DPBS and cells incubated in growth media containing 100 μg/mL until 2 hours post-

infection, followed by growth media containing 10 μg/mL gentamicin for the remainder of the experiment. For enumeration of intravacuolar bacteria, macrophages were lysed in lysis buffer (1% Triton X-100, 0.1% sodium-dodecyl sulphate (Sigma) in DPBS) for 10 minutes and serial dilutions plated on LB agar containing 50 μg/mL streptomycin. CFU counts were taken at 2 hours, and 24 hours post-infection.

2.3.9 THP-1 cell infections

THP-1 cells were seeded in 24-well plates at a density of 2 x 10^5 cells/well in complete RPMI media supplemented with 100 nM phorbol myristate acetate (PMA) 16-24 hours prior to infection for differentiation. Overnight bacterial cultures (stationary phase) were pelleted and resuspended in DPBS, and subsequently diluted in RPMI and added to the THP-1 cells at a MOI of ≈ 50:1. Plates were centrifuged at 170 *g* for 5 min at room temperature and incubated for 25 min at 37˚C in 5% CO_2. Non-internalized bacteria were removed by three washes in DPBS and cells incubated in RPMI containing 100 μg/mL until 2 hours post-infection, followed by RPMI containing 10 μg/mL gentamicin for the remainder of the experiment. CFU counts were taken at 2 hours, and 24 hours post-infection.

2.3.10 Antibodies

The goat polyclonal anti-*Salmonella* antibody CSA-1 (Kirkegaard and Perry Laboratories) was used at a dilution of 1:300; the mouse anti-LAMP1 antibody H4A3c developed by J.T. August and J. E. K. Hildreth, obtained from the Developmental Studies Hybridoma Bank developed under the auspices of the NICHD and maintained by the University of Iowa (Department of Biological Sciences, Iowa, USA) was used at a dilution of 1:100. The

mouse monoclonal anti-Golgin 97 antibody CDF4 (Molecular Probes) was used at a dilution of 1:100. Secondary antibodies were obtained from Thermo Fisher Scientific and used at a dilution of 1:500: Alexa 488-conjugated donkey anti-mouse, and Alexa 568-conjugated donkey anti-goat.

2.3.11 Immunofluorescence microscopy

Cell monolayers seeded on glass coverslips were fixed with 4% (vol/vol) paraformaldehyde in DPBS at room temperature for 10 minutes and washed three times in DPBS. Excess paraformaldehyde was quenched in 50 mM ammonium chloride for 10 minutes at room temperature followed by two washes in DPBS.

For LAMP1^{+}-tubules: Cells on coverslips were permeabilized in ice-cold acetone for 5 minutes at -20˚C and then blocked in 1% bovine serum albumin (BSA, wt/vol) (Sigma) in DPBS for 30 minutes at room temperature. Cells on coverslips were then incubated with primary antibodies diluted in 1% BSA in DPBS at room temperature for 1 hour followed by three washes in DPBS. Secondary antibodies diluted in 1% BSA in DPBS were added to the coverslips and incubated at room temperature for 1 hour and then washed once with DPBS. Cells were then incubated for 10 minutes at room temperature with DAPI (Invitrogen) in DPBS, followed by two DPBS washes. Cells were then washed in deionized water prior to mounting with ProLong Gold Antifade Mountant (Life Technologies) on glass slides. Microscopy was performed using Zeiss Axio Imager M2 (100x objective) and processed using Zeiss Zen Pro and ImageJ (NIH) software.

For Golgi-staining: Cells on coverslips were simultaneously permeabilized and blocked in 10% normal goat serum (NGS) (Invitrogen) and 0.1% Triton X-100 in DPBS for 30 minutes at room temperature. Cells on coverslips were then incubated with primary antibodies diluted in

10% NGS and 0.1% Triton X-100 in DPBS and incubated at room temperature for 1 hour followed by three washes in DPBS. Secondary antibodies diluted in 10% NGS and 0.1% Triton X-100 in DPBS were then added to the coverslips and incubated at room temperature for 1 hour followed by three washes in DPBS. Coverslips were mounted on glass slides using ProLong® Gold Antifade Mountant with DAPI (Life Technologies) and incubated at room temperature for 24 h prior to sealing. Microscopy was performed using Olympus IX81 microscope (100x objective) and SlideBook 4.1.0 software. Distances were quantified using ImageJ software (NIH).

2.3.12 Scoring of phenotypes by microscopy

To quantify the number of infected cells with LAMP1$^+$-tubules, we surveyed cells infected with *Salmonella* and immunolabelled for *Salmonella* and LAMP1. Uninfected cells were discarded from consideration. Infected cells were then scored for presence or absence of LAMP1$^+$-tubules radiating outwards from a labelled *Salmonella.* The number of tubules/*Salmonella* was not considered as we were only concerned with the presence or absence of LAMP1$^+$-tubules per each infected cell. At least 100 infected cells were scored blind in each experiment, and each experiment was repeated at least three times.

To quantify the distance from the Golgi, we surveyed cells infected with *Salmonella* and immunolabelled for *Salmonella* and Golgin-97. Distance from the Golgi was enumerated by measuring the distance from the center of individual *Salmonella* cells to the center of the Golgi (μM). At least 200 *Salmonella*-to-Golgi distances were measured blind in each experiment, and all experiments were repeated at least three times.

2.3.13 Murine gastroenteritis model

Specific pathogen free C57BL/6 female 6-week-old mice were obtained from The Jackson Laboratory (Bar harbor, Maine, USA) and housed in the animal facility at the University of British Columbia. Mice were pre-treated with 450 mg/L of streptomycin in drinking water as previously described [211]. Mice were orally gavaged with 2.8 x 10^7 CFU/mouse from overnight cultures of wild type and mutant SL1344 strains suspended in 0.1 mL DPBS. Mice were euthanized three days post-infection by anesthesia with isoflurane followed by CO_2 asphyxiation and tissues were aseptically harvested for further evaluation. Ceca, colons, ilea and spleens were collected in 1 mL of sterile DPBS and homogenized by a FastPrep Homogenizer (MP Biochemicals). CFU from each organ was enumerated by serial dilutions on LB agar plates containing 100 μg/mL of streptomycin.

2.3.14 ELISAs

Cecum and spleen homogenates were centrifuged twice for 10 minutes at 13,000 *g*, and the supernatants were collected, diluted 1:2 in DPBS, and stored at -20˚C. Levels of interferon-γ (IFN-γ) were determined by enzyme-linked immunosorbent assays (ELISAs) using BD OptEIA Mouse IFN-γ ELISA set (BD Biosciences) according for the manufacturer's instructions. IFN-γ levels were normalized to the weight of the organs.

2.3.15 Statistical analysis

Statistical analysis was performed using Prism 8 (GraphPad). *In vitro* infections, *S.* Typhimurium colonization in mice, and cytokine levels were analyzed. All data was found to not

adhere to a Gaussian distribution using the following normality tests: Shapiro-Wilk test, and the Kolmogorov-Smirnov normality test with Dallal-Wilkinson-Lilliefor P value test. Data sets were analyzed using Kruskal-Wallis one-way analysis of variance (ANOVA) with Dunn's multiple comparison post-test.

2.4 Results

2.4.1 Construction of multiple-effector deletion mutants

Through an extensive literature search we identified seven effectors of interest implicated in SIF biogenesis, SCV membrane maintenance, and intracellular SCV localization. These effectors include SseF, SseG, SteA, PipB2, SopD2, SseJ, and SifA (summarized in [80]) . In order to address the redundancy and coordination of these effectors, we constructed a series of effector-deletion mutants (see Table 2.1) in the wild type *S.* Typhimurium SL1344 genetic background. We generated multiple-effector deletion mutants of the seven effectors of interest in a stepwise manner, using a suicide vector-based approach and homologous recombination [209], to generate a strain lacking all seven effectors, as well as specific combinations of effectors (see Table 2.1). The Δ*sseFG* strain does not express the two T3SS2-secreted effectors SseF and SseG encoded y the genes *sseF* and *sseG*, respectively, which are a part of the *sseABCDEFG* operon [77]. Within epithelial cells the replication, SCV localization, and appearance and frequency of SIFs in the Δ*sseF* single-effector deletion mutant very closely resembles both the Δ*sseG* single-effector deletion mutant and the Δ*sseFG* double deletion mutant, likely owing to the functional link between the two effectors [112,172]. We therefore consider the double-deletion mutant Δ*sseFG* effectively as a single-effector deletion mutant.

Deleting one, or multiple coding regions for T3SS2-secreted effectors does not significantly impair the fitness of the effector deletion strains in LB broth (Figure 2.1).

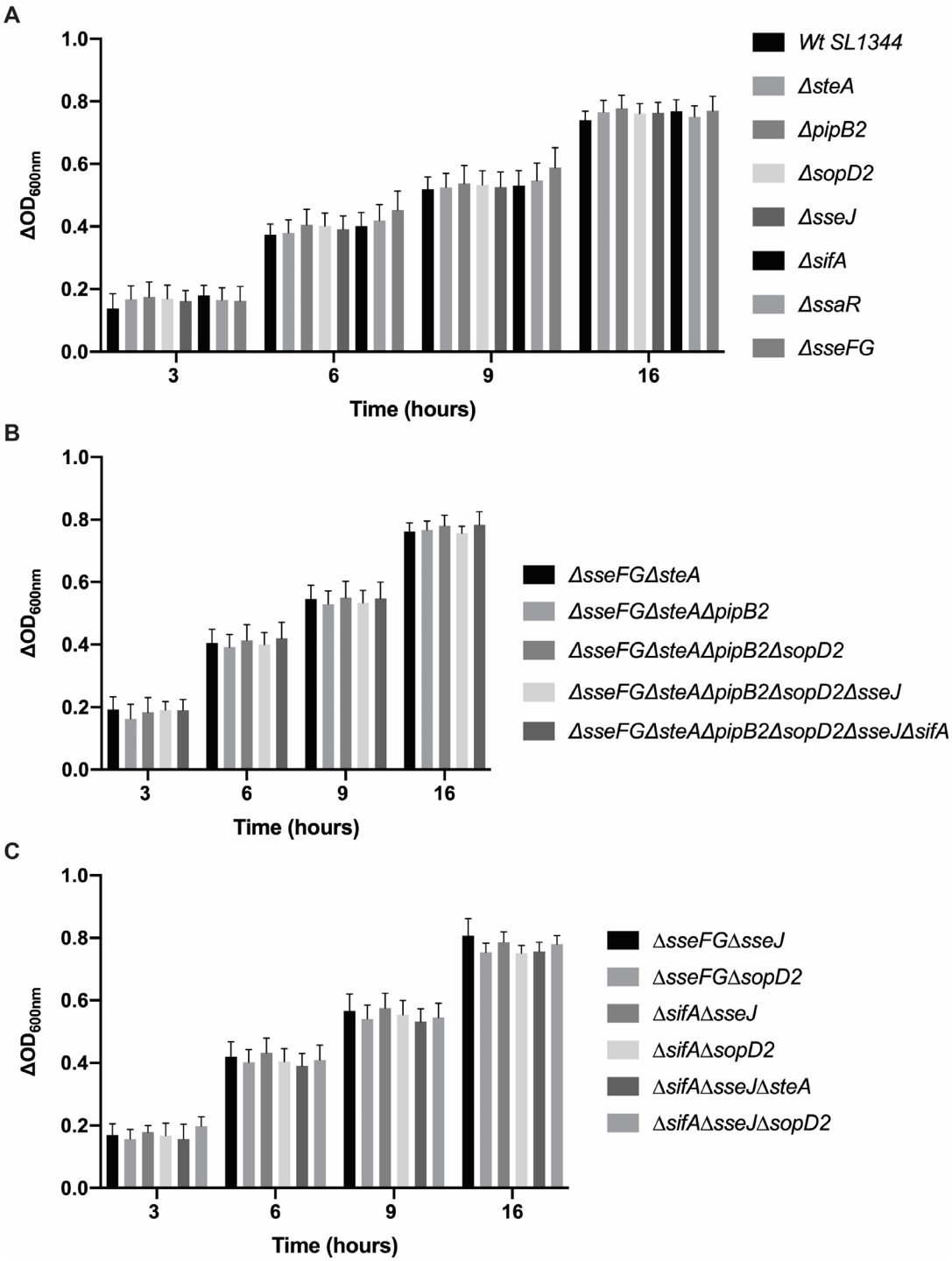

Figure 2.1 - Single- and multiple-effector deletion mutants do not have impaired growth in LB liquid culture. Change in OD_{600} (ΔOD_{600}) was calculated by subtracting the OD_{600} at Time=0 from the OD_{600} at each selected time point. Average ΔOD_{600} ± standard error of the mean is shown. **(A)** Growth of single-effector deletion mutants in LB. **(B)** Growth of sequential-effector deletion mutants in LB. **(C)** Growth of multiple-effector deletion mutants in LB.

2.4.2 Formation of LAMP1-positive tubules is dependent on multiple effectors

We analyzed the contribution of each of the effectors of interest to the formation of LAMP1-positive (LAMP1$^+$) tubules that radiate outwards from the SCV. SIFs, the first of the *Salmonella*-induced tubules to be described [129,154,212], are identified by the presence of the host membrane protein LAMP1 within their membranes [157,159]. HeLa human epithelial cells were infected with the various effector deletion mutants and evaluated for the frequency of SIF formation in infected cells. Infected HeLa cells were fixed at 8 hours post-infection and immunolabeled with an anti-LAMP1 antibody to label LAMP1-positive compartments (SCVs) and tubules (SIFs) and an anti-*Salmonella* antibody to label intracellular *S.* Typhimurium. Labeled cells were analyzed by indirect immunofluorescence microscopy. SIFs are, by definition, LAMP1$^+$-tubules comprised of an inner and outer membrane extending outwards from the SCV [129]. As we are unable to evaluate whether the SIFs observed have one or two membranes using this methodology, we will hereafter refer to them as LAMP1$^+$-tubules.

Cells infected with the wild type strain and single-deletion mutants (Figure 2.2) exhibit LAMP1$^+$-tubule formation consistent in both morphology and frequency to previous reports [72,129,154,160,172,179,180]. We observed "bulky" LAMP1$^+$-tubules extending outwards from the SCV of Δ*pipB2* infected cells, consistent with previous reports [180] (Figure 2.2A). All single-effector deletion mutant strains, except for Δ*sseJ*, had significantly fewer LAMP1$^+$-tubule-positive infected cells relative to wild type, while the Δ*sifA* and Δ*ssaR* strains failed to form LAMP1$^+$-tubules (Figure 2.2B).

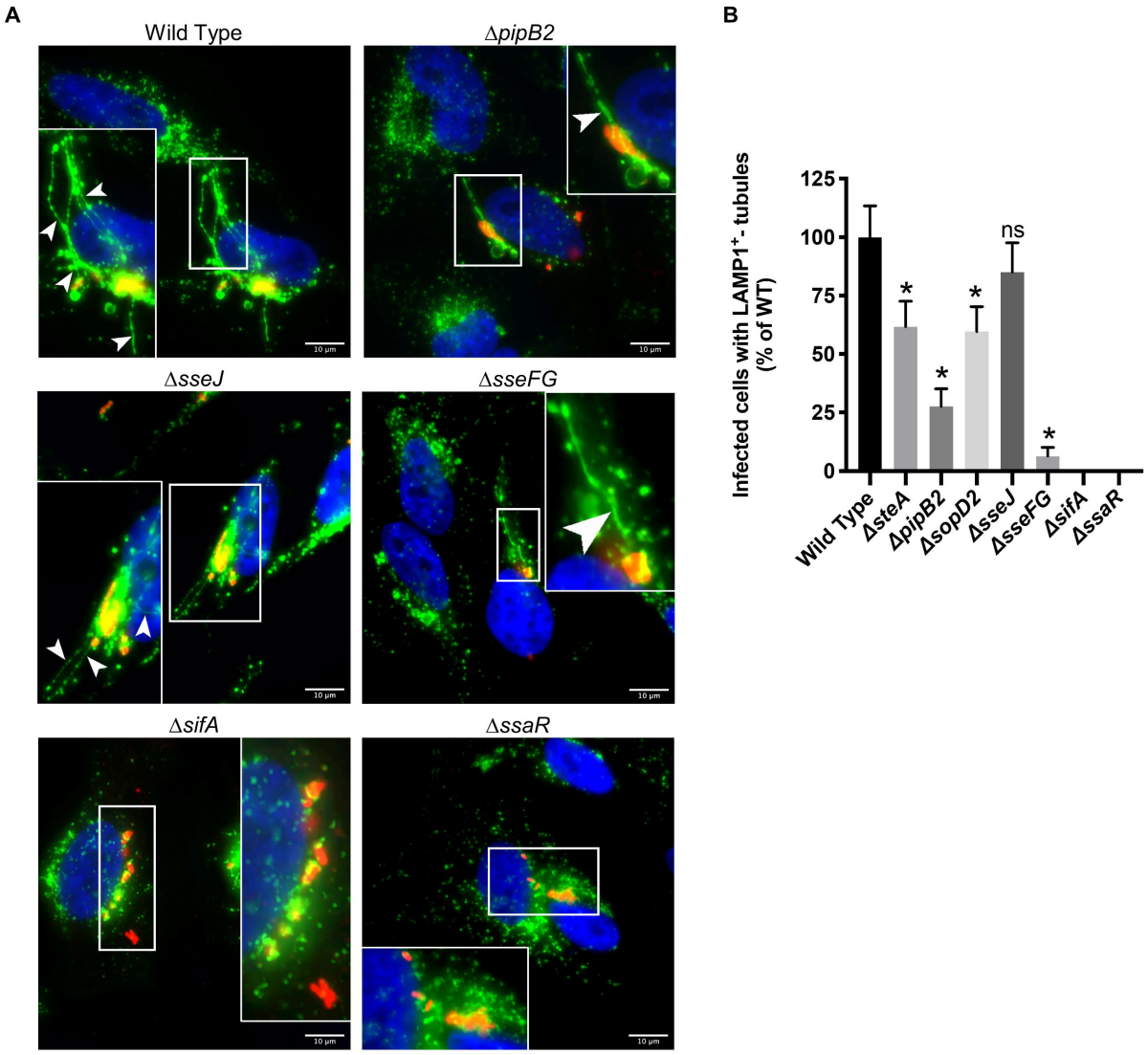

Figure 2.2 - LAMP1$^+$-tubule extension from single deletion mutants. (A) Comparison of frequency of LAMP1$^+$-tubule formation of wild type (WT) and isogenic single-effector deletion mutants in HeLa cells after 8 hours of infection. Cells were immunostained for *Salmonella* (red) and LAMP1 (green), and the nucleus was stained with DAPI (blue). Representative images of select strains are shown. The white boxes indicate zoomed-in region in inset. Arrowheads indicate LAMP1$^+$-tubules. Scale Bar = 10 μm. **(B)** Quantification of LAMP1$^+$-tubule frequency in HeLa cells infected with the single deletion mutants for 8 hours. The average frequency of infected cells with LAMP1$^+$-tubules relative to wild type infected cells ± standard error of the mean for three separate experiments is shown (n=3). At least 100 infected cells per strain were blindly analyzed in each experiment. An asterisk indicates a significant difference between the indicated mutant strain LAMP1$^+$-tubule frequency and the corresponding WT LAMP1$^+$-tubule frequency ($p < 0.02$) as determined by Kruskal-Wallis one-way ANOVA with Dunn's multiple comparison post-test. ns = not significant.

Cells infected with the multiple-effector deletion mutant strains (Table 2.1) exhibit a dramatic decrease in the frequency of LAMP1$^+$-tubule formation relative to both the wild type strain (Figure 2.3B) and the corresponding single-effector deletion mutants (Figure 2.2B). The sequential-effector deletion mutants (Figure 2.3B, strains ii-vi) —a subset of the multiple-effector deletion mutants—were found to have LAMP1$^+$-tubules extending outwards from intracellular *Salmonella* in 2-8% of infected cells relative to wild type infected cells (Figure 2.3, strain i). The frequency of LAMP1$^+$-tubule-positive infected cells was not statistically different between the sequential-effector deletion mutants. Sequential deletion of effectors does not dramatically reduce LAMP1$^+$-tubule frequency (*i.e.,* Δ*sseFG*Δ*steA* vs. Δ*sseFG*Δ*steA*Δ*pipB2* vs. Δ*sseFG*Δ*steA*Δ*pipB2*Δ*sopD2*). The sequential-effector deletion mutants Δ*sseFG*Δ*steA*, Δ*sseFG*Δ*steA*Δ*pipB2,* Δ*sseFG*Δ*steA*Δ*pipB2*Δ*sopD2,* and Δ*sseFG*Δ*steA*Δ*pipB2*Δ*sopD2*Δ*sseJ* (Figure 2.3, strains ii-v) all induce formation LAMP1$^+$-tubules and only the sequential-effector deletion mutant with all seven effectors deleted (Δ*sseFG*Δ*steA*Δ*pipB2*Δ*sopD2*Δ*sseJ*Δ*sifA,* strain vi) fails to induce LAMP1$^+$-tubules. This is consistent with previous evidence suggesting that SifA plays a major role in inducing LAMP1$^+$-tubules [71] as all the sequential-effector deletion mutants are able to induce LAMP1$^+$-tubule formation except for the strain with the *sifA* deletion.

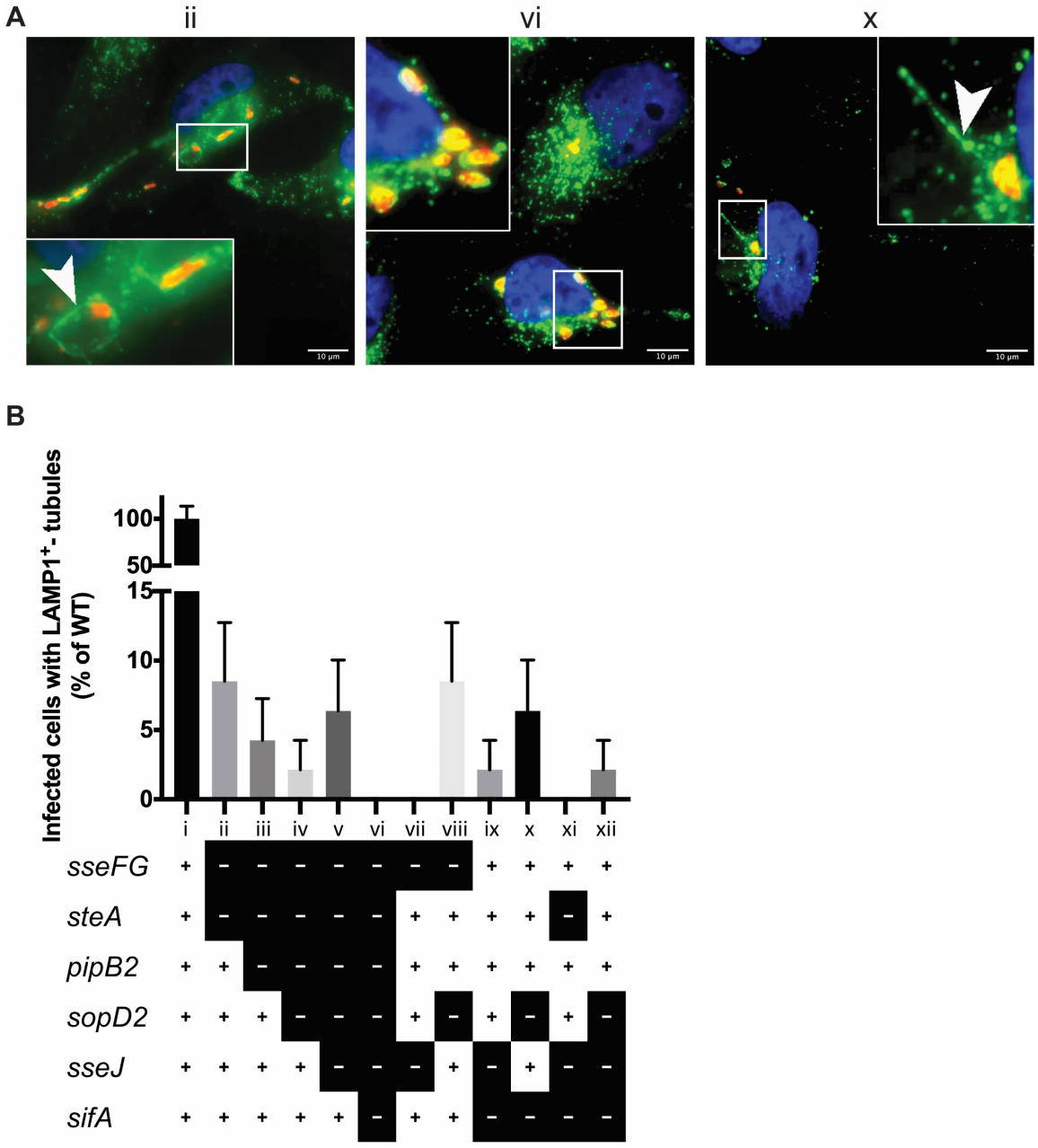

Figure 2.3 - LAMP1$^+$-tubule extension from the SCV results from the actions of several effectors. (A) Comparison of frequency of LAMP1$^+$-tubule formation of wild type and isogenic multiple-effector deletion mutants in HeLa cells after 8 hours of infection. Cells were fixed at 8 hours post-infection, immunostained, and analyzed as described in the legend of Fig 2.2. Representative images of select strains are shown. Strain designation (ii, vi, and x) corresponds to strains described in the legend of (B). **(B)** Quantification of LAMP1$^+$-tubule frequency in HeLa cells infected with the multiple-effector deletion mutants for 8 hours. LAMP1$^+$-tubule frequency was quantified and analyzed as described in the legend of Fig 2.2. The average frequency of infected cells with LAMP1$^+$-tubules relative to wild type infected cells ± standard error of the mean for three separate experiments is shown (n=3). At least 100 infected cells per strain were blindly analyzed in each experiment. Strain legend: "+" = gene present, "-" = gene deleted. A "+" for all genes indicates wild type (strain i). Results analyzed by a Kruskal-Wallis test with Dunn's correction for multiple comparisons. All LAMP1$^+$-tubule frequencies in the multiple-deletion mutant strains were significantly different from wild type, however there was no significance between the multiple-deletion mutants themselves.

Infection of HeLa cells with the remainder of the multiple-effector deletion mutants with different combinations of deleted effectors reveals that the mechanism of LAMP1$^+$-tubule extension is indeed very intricate. The strain Δ*sseFG*Δ*sseJ* (Figure 2.3, strain vii) is unable to form LAMP1$^+$-tubules even though this strain has SifA. This contrasts with the above results from the sequential-effector deletion mutants suggesting that mutant strains can form LAMP1$^+$-tubules so long as *sifA* was not deleted. Unlike Δ*sseFG*Δ*sseJ,* the strain Δ*sseFG*Δ*sopD2* (Figure 2.3, strain viii) was able to form LAMP1$^+$-tubules. This may suggest an interaction or coordinated roles between SseJ and SseF/G that facilitates LAMP1$^+$-tubule extension. For example, SseF/G may require the activity of SseJ in order to induce LAMP1$^+$-tubulation which could explain the presence of LAMP1$^+$-tubules in Δ*sseFG*Δ*sopD2* infected cells but not Δ*sseFG*Δ*sseJ* infected cells. Further studies are required to delve deeper into the reasons behind the formation of LAMP1$^+$-tubules in some multiple-effector deletion strains and not in others.

The ability to form SIFs (LAMP1$^+$-tubules) has long been thought to be heavily dependent on SifA as ectopic expression of *sifA* in HeLa cells induces LAMP1$^+$-tubule formation [69,71]. We observed LAMP1$^+$-tubules radiating outwards from the SCV in cells infected with both Δ*sifA*Δ*sseJ* and Δ*sifA*Δ*sopD2* double deletion mutants (Figure 2.3, strains ix and x, respectively), albeit at a very low frequency. Both strains lack the gene encoding *sifA*, yet they retain the ability to form LAMP1$^+$-tubules. Intriguingly, we did not observe any LAMP1$^+$ tubules in the Δ*sifA*Δ*sseJ*Δ*sopD2* triple-effector deletion mutant (Figure 2.3, strain xi). This may indicate a required sequential or coordinated actions of SifA, SopD2, and SseJ, in order to extend LAMP1$^+$-tubules.

2.4.3 Intracellular localization of *S.* Typhimurium is modulated by multiple effectors

Intracellular *S.* Typhimurium typically forms microcolonies near the microtubule-organizing center and Golgi-complex several hours post-infection in infected epithelial cells [110–112,213]. The T3SS2-secreted effectors SseF, SseG, SifA, PipB2, and SteA have been individually implicated in SCV localization during infection [110–112,174,186,213,214]. We used our library of multiple-effector deletion mutants to examine the effect of multiple effector deletions on intracellular localization. We quantified the distribution of *S.* Typhimurium relative to the Golgi complex by measuring the distance between intracellular *S.* Typhimurium and the Golgi complex 8 hours after infection in HeLa cells immunostained for *S.* Typhimurium and Golgin-97 (Figure 2.4).

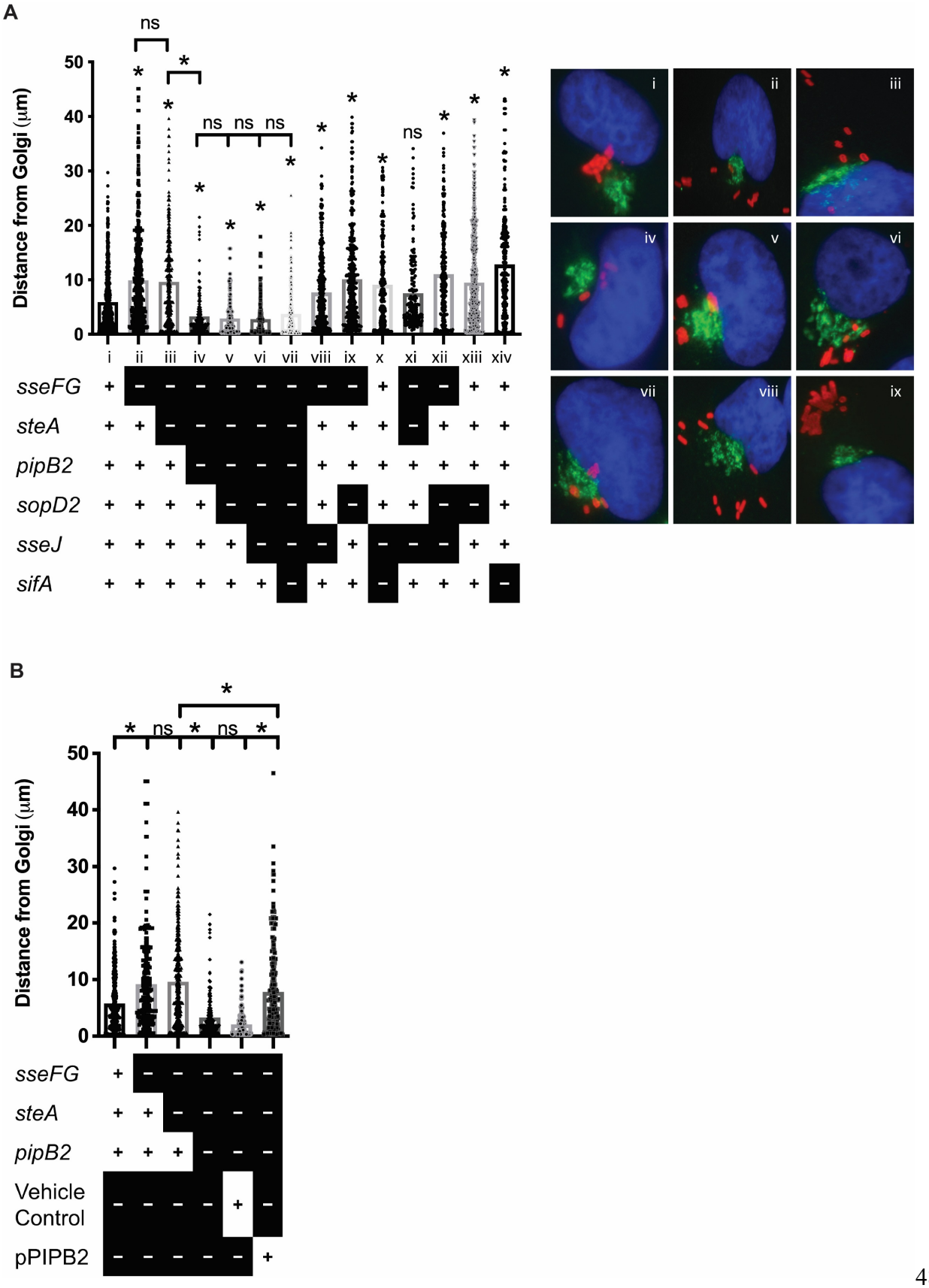
A
Distance from Golgi (μm)
ns
ns ns ns
ns
i ii iii iv v vi vii viii ix x xi xii xiii xiv
sseFG
steA
pipB2
sopD2
sseJ
sifA
i
ii
iii
iv
v
vi
vii
viii
ix
B
Distance from Golgi (μm)
* ns * ns *
sseFG
steA
pipB2
Vehicle Control
pPIPB2

Figure 2.4 - Multiple effectors drive SCV movement away from the Golgi complex. HeLa cells were infected with the indicated *S.* Typhimurium strains for 8 hours, fixed, and immunostained for *Salmonella* (red) and Golgin-97 (green), and the nucleus was stained with DAPI (blue). An asterisk indicates a significant difference ($p < 0.003$) between the indicated mutant strain and the WT strain or other strain if indicated by ⌐¬ as determined by a Kruskal-Wallis one-way ANOVA with Dunn's multiple comparison post-test. ns = not significant. **(A)** Quantification of *S.* Typhimurium position relative to the Golgi. The distance from the center of individual bacteria to the nearest edge of the Golgi complex was measured in infected cells. Strain legend: "+" = gene present, "-" = gene deleted. All data points are shown to accurately indicate the spread of the data with averages shown for three separate experiments (*n* = 3). **(B)** Select representative images used to enumerate distances in (A). **(C)** SL1344 strain *ΔsseFGΔsteAΔpipB2* was complemented with a low-copy plasmid expressing *pipB2*. HeLa cells were infected, fixed, stained, and analyzed as described in (A).

Consistent with previous reports, the deletion of Δ*sseFG* alters SCV localization such that Δ*sseFG* mutants are scattered throughout the host cell cytoplasm, rather than remaining in close proximity to the Golgi apparatus like wild type *S.* Typhimurium (Figure 2.4A, strains ii and i, respectively) [109–113,201,214]. The additional deletion of *steA* (resulting in the Δ*sseFG*Δ*steA* triple-effector deletion mutant, strain iii in Figure 2.4A) does not significantly alter *S.* Typhimurium positioning relative to the Golgi as compared to the Δ*sseFG* double deletion mutant, which is consistent with the findings of Domingues *et al.*, (2014). Further deletion of PipB2 (resulting in the Δ*sseFG*Δ*steA*Δ*pipB2* quadruple-effector deletion mutant, strain iv in Figure 2.4) results in a strain that remains closer to the Golgi than wild type *S.* Typhimurium. Δ*pipB2* and Δ*steA* single-effector deletion mutants have previously been shown to be positioned close to the nucleus at 8-14 hours-post infection while a Δ*sseF*Δ*pipB2* double deletion mutant is found scattered throughout the cytosol [174,200]. Our results indicate potential interplay between SteA and PipB2 to promote movement away from the Golgi as both effectors must be deleted in the Δ*sseFG* background to maintain close apposition to the Golgi. Subsequent sequential deletions of *sopD2*, *sseJ*, and *sifA* (Figure 2.4A, strains v, vi, and vii, respectively), do not impact intracellular localization of these *S.* Typhimurium mutant strains as they all reside very close to the Golgi. This is unexpected as the single-effector deletion mutants Δ*sseFG*, Δ*sopD2*, and Δ*sifA* all have a scattered distribution SCVs throughout the host cell (Figure 2.4A,

strains ii, xiii, and xiv, respectively). In fact, strains Δ*sseFG*Δ*steA*Δ*pipB2*Δ*sopD2*, Δ*sseFG*Δ*steA*Δ*pipB2*Δ*sopD2*Δ*sseJ*, Δ*sseFG*Δ*steA*Δ*pipB2*Δ*sopD2*Δ*sseJ*Δ*sifA* are positioned closer to the Golgi than even wild type *S.* Typhimurium. The PipB2-dependent SCV scattering was complemented when a plasmid expressing PipB2 was introduced in the Δ*sseFG*Δ*steA*Δ*pipB2* mutant strain (Figure 2.4B). All the remainder of the multiple-effector deletion strains in Figure 2.4, apart from Δ*sseFG*Δ*steA*Δ*sseJ,* have altered SCV positioning relative to wild type. Our results indicate that these effectors are involved in keeping intracellular *S.* Typhimurium close to the Golgi and that it seems likely that there is interplay between PipB2 and SteA which plays a critical role in SCV localization during infection.

2.4.4 Multiple-effector deletion mutants of *S.* Typhimurium do not replicate in macrophages

The effectors SseJ, SopD2, SifA, PipB2, and SteA modulate SCV membrane dynamics to promote intracellular replication [80]. In macrophages, *S.* Typhimurium that escape the SCV and enter the host cell cytoplasm are eliminated by host defenses [215]. Therefore, maintaining the SCV membrane is critical to replication in macrophages. Previous studies have demonstrated that multiple T3SS2-secreted effectors, including the seven effectors in this study, contribute to replication within mouse macrophages [202,216]; specifically, the single-effector deletion mutants *sifA*, *sseJ*, *sopD2*, and *sseFG* exhibit decreased replication relative to wild type *S.* Typhimurium [216]. Given that several effectors are implicated in promoting replication in macrophages, we wanted to evaluate if our effectors of interest act independently, sequentially, or cooperatively to promote intramacrophage replication.

RAW 264.7 mouse macrophages were infected with our library of deletion mutants and CFUs enumerated at 2 hours and 24 hours post-infection. Most single-effector deletion mutants

replicated in RAW 264.7 cells as indicated by a fold change greater than 1, while the T3SS2-secretion negative control Δ*ssaR* mutant and the Δ*sifA* mutant did not replicate which is consistent with previous reports (Figure 2.5A) [69,176]. Conversely, the sequential deletion mutants (strains ix-xiii in Figure 2.5A) were unable to replicate as were the multiple-effector deletion mutants shown in Figure 2.5B.

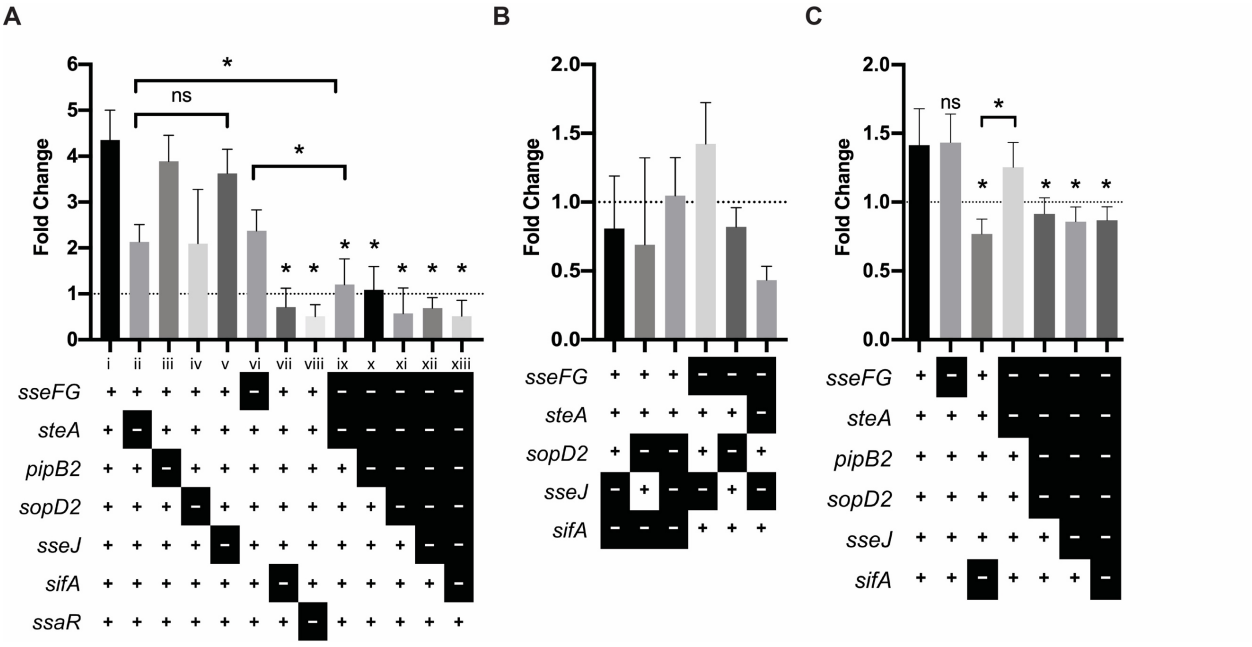

Figure 2.5 - Multiple effectors are required for replication in macrophages. Strain legend: "+" = gene present, "-" = gene deleted. A "+" for all genes indicates wild type. An asterisk indicates a significant difference ($p < 0.03$) between the indicated mutant strain and WT or other strain if indicated by ⌐ as determined by a Kruskal-Wallis one-way ANOVA with Dunn's multiple comparison post-test. ns = not significant. The average fold change ± standard deviation for three experiments is shown (n=3). **(A)** Replication of *S.* Typhimurium single- and sequential-deletion mutants in RAW 264.7 macrophages. RAW 264.7 cells were infected with the indicated strains at a MOI of 10. Fold change was determined by dividing CFU counts at 24 hours post-infection by CFU counts at 2 hours post-infection. **(B)** Replication of *S.* Typhimurium multiple-effector deletion mutants in RAW 264.7 macrophages. Experiment was performed and analyzed as described in (A). **(C)** Replication of *S.* Typhimurium strains in THP-1 monocytes. THP-1 monocytes were infected with select *S.* Typhimurium strains and results analyzed as described in (A). Representative results from one experiment is shown.

We anticipated that sequential and successive deletion of effectors would have a cumulatively negative impact on intramacrophage replication. As such, we expected a strain with

three effectors deleted would experience decreased replication as compared to a strain with only two effectors deleted. However, while deletion of a single effector is permissive of intramacrophage replication, deletion of two or more effectors results in an inability to replicate within the macrophage. For example, the double-effector deletion strain Δ*sseFG* (considered a single-deletion mutant, Figure 2.5A strain vi) and the single-effector deletion strain Δ*steA* (Figure 2.5A, strain ii) are able to replicate within RAW 264.7 cells (fold change > 1), however the triple-effector deletion mutant Δ*sseFG*Δ*steA* (Figure 2.5A, strain ix) is unable to replicate (fold change < 1). We found a similar effect with select multiple-effector deletion mutants in human THP1 monocytes (Figure 2.5C). The inability of the sequential- and multiple-effector deletion mutants to replicate within macrophages was not driven by the specific effectors deleted, but rather by the number of effectors deleted. Simply put, intramacrophage replication does not occur when two or more of the effectors examined in this study are deleted. We can therefore conclude that intramacrophage replication is driven by the actions of multiple effectors.

2.4.5 Multiple effector deletion mutants of *S.* Typhimurium have impaired virulence in a mouse model of infection

We have demonstrated that these seven effectors (SseF, SseG, SteA, PipB2, SopD2, SseJ, and SifA) are all required to establish an intracellular replicative niche within both epithelial cells and macrophages. While these models provide insight into the cellular events within host cells, they do not provide any information regarding virulence. We therefore investigated the contribution of these seven effectors to virulence in an *in vivo* infection model. We chose to use a low-dose streptomycin pre-treatment murine model of gastroenteritis as it more closely models *S.* Typhimurium infections in humans and produces consistent results in our hands. In this

model, pre-treatment of C57BL/6 mice with low-dose of streptomycin induces susceptibility to gastroenteritis upon infection with wild type *S.* Typhimurium [211].

Streptomycin-treated mice were infected with either wild type SL1344, Δ*sseFG*Δ*steA*Δ*pipB2*Δ*sopD2*, or Δ*sseFG*Δ*steA*Δ*pipB2*Δ*sopD2*Δ*sseJ*Δ*sifA* multiple-effector deletion strains. These two multiple-effector deletion strains were selected as they both exhibit reduced frequency of LAMP1^{+}-tubulation and an inability to replicate in macrophages. *S.* Typhimurium colonization in intestinal and systemic sites were determined at three days post-infection by CFU counts from the spleen, cecum, ileum, and colon. Both multiple-effector deletion strains colonized the spleen, cecum, and colon significantly less than the wild type strain (Figure 2.6A). Both multiple-effector deletion strains also colonized the ileum to a lesser extent than the wild type strain, though the Δ*sseFG*Δ*steA*Δ*pipB2*Δ*sopD2*Δ*sseJ*Δ*sifA* was not statistically significantly different from wild type (Figure 2.6A). There was no significant difference in colonization at the four sites between Δ*sseFG*Δ*steA*Δ*pipB2*Δ*sopD2* and Δ*sseFG*Δ*steA*Δ*pipB2*Δ*sopD2*Δ*sseJ*Δ*sifA*. This suggests that successful colonization, at both intestinal and systemic sites, requires the action of multiple effectors.

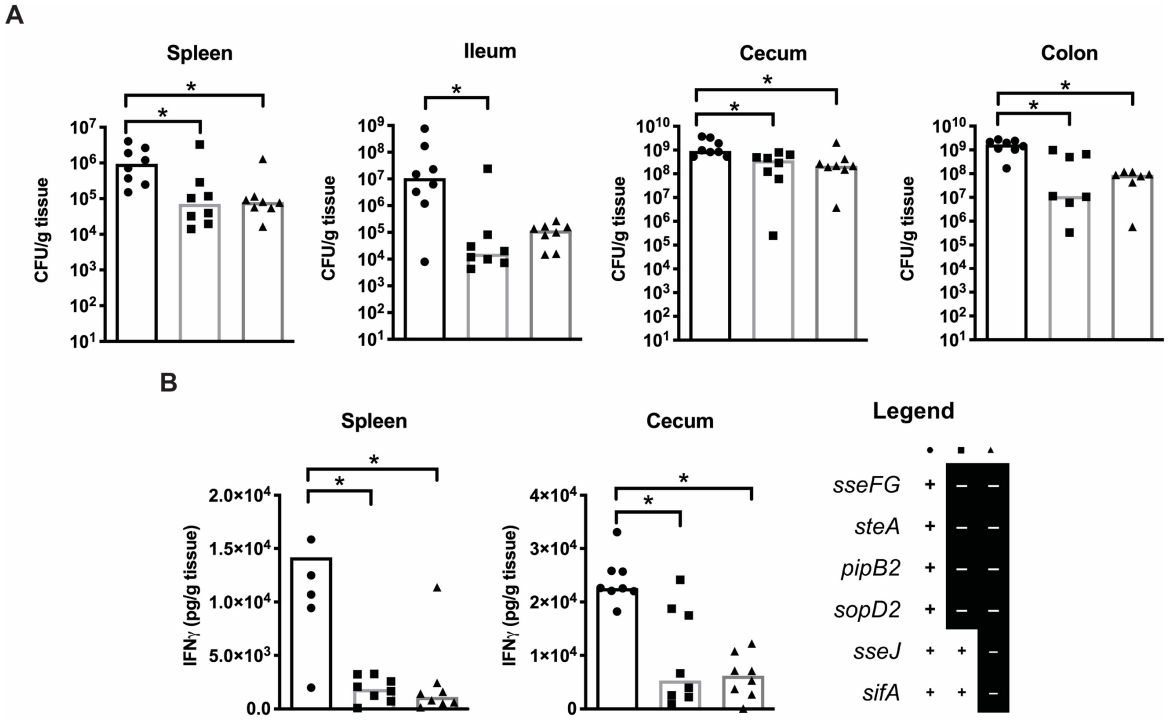

Figure 2.6 - Gastroenteritis model of *S.* Typhimurium infection. Mice were treated with streptomycin for two days prior to oral infection with select *S.* Typhimurium strains to induce gastroenteritis as per Sekirov et al., 2008. Strain legend found on bottom right of figure: "+" = gene present, "-" = gene deleted. A "+" for all genes indicates wild type. A single asterisk indicates a significant difference between the indicated strains ($p < 0.03$) as determined by a Kruskal-Wallis one-way ANOVA with Dunn's multiple comparison post-test. **(A)** Bacterial counts were recovered from systemic and intestinal organs of mice three days post-infection. Counts given represent colony forming units per gram of tissue. The median CFU/g for three separate experiments is shown with individual data points visible to accurately represent the spread of the data. **(B)** IFNγ-levels as determined by ELISA. The median amount of IFNγ (pg of IFNγ/g of tissue) is shown with individual data points visible to accurately represent the spread of the data.

One of the hallmarks of non-typhoidal salmonellosis infection is acute intestinal inflammation [217]. Therefore, elevated levels of gastrointestinal inflammation—reflected by the levels of IFNγ—indicate *S.* Typhimurium infection within the intestinal epithelium. We found significantly decreased IFNγ in the spleen and cecum of mice infected with the multiple-effector deletion strains Δ*sseFG*Δ*steA*Δ*pipB2*Δ*sopD2* and Δ*sseFG*Δ*steA*Δ*pipB2*Δ*sopD2*Δ*sseJ*Δ*sifA* as compared to mice infected with wild type strain (Figure 2.6B). The additional deletion of *sifA* and *sseJ* to the Δ*sseFG*Δ*steA*Δ*pipB2*Δ*sopD2* strain does not further decrease colonization or

inflammation, mirroring our results in the macrophage infection models (both RAW 264.7 and THP-1 cells). This suggests that the multiple-effector deletion strains did not elicit as strong of an inflammatory response as the wild type strain. The combination of decreased colonization and decreased inflammation induced by the multiple-effector deletion strains suggests that multiple effectors are required for both colonization and virulence of *Salmonella* within a gastroenteritis model of infection.

2.5 Discussion

The importance of T3SS2-secreted effectors during infection is widely recognized, but the precise biochemical activity and function of many of these effectors is poorly understood. Previous attempts to identify the functions and targets of T3SS2-secreted effectors often involve studying effectors separately [113,114,177,218]; however increasing evidence suggests that the effectors have overlapping yet distinct roles during infections. As infections involve dynamic and complex processes, the effect of one effector may require prior action by another effector, or their activities may be linked. It is therefore necessary to study effector activities in the presence or absence of other related effectors to discover the precise function of each effector.

SIF biogenesis is a complex and dynamic process involving the action of several effectors as shown by multiple studies [129,156,160]. Here, we demonstrate the complexity of LAMP1$^+$-tubule extension (*i.e.,* SIF biogenesis) by infecting HeLa cells with a library of single-effector and multiple-effector deletion strains. Most single-effector deletion mutant strains can form LAMP1$^+$-tubules at a frequency of at least 25% relative to wild type, whereas all 11 multiple-effector deletion strains fail to induce LAMP1$^+$-tubules at a frequency greater than 10% relative to wild type. The fact that single-effector deletion mutants form more LAMP1$^+$-tubules

as compared to the multiple-effector deletion mutants implies that more than one effector is required to extend LAMP1$^+$-tubules and that at least two or more of the effectors are working in conjunction with one another. Furthermore, the sequential deletion of effectors does not decrease the frequency of LAMP1$^+$-tubule formation in a step wise manner indicating unequal contribution by each effector to this process. The severe and non-cumulative defects in LAMP1$^+$-tubule formation observed in the multiple-effector deletion mutants strongly suggests that extensive LAMP1$^+$-tubule extension requires multiple effectors mediating the process.

Previous studies show that multiple T3SS2-secreted effectors are required to mediate LAMP1$^+$-tubule extension [112,165]. While one study indicates that ectopically expressed *sifA* in HeLa cells is sufficient to induce LAMP1$^+$-tubulation, others studies report significantly higher frequencies of LAMP1$^+$-tubulation when *sifA* is co-expressed with either *sopD2* or *sseJ* [161,165]. SifA and SseJ cooperate through interactions with the host kinesin-binding protein SKIP and RhoA family GTPases to induce LAMP1$^+$-tubulation [165]. We observed similar frequencies of LAMP1$^+$-tubulation in a strain with functional SifA and SseJ (Δ*sseFG*Δ*steA*Δ*pipB2*Δ*sopD2*) and a strain with only functional SifA (Δ*sseFG*Δ*steA*Δ*pipB2*Δ*sopD2*Δ*sseJ*), while LAMP1$^+$-tubules were not observed in the strain that lacks all seven effectors of interest (Δ*sseFG*Δ*steA*Δ*pipB2*Δ*sopD2*Δ*sseJ*Δ*sifA*). From this we can conclude that SifA is sufficient to induce LAMP1$^+$-tubule formation on its own. However, the frequency of LAMP1$^+$-tubulation was not significantly higher when both SifA and SseJ are functional than with SifA alone, suggesting that the previously described cooperative actions between SifA and SseJ, resulting in the increased LAMP1$^+$-tubulation, possibly involves other *S.* Typhimurium effectors or other host proteins to increase the frequency of LAMP1$^+$-tubules. The discrepancy between our results and others, regarding the cooperation between SifA and SseJ,

may be explained by previous studies observing increased LAMP1$^+$-tubule frequencies with ectopically expressed SifA and SseJ through transfection [121,165] whereas our study is in the context of a *S.* Typhimurium infection. Our results strongly suggest that multiple T3SS2-secreted effectors are required to facilitate efficient formation and extension of LAMP1$^+$-tubules.

Previous studies have demonstrated that neither the Δ*sifA* single-effector deletion mutant nor the Δ*sifA*Δ*sseJ* double-effector deletion mutant form SIFs. However, the Δ*sifA* mutant escapes the SCV while the Δ*sifA*Δ*sseJ* mutant remains in the SCV [69,121,154,175,219]. While the N-terminal domain of SifA is required for interactions with the host protein SKIP (PLEKHM2) and PLEKHM1 [110,164,167,177,220], the C-terminal domain promotes LAMP1 recruitment to *Salmonella*-induced tubules via interactions with the GTPase Arl8b [221]. Studies have demonstrated that Arl8b controls membrane fusion events with late endocytic compartments and is associated with LAMP1 accumulation in SIFs [221,222]. In our study, the Δ*sifA* deletion mutant was unable to extend LAMP1$^+$-tubules, yet we observed LAMP1$^+$-tubules in HeLa cells infected with Δ*sifA*Δ*sseJ* and Δ*sifA*Δ*sopD2* strains, suggesting that LAMP1 recruitment, and subsequent LAMP1$^+$-tubule extension, can occur via a SifA-independent mechanism. Further work is required to determine if LAMP1 recruitment in these strains is mediated by an additional effector interacting with Arl8b, or if an alternative Arl8b-independent mechanism is at play. The fact that the additional deletion of *sseJ* or *sopD2* in the Δ*sifA* background restores the ability to extend LAMP1$^+$-tubules indicates potential antagonistic action between SifA, SseJ, or SopD2 and other effectors to mediate SIF biogenesis.

The low frequency of LAMP1$^+$-tubule extension observed in multiple-effector deletion mutants lacking Δ*sseFG* may be directly related to the role of SseF and SseG during infection. Both SseF and SseG, while not required for the formation of single membrane SIFs, are required

for the conversion of single-membraned SIFs (also known as pseudo-SIFs) to double-membrane SIFs [129]. The inability to convert from single- to double-membraned SIFs may explain the thinner appearance of SIFs in cells infected Δ*sseF/G* strains as compared to wild type infected cells [172,180]. The methods used in our study may fail to detect these thinner pseudo-SIFs and may therefore account for low frequency of LAMP1$^+$-tubules in the Δ*sseFG* mutant strains.

Multiple studies have established that precise intracellular SCV positioning plays a key role during infection [109–111,223,224]. Mutant *S.* Typhimurium strains that fail to cluster near the Golgi at 8 hours-post infection in epithelial cells have lower frequencies of LAMP1$^+$-tubule extension and impaired intracellular replication [111,112,190]. The *sseF* and/or *sseG* deletion mutants are found scattered throughout the host cell's cytoplasm which could be a consequence of dysregulated microtubule motors [201]. Alternatively, the scattered phenotype caused by *sseF/G* deletion could also result from the absence of SseF and SseG mediated tethering to the Golgi-associated protein ACBD3 [113]. SifA and PipB2 also play a role in SCV localization during infection. T3SS2-secreted effector SifA inserts into the SCV membrane where it binds to the C-terminal PH domain of SKIP (PLEKHM2) [110,225]. Meanwhile, PipB2 tethers auto-inhibited kinesin-1 to the SCV membrane [114] in a process involving the small GTPase Arl8b [222,226]. Kinesin-1 is then activated by binding to the SifA-SKIP complex [167]. Deletion of *pipB2* prevents centrifugal displacement of SCVs at later timepoints in infection [200]. SteA may play a role in SCV positioning as it is thought to activate kinesin-1 or inhibit dynein [174]. While we have many pieces of the puzzle, the exact mechanisms controlling SCV localization during infection remains unclear.

A previous study investigated the role of up to three effectors on the intracellular localization of *S.* Typhimurium during infection. The authors found that intracellular wild type,

Δ*steA*, and Δ*pipB2* single-effector deletion mutants tend to reside close to the Golgi-apparatus at up to 14 hours post-infection, whereas any multiple deletion mutant that also had *sseF* and/or *sseG* deleted were more likely to be scattered throughout the host cell cytosol [174,200]. We found that the additional deletion of *pipB2* in the Δ*sseFG*Δ*steA* background (resulting in Δ*sseFG*Δ*steA* Δ*pipB2*) restores SCV localization close to the Golgi-apparatus. Subsequent deletion of additional effectors in the Δ*sseFG*Δ*steA*Δ*pipB2* background did not alter this close apposition of the SCV to the Golgi. Conversely, SCVs in mutant strains with functional PipB2 and SteA tend to be scattered throughout the host cell cytosol. These results suggest that PipB2 may be the first effector in a series of events involving SteA that leads to outwards centrifugal movement of SCV at 8 hours post-infection (and later time points as well) and without the initial action of PipB2, the SCV remains near the Golgi. The intracellular positioning of *Salmonella* must therefore rely on a delicate balance of effector actions to precisely regulate SCV positioning during infection. We can therefore conclude that multiple effectors are required to regulate positioning of the SCV during infection.

The question remains as to what the link is, if any, between SCV localization, LAMP1$^+$-tubule extension, and intracellular replication? Does effector deletion alter SCV localization, which directly impairs LAMP1$^+$-tubule extension, thereby limiting intracellular replication? Or does effector deletion itself impair LAMP1$^+$-tubule extension, resulting in decreased intracellular replication and altered SCV localization is merely a coincidental phenotype? An example that brings causality into question is the effect of deletion of *sseF* and *sseG* (Δ*sseFG*). We, and others, have shown that deletion of *sseFG* results in altered SCV localization and decreased LAMP1$^+$-tubule formation in HeLa cells, as well as reduced intracellular replication. Other studies have found that Δ*sseFG* strains also have altered SIF morphology [129,172]. SIFs

(LAMP1^{+}-tubules) are necessary for supplying intravacuolar *S.* Typhimurium with nutrients [193]. Intravacuolar *S.* Typhimurium forms SIFs by converting the host's endosomal system into SIFs to siphon nutrients from the host [194]. So then, does the replication defect of the Δ*sseFG* double mutant result from altered SCV localization, or does the altered SIF morphology itself limit nutrient acquisition from the host causing impaired intracellular replication? Alternatively, does altered SIF morphology result directly from altered SCV localization, impacting interactions with the host's endosomal system, and thus limiting nutrient acquisition, resulting in impaired intravacuolar replication? Further studies are necessary to elucidate the cause and effect of these processes. Intracellular localization, SIF formation, and replication are likely very intertwined and deletion of one effector critical to one of these processes could dramatically impact the others.

Multiple effectors are required to promote intracellular replication in macrophages. Most single-effector deletion mutants replicate within both RAW 264.7 macrophages and THP-1 monocytes, whereas multiple-effector deletion mutants do not. The precise reason for impaired replication is unclear, however a potential explanation is that deletion of multiple effectors alters interactions with the host's endocytic pathway which would then alter or limit SIF formation and thereby decrease nutrient acquisition from the host [129,130,193,194]. The fact that all multiple-effector deletion mutants have impaired intramacrophage replication regardless of the effectors deleted, suggests that all effectors are required in combination with each other to successfully replicate within host cells.

The importance of these SPI-2 effectors during infection was reinforced by examining colonization and inflammatory response in an *in vivo* infection model. It has been reported that SifA is not required to induce inflammation in the colon of mice [227]; however another group

showed that strains lacking SifA in addition to other T3SS2-decreted effectors (SseF, SseJ, SteA, and SpvB) have dramatically reduced inflammation during infection suggesting that intestinal inflammation requires the cooperative effects of at least these five effectors [228]. In line with these findings, both multiple-effector deletion strains in our study Δ*sseFG*Δ*steA*Δ*pipB2*Δ*sopD2* and Δ*sseFG*Δ*steA*Δ*pipB2*Δ*sopD2*Δ*sseJ*Δ*sifA* exhibited decreased virulence in a low-dose streptomycin pre-treatment mouse model of gastroenteritis. Both multiple-effector deletion strains are impaired to a similar degree with respect to colonization and inflammation in mice as compared to the mice infected with wild type *S.* Typhimurium. This means that SifA and SseJ are insufficient to mount a successful infection without the other five effectors of interest: SseF, SseG, PipB2, SteA, and SopD2. The impaired colonization observed in the two multiple-effector deletion mutants used in the mouse model of infection means that deletion of these effectors either impacts the ability of these strains to invade the host cells, the ability to replicate within host cells, or the ability to evade the host's immune system. The decreased inflammation in mice infected with either multiple-effector deletion strain also suggests that these strains may not invade host cells as efficiently as wild type strains, or they were easily eliminated from the host before the end point of the experiment. Similar to the conclusions of Matsuda *et al.* (2019), we can surmise that the seven effectors of interest in this study are required to mount a successful infection in a mouse model of gastroenteritis

We have shown that the processes of SIF biogenesis, intracellular localization, replication in macrophages, and colonization and inflammation in a mouse model, all require multiple effectors present and working together to successfully mount an infection. Our study highlights the fact that not one single effector of our seven of interest, is solely responsible for mediating complex infection phenotypes. It seems likely that several effectors act on the same process,

either in conjunction with one another, or in a sequential manner. If these effectors work sequentially, then deletion of an effector that works early within the pathway will have dramatic results. As an example: deletion of *pipB2* helps *S.* Typhimurium mutants remain very close to the Golgi during infection regardless of the presence or absence of other effectors, indicating that PipB2 likely acts early within the pathway. Similarly, these effectors could interact within much larger complexes, and deletion of a key effector could render the entire complex ineffective. If we want to elucidate the exact mechanisms underpinning *Salmonella*'s intracellular replicative niche, we must study the role of each effector in the context of other effectors, rather than deleting single effectors, or transfecting a single effector into tissue culture cells and examining their effect. Further studies are required to examine how these effectors interact with each other, or on similar host processes.

Chapter 3: *ssrB* overexpression enables study of SPI-2 effectors during infection

3.1 Synopsis

Many bacterial pathogens use secretion apparatuses to translocate virulence proteins (effectors) into host cells. These effectors mediate a wide variety of events within host cells to establish a successful infection. *Salmonella* Typhimurium makes use of its T3SS2 to translocate effectors into the host cell to create a unique replicative niche following invasion. Significant efforts over the years to identify T3SS2 effector-host binding partners, effector biochemical activity, and effector roles during infection have been met with mixed amounts of success. Such efforts have relied heavily on transfection of single effectors into host cells. Here, I design a toolkit comprised of a *S.* Typhimurium strain secreting increased abundance of T3SS2-secreted effectors and tagged versions of T3SS2 effectors of interest enabling study of effector-host interactions of several effectors implicated manipulating host endomembrane trafficking during infection.

3.2 Introduction

Understanding T3SS2-secreted effectors has been a challenge ever since SPI-2 and its associated T3SS were first described over 25 years ago [76,229]. Since then, the quest is ongoing to identify the T3SS2 effectors, their host targets, and their biochemical activity during infection. Great progress has been made to identify T3SS2-translocated effectors and their host targets. However, many questions remain.

One area of great interest is understanding how *S.* Typhimurium establishes its intracellular replicative niche. Complicating this effort is the fact that T3SS2-translocated effectors have seemingly redundant and overlapping roles. In Chapter 2 we demonstrate the magnitude of the complexities surrounding the effectors associated with SIF biogenesis, SCV positioning, intramacrophage replication, and virulence in a mouse model of infection. Our work has shown that studying T3SS2-translocated effectors individually leads to oversimplification of the complex host-pathogen interaction. Not only is it clear that these effectors work together to create the unique features of *S.* Typhimurium infection, but it is probable that two or more effectors bind to the same host target. Such a scenario would explain why precise mechanisms of SIF biogenesis, SCV positioning, or SCV maturation remain unclear. Indeed, another group recently found that the effectors PipB2 and SifA can both interact with host kinesin-1 and that there is a specific and direct interaction between SifA and PipB2 [115]. Commonly used transfection-based approaches with single T3SS2-translocated effectors fails to address the possibility that two effectors could be binding to the same host protein to mediate infection.

A barrier to identifying specific and significant T3SS2-secreted effector interactions is that the quantity of T3SS2-secreted effectors pales in comparison to the abundance of both T3SS1-secreted effectors and host proteins. It is thus inadequate to rely on native expression of T3SS2 effectors to identify binding partners as T3SS2-effector binding partners can be lost in the background noise of mass spectrometry. To mitigate this limitation, I aimed to create an isogenic strain of *S.* Typhimurium SL1344 that specifically secretes increased amounts of T3SS2-secreted effectors, but not increased T3SS1-secreted effectors. T3SS2-effector secretion is easily analyzed as T3SS2-secreted proteins are readily secreted into the culture supernatant of *S.* Typhimurium grown in SPI-2 inducing media that mimics the environment within the SCV [230].

The regulation of T3SS2-secretion is complex. Secretion is regulated at several levels by multiple proteins including, but not limited to: nucleoid-associated proteins IHF and Fis, the regulatory protein SlyA, the DNA binding protein HilD and the two component systems PhoP/PhoQ, OmpR/EnvZ, and SsrA/SsrB [75]. The SsrA/SsrB two component system is encoded within SPI-2 wherein SsrA (often referred to as SpiR, and not to be confused with SsaR) functions as the integral membrane sensor with the cognate response regulator SsrB [76,85]. The SsrB protein binds to and promotes expression of all functional gene clusters within SPI-2 [83] in addition to being critical for T3SS2 expression and T3SS2-secreted effectors, including those encoded outside of SPI-2 [84,93,231]. Creation of a *ssrB* overexpression mutant could therefore increase expression and secretion/translocated of all T3SS2 effectors.

This chapter and the next aim to identify T3SS2-translocated effector binding partners in the context of an infection wherein all T3SS2-effectors are present. Many groups have successfully found host binding partners of T3SS2 effectors by transfecting their chosen epitope-tagged effector into host cells and identifying effector-host interactions. While this is a robust method, it fails to address the interplay between effectors and the potentiality that more than one effector could be required to bind to a host protein to carry out its biochemical function. In this chapter, I create a *ssrB* overexpression mutant, termed T3SS2^{+}, that secretes increased amounts of SPI-2 effectors and create a toolkit to investigate effector binding partners for SifA, SopD2, SteA, PipB2, SseJ, and SseF. Together, Chapters 3 and 4 aim to unravel the complicated interplay between these effectors.

3.3 Materials and Methods

3.3.1 Bacterial strains and culture conditions

Bacterial strains used in this work are described in (Table 3.1). All strains were routinely grown in Luria-Bertani (LB) medium at 37˚C with shaking. For growth of the *E. coli* MFD*pir* strain, media was supplemented with DL-2,6-Diaminopimelic acid (DAP) at a final concentration of 0.3 mM when appropriate. Antibiotics were used at the following concentration when required: streptomycin 50 μg/mL, chloramphenicol 30 μg/mL, kanamycin 50μg/mL.

Table 3.1 - Bacterial strains used in this study

Strain Designation	Relevant Characteristics/Genotype	Source/Reference
SL1344	Wild-type strain, *hisG*	[206]
T3SS2$^+$	chromosomal duplication of *ssrB* resulting in increased expression of SPI-2 and its associated effectors	This study
MC1061*λpir*	*hsdR mcrB araD139 Δ(araABC-leu)7679 ΔlacX74 gal1 galK rpsL thiλpir*	[203]
MFD*pir*	*MG1655 RP4-2-TC::[ΔMu1::aac(3)IV-ΔaphA-Δnic35-ΔMu2::zeo] ΔdapA::(erm-pir) ΔrecA*	[204]
DH10B	*F- araDJ39 Δ(ara, leu)7697 ΔlacX74 galU galK rpsL deoR ϕ80dlacZΔM15 endAI nupG recAl mcrA Δ(mrr hsdRMS mcrBC)*	[205]
SL1344 pSifA-2HA	Wild type SL1344 transformed with 2x HA-tagged *sifA* in pACYC184	This study
SL1344 pSopD2-2HA	Wild type SL1344transformed with 2x HA-tagged *sopD2* in pACYC184	This study
SL1344 pPipB2-2HA	Wild type SL1344 transformed with 2x HA-tagged *pipB2* in pACYC184	This study
SL1344 pSteA-2HA	Wild type SL1344 transformed with 2x HA-tagged *steA* in pACYC184	This study
SL1344 pSseJ-2HA	Wild type SL1344 transformed with 2x HA-tagged *sseJ* in pACYC184	This study
SL1344 pSseF-2HA	Wild type SL1344 transformed with 2x HA-tagged *sseF* in pACYC184	This study
T3SS2$^+$ pSifA-2HA	*ssrB* overexpressing mutant transformed with 2x HA-tagged *sifA* in pACYC184	This study
T3SS2$^+$ pSopD2-2HA	*ssrB* overexpressing mutant transformed with 2x HA-tagged *sopD2* in pACYC184	This study
T3SS2$^+$ pPipB2-2HA	*ssrB* overexpressing mutant transformed with 2x HA-tagged *pipB2* in pACYC184	This study
T3SS2$^+$ pSteA-2HA	*ssrB* overexpressing mutant transformed with 2x HA-tagged *steA* in pACYC184	This study
T3SS2$^+$ pSseJ-2HA	*ssrB* overexpressing mutant transformed with 2x HA-tagged *sseJ* in pACYC184	This study

Table continued on next page

T3SS2$^+$ pSseF-2HA	*ssrB* overexpressing mutant transformed with 2x HA-tagged *sseF* in pACYC184	This study
T3SS2$^+$ Δ*sifA*-pSifA-2HA	*sifA* single deletion mutant in the *ssrB* overexpressing mutant complemented with 2x HA-tagged *sifA* in pACYC184	This study
T3SS2$^+$ Δ*sopD2*-pSopD2-2HA	*sopD2* single deletion mutant in the *ssrB* overexpressing mutant complemented with 2x HA-tagged *sopD2* in pACYC184	This study
T3SS2$^+$ Δ*pipB2*-pPipB2-2HA	*pipB2* single deletion mutant in the *ssrB* overexpressing mutant complemented with 2x HA-tagged *pipB2* in pACYC184	This study
T3SS2$^+$ Δ*steA*-pSteA-2HA	*steA* single deletion mutant in the *ssrB* overexpressing mutant complemented with 2x HA-tagged *steA* in pACYC184	This study
T3SS2$^+$ Δ*sseJ*-pSseJ-2HA	*sseJ* single deletion mutant in the *ssrB* overexpressing mutant complemented with 2x HA-tagged *sseJ* in pACYC184	This study
T3SS2$^+$ Δ*sseF*-pSseF-2HA	*sseF* single deletion mutant in the *ssrB* overexpressing mutant complemented with 2x HA-tagged *sseF* in pACYC184	This study

3.3.2 Plasmid construction

Plasmids constructed and used in this study are listed in Table 3.2. Plasmid pRE112-*ssrB* was constructed using the Gibson Assembly method of cloning [208] Plasmids pSopD2-2HA and pSifA-2HA were previously made in our lab [171,176]. Plasmids pRE112Δ*sifA*, pRE112Δ*sopD2*, pRE112Δ*pipB2*, pRE112Δ*steA*, pRE112Δ*sseJ*, and pRE112Δ*sseF* were all constructed previously (see section 2.3.4). Complementation vectors and gene deletion/insertion vectors were routinely maintained in *E. coli* DH10B and MC1061*λpir* respectively.

Table 3.2 - Plasmids used in this study

Plasmid Designation	Relevant Characteristics/Genotype	Source/Reference
pRE112-*ssrB*	pRE112 containing *ssrB* and homologous regions for insertion	This study
pRE112Δ*sifA*	pRE112 containing homologous regions surrounding *sifA* for chromosomal *sifA* deletion	Section 2.3.4
pRE112Δ*sopD2*	pRE112 containing homologous regions surrounding *sopD2* for chromosomal *sopD2* deletion	Section 2.3.4
pRE112Δ*pipB2*	pRE112 containing homologous regions surrounding *pipB2* for chromosomal *pipB2* deletion	Section 2.3.4
pRE112Δ*steA*	pRE112 containing homologous regions surrounding *steA* for chromosomal *steA* deletion	Section 2.3.4
pRE112Δ*sseJ*	pRE112 containing homologous regions surrounding *sseJ* for chromosomal *sseJ* deletion	Section 2.3.4
pRE112Δ*sseF*	pRE112 containing homologous regions surrounding *sseF* for chromosomal *sseF* deletion	Section 2.3.4
pSopD2-2HA	SopD2 with a tandem C-terminal HA tag in pACYC184	[171]
pSifA-2HA	Tandem HA tag in middle of SifA in pACYC184	[176]
pPipB2-2HA	PipB2 with a tandem C-terminal HA tag in pACYC184	This study
pSteA-2HA	SteA with a tandem C-terminal HA tag in pACYC184	This study
pSseJ-2HA	SseJ with a tandem C-terminal HA tag in pACYC184	This study
pSseF-2HA	SseF with a tandem C-terminal HA tag in pACYC184	This study

For PCR, Phusion High-Fidelity DNA Polymerase (NEB) was used. The plasmid pRE112-*ssrB* was constructed by using primers KK_001 and KK_002 to amplify linear pRE112 from the KpnI to SacI unique restriction sites (Table 3.3). Linearized pRE112 plasmid backbone was subsequently digested with DpnI (NEB) to remove any remaining circular template DNA. To generate an unmarked gene insertion, the region upstream of the *ssrB* insertion site was amplified using primers KK_003 and KK_004 and the region downstream of the insertion site was amplified using primers KK_007 and KK_008. The *ssrB* coding region was amplified using primers KK_005 and KK_006. Linearized pRE112, upstream insertion site fragment, *ssrB* fragment, and downstream insertion site fragment were assembled to form pRE112-*ssrB* using Gibson Assembly.

Table 3.3 - Primers used in this study

Primer Name	5' to 3' Sequence	Description
KK_001	GAGCTCTCCCGGGAATTCATGCAGTTCAC	Linearization of pRE112 maintaining SacI and **KpnI** cut sites
KK_002	**GGTACC**TCTAGAAGAAGCTTGGGA	
KK_003	CAAGCTTCTTCTAGAGGTACC CCGTCTTCGCTGATATCCCAC	Amplification of region upstream of *ssrB* insertion
KK_004	CTCAGATAATCAACATATCGAAAGAAATTTTTC	
KK_005	CGATATGTTGATTATCTGAGCAGATGATATGGTCATT AATAGCAAG	Amplification of *ssrB* and native promoter
KK_006	GCGTTAGTGGTATTAATCGTTAATACTCTATTAACCTC ATTCTTCGGGC	
KK_007	GAGGTTAATAGAGTATTAACGATTAATACCACTAACG CTAAAACGCAC	Amplification of region downstream of *ssrB* insertion
KK_008	ATGAATTCCCGGGAGAGCTCGGTGATGCGGTAATGTC GCTGC	
KK_009	GTACGCGTCGACCCGAGACGGTAGCCTGATTGAGTTA AACG	Amplification of *pipB2* plus native promoter, SalI and **Xho1** cut sites
KK_010	GTACGC**CTCGAG**AATATTTTCACTATAAAATTCGTTA AAGAGTGTTTGTGTGC	
KK_011	GTACGCGTCGACGCGCTTCCCCATCCCAAACCACC	Amplification of *sseJ* plus native promoter, SalI and **Xho1** cut sites
KK_012	GTACGC**CTCGAG**TTCAGTGGAATAATGATGAGCTATA AAACTTTCTAACATTATGGC	
KK_013	GTACGCGTCGACGCGACGGGCGCTCACCAATC	Amplification of *steA* plus native promoter, SalI and **Xho1** cut sites
KK_014	GTACGC**CTCGAG**ATAATTGTCCAAATAGTTATGGTAG CGAGCTTTTATGTCGG	
KK_015	GTACGCGTCGACGAAGAGAACAACGGCAAGTTACAG GATCCGC	Amplification of *sseABCDEFG* operon promoter, SalI cut site
KK_016	GATTGTTATTTTCACGTGCCCCTCCATATACACGATAG ATAATTAACGTGCTAAC	
KK_017	CTATCGTGTATATGGAGGGGCACGTGAAAATAACAAT CAATAGGTATGATGATGAAAG	Amplification of SscB chaperone and *sseF*
KK_018	GTACGC**CTCGAG**TGGTTCTCCCCGAGATGTATGATCA G	Reverse primer to amplify *sseF* and *sscB,* **XhoI** cut site

Plasmids pPipB2-2HA, pSteA-2HA, pSseJ-2HA, and pSseF-2HA were constructed based off the pSopD2-2HA plasmid [171]. Briefly, pSopD2-2HA was SalI/XhoI digested. Protein coding regions plus 300-500 bp upstream of the coding regions containing each gene's native promoter were amplified from genomic DNA from SL1344 as follows: *pipB2*: KK_009 and KK_010, *sseJ*: KK_011 and KK_012, *steA*: KK_013 and KK_014.The pSseF-2HA plasmid was constructed by amplifying the *sseABCDEFG* operon promoter the using primers KK_015 and

KK_016. Expression and secretion of SseF is dependent on the chaperone protein SscB [232]. The coding region of *sscB* and sseF were amplified using primers KK_017 and KK_018. The *sseABCDEFG* operon promoter was ligated to upstream end of *sscB* using Gibson Assembly. Each coding region plus native promoters were SalI/XhoI digested and inserted into the SalI/XhoI digested pSopD2 resulting in tandem double hemagglutinin (HA)-tag the C-terminal end of each effector. All cloned constructs were verified by DNA sequencing (Genewiz).

3.3.3 Generation of mutants by allelic exchange

The chromosomal duplication of *ssrB* resulting the T3SS2^{+} SPI2 overexpression mutant was created by conjugating MFD*pir* transformed with the plasmid pRE112-*ssrB* with wild type SL1344 to make an unmarked chromosomal duplication of *ssrB* in the SL1344 chromosome between the genes *dppA* and SL1344_3597 (a putative xanthine permease), specifically at the 3,837,749 base pair position according genome assembly NCBI_accession: NC_016810. This location was chosen as it is an intergenic region distant from SPI-2 within the SL1344 chromosome. Pro-conjugation single crossover mutants between pRE112-*ssrB* and the SL1344 chromosome were selected on LB agar plates containing chloramphenicol. Sucrose counter-selection was performed as previously described [209] to select for the second crossover event, thus inserting *ssrB* into the chromosome and creating the T3SS2^{+} mutant. Unmarked complete deletion mutants in the T3SS2^{+} background was generated as previously described (see Section 2.3.5)

3.3.4 Cell lines

HeLa (ATCC® CCL-2™) cells were obtained directly from ATCC. HeLa cells were routinely maintained at 37˚C in a 5% CO_2 atmosphere and cultured in Dulbecco's Modified Essential Medium (DMEM) (Hyclone) containing 10% (v/v) heat-inactivated fetal bovine serum (FBS) (Gibco), 1% (v/v) GlutaMax (Gibco), and 1% (v/v) non-essential amino acids (Gibco). HeLa cells were used until passage 15.

3.3.5 HeLa cell infections

For immunofluorescence: HeLa cells were seeded on 12 mm diameter coverslips in 24-well plates (Corning) at a density of 5 x 10^4 cells/well, 16-24 hours prior to infection. For detection of tagged effectors: HeLa cells were seeded in 100 mm tissue culture dishes (Corning) at a density of 2.0 x 10^6 cells/dish, 16-24 hours prior to infection. For all HeLa cell infections: overnight bacterial cultures were subcultured 1:33 in LB without antibiotic and incubated for 3 hours at 37˚C with shaking. 1 mL of bacterial cultures were pelleted and resuspended in Dulbecco's Phosphate-Buffered Saline (DPBS) (Hyclone), diluted in DMEM, and added to the HeLa cells at a multiplicity of infection (MOI) of ≈ 100:1. The infection proceeded for 15 minutes at 37˚C in 5% CO_2 before non-internalized bacteria were removed by three washes in DPBS and cells incubated in growth media containing 100 μg/mL gentamicin until 2 hours post-infection, followed by growth media containing 10 μg/mL gentamicin for the remainder of the experiment. HeLa cells were infected for a total of 8 hours.

3.3.6 Antibodies for immunofluorescence

The goat polyclonal anti-*Salmonella* antibody CSA-1 (Kirkegaard and Perry Laboratories) was used at a dilution of 1:300; the mouse anti-LAMP1 antibody H4A3c developed by J.T. August and J.E.K. Hildreth, obtained from the Developmental Studies Hybridoma Bank developed under the auspices of the NICHD and maintained by the University of Iowa (Department of Biological Sciences, Iowa, USA) was used at a dilution of 1:300. Secondary antibodies were obtained from Thermo Fisher Scientific and used at a dilution of 1:500: Alexa 488-conjugated donkey anti-mouse, and Alexa 568-conjugated donkey anti-goat.

3.3.7 Immunofluorescence microscopy

Cell monolayers seeded on glass coverslips were fixed with 4% (v/v) paraformaldehyde in DPBS at room temperature for 10 minutes and washed three times in DPBS. Excess paraformaldehyde was quenched with 50 mM ammonium chloride for 10 minutes at room temperature followed by two washes in DPBS. Cells were permeabilized in ice-cold acetone for 5 minutes at -20˚C and then blocked in 1% bovine serum albumin (BSA, wt/vol) (Sigma) in DPBS for 30 minutes at room temperature. Cells on coverslips were then incubated with primary antibodies diluted in 1% BSA in DPBS at room temperature for 1 hour followed by three washes in DPBS. Secondary antibodies diluted in 1% BSA in DPBS were added to the coverslips and incubated at room temperature for 1 hour and then washed once with DPBS. Cells were then incubated for 10 minutes at room temperature with DAPI (Invitrogen) diluted in DPBS followed by two DPBS washes. Cells were then washed in deionized water prior to mounting with ProLong Gold Antifade Mountant (Life Technologies) on glass slides. Microscopy was performed using Olympus IX81 (100x objective) and Zeiss Axio Imager M2 (100x objective)

microscopes using SlideBook 4.1.0 and Zeiss Zen Pro softwares, respectively. Images were further analyzed with ImageJ version 2.1.0/1.53c and Adobe Photoshop version 21.0.1.

3.3.8 Phenotype scoring by microscopy

To quantify the number of infected cells with LAMP1$^+$-tubules, we imaged at least one infected cell per field of view, then quantified the number of infected and uninfected cells per field of view. Infected cells were then scored for the presence or absence of LAMP1$^+$-tubules radiating outwards from labelled *Salmonella*. The number of tubules per *Salmonella* bacterium or number of tubules per infected cell was not considered. At least 60 infected cells per strain were scored blind in each experiment, and each experiment was repeated at least three times.

3.3.9 *In vitro* secretion assays

3.3.9.1 Protein secretion analysis

Effectors secreted by SPI-1 encoded type III secretion system (T3SS1) were analyzed by way of a SPI-1 secretion assay as previously described [30,233]. Overnight cultures of *S.* Typhimurium strains in LB-broth were subcultured 1:100 in fresh LB broth containing no antibiotics. Cultures were grown at 37˚C for 6 hours with shaking after which the optical density at 600 nm was measured. 3 mL of culture were centrifuged at 9500 x *g* for 10 mins at 4˚C. Culture supernatant was passed through a 0.22 μm filter, precipitated with trichloroacetic acid (TCA; Sigma) at a final concentration of 10%, and incubated on ice at 4˚C overnight.

Effectors secreted by T3SS2 were analyzed by way of a SPI-2 secretion assay as previously described [230]. 1 mL of overnight *S.* Typhimurium cultures were washed twice in a low phosphate and low magnesium-containing medium (LPM), then inoculated at a 1:50 dilution

in 30 mL of LPM at a pH of 5.8. LPM composition was 5 mM KCl, 7.5 mM $(NH_4)_2SO_4$, 0.5 mM K_2SO_4, 80 mM MES, 38 mM glycerol (0.3% v/v), 0.1% casamino acids, 24 μM $MgCl_2$, 337 μM PO_4^{3-}. Cultures were grown at 37˚C with shaking for 9 hours after which the optical density at 600 nm was measured. Bacteria were collected by centrifugation for 30 mins at 3000 x g in a 4˚C centrifuge. Culture supernatant was passed through a 0.22 μm filter, precipitated with TCA at a final concentration of 10%, and incubated on ice at 4˚C overnight.

3.3.9.2 Analysis of secreted proteins

For T3SS1-secreted proteins: The TCA insoluble fraction was collected by centrifugation for 45 minutes at 13,000 x g at 4˚C. Precipitate pellets were then washed in ice cold acetone and centrifuged at max speed in a 4˚C microfuge. Pellets were air-dried before resuspension in a volume of 2x SDS-PAGE sample buffer (100 mM Tris-HCL, pH 6.8, 20% glycerol, 4% SDS, 0.002% bromophenol blue, and 200 mM dithiothreitol) normalized to A_{600} of the original culture and boiled for 10 minutes. Samples were separated by SDS-PAGE using 12% polyacrylamide gels and stained with Coomassie Brilliant Blue R-250. Secreted proteins were annotated based on molecular weight as per [234].

For T3SS2-secreted proteins: The TCA insoluble fraction was collected by centrifugation for 45 minutes at 14,000 x g at 4˚C. Precipitate pellets were centrifuged at 14,000g at 4˚C for 45 mins. Pellets were solubilized with a volume of 2x SDS-PAGE sample buffer adjusted according to the A_{600} of the original culture.

Proteins from equivalent numbers of bacterial cells, as determined by the A_{600}, were separated on 12% SDS-polyacrylamide gels, transferred to Pure Nitrocellulose membranes (Bio-Rad) using a wet transfer cell. Membranes were blocked in blocking buffer (Tris-buffered saline containing 0.1% (v/v) Tween 20 (TBS-T) and 5% non-fat milk) overnight at 4˚C. Blots were

incubated with the following primary antibodies in blocking buffer for one hour at room temperature: rabbit affinity-purified antibodies raised against recombinant SseB and SseD (1:1500), rat anti-HA monoclonal antibody (1:2000, Roche), or mouse anti-beta-tubulin (1:1500, Abcam). Three 5-minute wash steps were performed using TBS-T followed by room temperature incubation of membranes with secondary antibody. Secondary antibodies conjugated to horseradish peroxidase (HRP; goat anti-rat, goat anti-rabbit, or goat anti-mouse) were diluted to 1:5000 in blocking buffer. Antibody complexes were detected using ClairtyTM Western ECL Substrate (Bio-Rad Laboratories, Inc) prior to detection in a BioRad Gel Imaging System.

3.3.10 Immunoprecipitation of tagged effectors from HeLa lysate

Lysates were harvested from infected HeLa cells grown in 100 mm dishes. Culture dishes were placed on ice at 8 hours post infection and washed three times with ice-cold DPBS. Cells were manually detached from the culture dish containing 5 mL ice-cold DPBS and transferred into 15 mL tubes. Cells were spun at 300 x *g* for 10 minutes in a centrifuge set to 4˚C. The supernatant was removed, cell pellets snap frozen in liquid nitrogen, and stored at -80˚C. Cell pellets were thawed on ice and resuspended in RIPA buffer (25 mM Tris-HCl pH 7.6, 150 mM NaCl, 1% NP-40, 1% sodium deoxycholate, 0.1% sodium-dodecyl sulphate (SDS), supplemented with cOmplete protease inhibitor cocktail (Roche)). Cell lysates were centrifuged for 10 minutes in a 4˚C microcentrifuge for 10 minutes at max speed. Protein concentration of the supernatant was determined by Pierce BCA Protein Assay Kit (Thermo Fisher Scientific). HA-tagged proteins were immunoprecipitated using Pierce Anti-HA magnetic beads (Thermo Fisher Scientific) according to manufacturer specifications. Samples were eluted in 50 mM NaOH and analyzed by Western blot.

3.3.11 Statistical analyses

Statistical analysis was performed using Prism9 (GraphPad). Analysis was performed using a Mann-Whitney test to compare two groups and two-way ANOVA for more than one group with Tukey's multiple comparison test as appropriate. Aggregate results represent the mean ± standard error on the mean.

3.4 Results

The results from Chapter 2 of this dissertation indicate that multiple T3SS2-secreted effectors are required to mediate the processes of LAMP1^{+}-tubule extension, subcellular SCV positioning, intramacrophage replication, and replication *in vivo*. To help delineate these complex processes, I aimed to design a robust system to identify T3SS2-secreted effector-host binding partners in the context of an infection with natural effector delivery.

Overexpression of plasmid-encoded *ssrB* has previously led to discovery of additional T3SS2-secreted effectors within an *in vitro* T3SS2-secretome analysis [235] but has to our knowledge never been used to identify effector-host binding partners. Four different isogenic strains of *S.* Typimurium were used to assess secretion of T3SS2 effectors: the wild type SL1344, T3SS2^{+}, Δ*invA,* Δ*ssaR*. The T3SS2^{+} strain has a duplicated copy of the promoter and protein coding region for *ssrB* inserted within the chromosome of SL1344 in an intergenic region distant from SPI-2 between the genes *dppA* and SL1344_3597 (a putative xanthine permease) (Figure 3.1). The coding region for the duplicated *ssrB* does not reside within the SPI-2 locus, like many of the effectors secreted by the T3SS2.

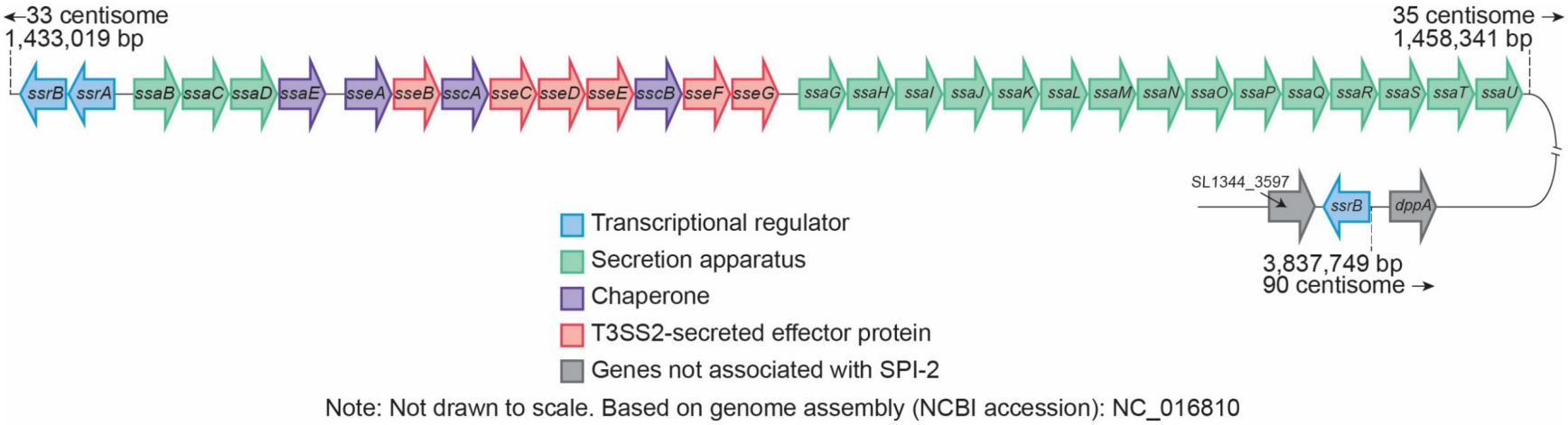

Figure 3.1 - Genetic organization of SPI-2 and *ssrB* duplication insertion site. Genetic organization of *Salmonella*-pathogenicity island 2. The duplicated *ssrB* coding region and its native promoter were inserted at a distant location within the chromosome to enhance secretion of T3SS2-secreted effectors.

3.4.1 Chromosomal duplication of *ssrB* increases T3SS2-effector secretion

To assess the impact of overexpression of *ssrB* in the T3SS2$^+$ strain, I performed both SPI-1 and SPI-2 secretion assays to evaluate the relative amount of effector secretion under both SPI-1 and SPI-2 inducing conditions (Figure 3.2).

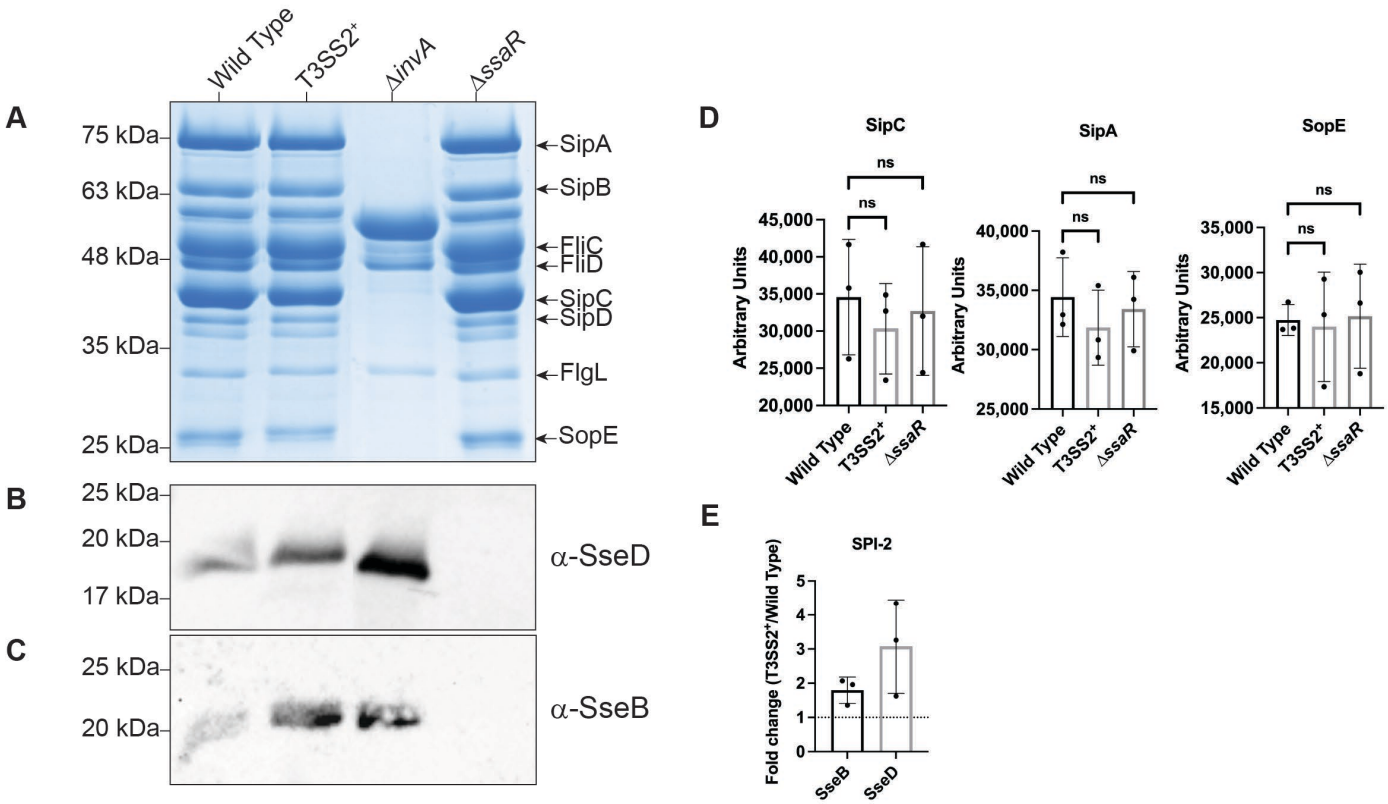

Figure 3.2 - Effector secretion by T3SS2$^+$ *ssrB* overexpression mutant. Images shown are representative of *n*=3 experiments. **(A)** Secreted proteins from indicated strains grown under SPI-1 inducing conditions were separated by SDS-PAGE and stained with Coomassie Brilliant R250. **(B)** and **(C)** Secreted proteins from indicated strains grown under SPI-2 inducing conditions were precipitated and separated on a SDS-PAGE gel and immunoblotted with α-SseD **(B)** or α-SseB **(C)**. **(D)** Densitometric analysis of SPI-1 secreted effectors SipA, SipC, and SopE as determined by 3 SDS-PAGE gels stained by Coomassie. Ns= Not significant as determined by a Kruskal-Wallis test with Dunn's correction for multiple comparisons **(E)** Fold change determined by densitometry of 3 Western blots from independent experiments. Mean fold change ± standard deviation is shown. Fold change = (Densitometry of T3SS2$^+$)/(Densitometry of wild type). Dashed line = 1.

The wild type strain secreted significant amounts of the T3SS1-secreted effectors SipA, SipB, SipC, SipD, and SopE (Figure 3.2A and D). SPI-1 inducing growth conditions that induce T3SS1-secretion also induce the secretion of flagellar proteins FliC, FliD, and FlgL (Figure

3.2A) [234]. Chromosomal duplication of *ssrB* (T3SS2$^+$) did not significantly increase or decrease secretion of T3SS1-secreted proteins relative to wild type (Figure 3.2 A and D).

The Δ*invA* mutant is unable to secrete proteins through the T3SS1 secretion apparatus [236] and served as a negative control. T3SS1-secreted effectors were not secreted by the Δ*invA* strain, while the T3SS2-independent flagellin proteins were still detected in the culture supernatant. The SPI-2 apparatus mutant Δ*ssaR* [207] secretes approximately equivalent amounts of SPI-1 effectors as both wild type and T3SS2$^+$ (Figure 3.2 A and D). These results suggest that overexpression of *ssrB* from the chromosome does not impact T3SS1-secretion.

While overexpression of *ssrB* from the chromosome (T3SS2$^+$) does not seem to affect T3SS1-effector secretion, it does increase T3SS2-effector secretion. Our lab previously made affinity purified antibodies against the SPI-2 encoded proteins SseB and SseD (filament and pore forming components of the T3SS2 secretion apparatus, respectively [230]) providing a convenient means to detect T3SS2 proteins. Growth of bacteria under SPI-2-inducing conditions indicates that the T3SS2$^+$ strain secretes more SseD (Figure 3.2B) and SseB (Figure 3.2C) than wild type as shown by a fold change (T3SS2$^+$/wild type) greater than 1 (Figure 3.2E). The Δ*ssaR* mutant (known to have a defective T3SS2-secretion apparatus) failed to secrete either SseD/B.

3.4.2 T3SS2$^+$ mutants produce more SIFs during infection

I hypothesized that the increased T3SS2-effector secretion of the T3SS2$^+$ strain would affect primarily T3SS2-, but not T3SS1-, mediated processes. Strains with increased T3SS2-effector secretion should also have increased T3SS2-mediated effects during infection, such as increased frequency of SIF biogenesis. I therefore decided to use the frequency of SIF biogenesis in infected cells as evidence of increased T3SS2-effector secretion during infection. HeLa cells

were infected for 8 hours with wild type, T3SS2^{+}, and Δ*ssaR* strains to determine percentage of infected cells and the percentage of infected cells with SIFs (Figure 3.3).

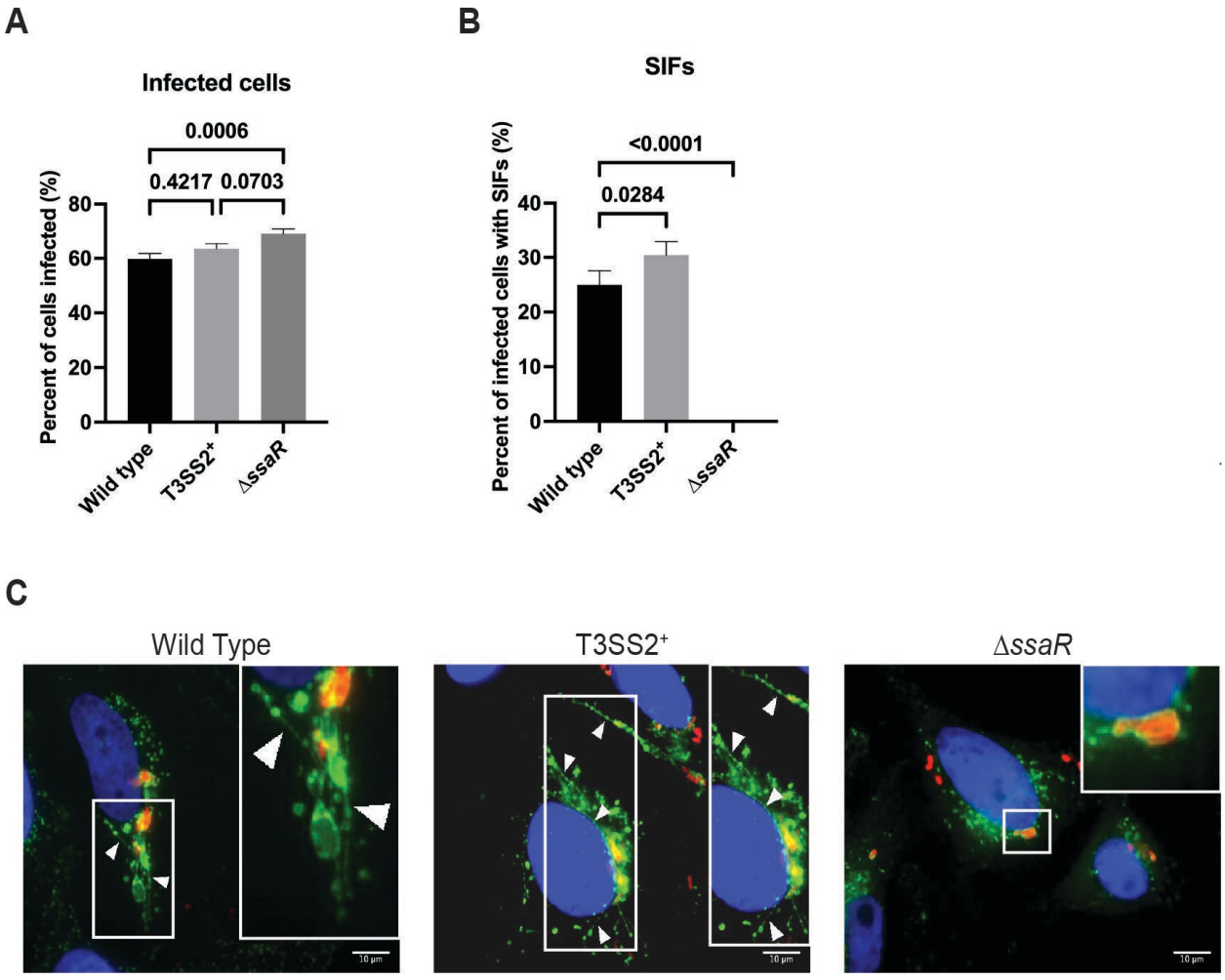

Figure 3.3 - *ssrB* overexpression in HeLa cells increases the number of infected cells with SIFs. For quantifications, bars represent mean ± standard error of the mean for three separate experiments (*n*=3). Significance was determined by Kruskal-Wallis test with Dunn's correction for multiple comparisons. *p* values are as indicated. HeLa cells were infected with an MOI ≈ 100 for 8 hours prior to cell fixation. Cells were immunostained for *Salmonella* (red) and LAMP1 (green), and the nucleus was stained with DAPI (blue). 60 distinct fields of view were used for quantification per experiment with at least 1 infected cell per field of view. **(A)** Quantification of percent of cells infected as determined by counting the number of infected and uninfected cells in each field of view. **(B)** Quantification of percentage of infected cells with LAMP1^{+}-tubules (SIFs) as determined by enumerating the number of infected cells per field of view and the number of infected cells with SIFs. **(C)** Representative images of HeLa cells infected with a MOI ≈ 100 with strains wild type, T3SS2^{+}, or *ΔssaR* at 8 h.p.i. Scale bar = 10 µm.

The percentage of cells infected is an indicator of whether *ssrB* overexpression impacts invasion, a T3SS1-mediated process. The T3SS2$^+$ strain infected about the same proportion of cells as the wild type (Figure 3.3A). The Δ*ssaR* strain infected significantly more cells than both the wild type and T3SS2$^+$ strains. These results indicate that the T3SS2$^+$ mutant is not more effective at invading host cells than wild type and therefore likely does not have altered T3SS1-mediated processes.

Infected HeLa cells were examined for the presence or absence of SIFs with the idea that increased T3SS2-effector secretion should increase the frequency of SIF biogenesis. There was a significant increase in the percentage of infected cells exhibiting SIFs in the T3SS2$^+$ strain relative to wild type infected cells (Figure 3.3B). As previously reported, the Δ*ssaR* strain failed to induce SIFs [207,237]. From these experiments, we can conclude that the T3SS2$^+$ strain does not infect a higher proportion of cells than wild type but does have significantly more infected cells with SIFs relative to the wild type strain.

3.4.3 T3SS2$^+$ mutant secretes tagged effectors

I wanted to epitope tag six effectors of interest examined in Chapter 2 of this dissertation (SifA, SopD2, PipB2, SteA, SseJ, and SseF) to facilitate immunoprecipitation and identification of effector binding partners (Chapter 4 of this dissertation). A previous lab member constructed tandem double hemagglutinin (HA)-tagged SopD2 [171] and SifA [166] under the control of their respective native promoters in a low copy bacterial expression plasmid. I transformed these constructs into both wild type and the T3SS2$^+$ mutant to evaluate whether A) SL1344 expresses and secretes tagged effectors, and B) T3SS2$^+$ expresses and secretes increased amounts of the tagged effectors relative to wild type cells transformed with the same plasmid.

T3SS2$^+$ strains transformed with either pSopD2-2HA or pSifA-2HA were grown to stationary phase under SPI-2 inducing conditions and secreted proteins were enriched from the culture supernatant. Increased amounts of both SopD2-2HA and SifA-2HA were detected in the culture supernatant of the T3SS2$^+$ strains as compared to SL1344 cells transformed with the same plasmids (Figure 3.4A).

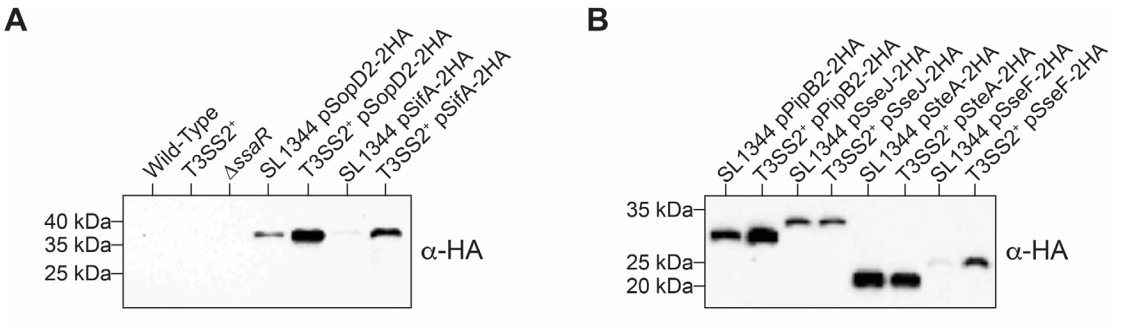

Figure 3.4 - Epitope-tagged effectors are secreted by *S.* Typhimurium. Secretion of tandem double HA-tagged effectors into culture supernatant. All blots are representative of *n*=3 experiments. The indicated strains were cultured for 9 hours in a minimal medium optimized for induction of SPI-2 gene expression and subsequent SPI-2 effector secretion. Bacterial cultures were pelleted by centrifugation and the culture supernatant proteins were precipitated using trichloroacetic acid and dissolved in SDS-PAGE sample buffer. Samples were resolved on a 12% SDS-PAGE gel, Western blotted, and probed with anti-HA antibodies. **(A)** Secretion of previously made tagged effectors by both the SL1344 and T3SS2$^+$ strain. **(B)** Secretion of newly made tagged effects by both SL1344 and T3SS2$^+$ strains.

The remainder of the effectors of interest were tandem double HA-tagged at their C-terminus under the control of their native promoter in a low-copy number bacterial expression plasmid. pPipB2-2HA, pSteA-2HA, pSseJ-2HA, and pSseF-2HA were all successfully transformed, expressed, and secreted in both the SL1344 and the T3SS2$^+$ strains (Figure 3.4B). Generally, the T3SS2$^+$ strains secreted more of some effectors, and approximately the same amount of other effectors relative to SL1344 strains secreting the same effectors.

3.4.4 Secretion of tagged effectors in complemented single-effector deletion mutants

The overall goal for the T3SS2$^+$ mutants and tagged effectors is identify the interaction partners for each of the effectors of interest (Chapter 4 of this dissertation). To achieve maximum translocation of purely tagged effectors during infection, the native chromosomal copy of each effector was deleted in the T3SS2$^+$ genetic background to create unmarked deletions. Each of the six single-effector deletion mutants Δ*sifA*, Δ*sopD2*, Δ*steA*, Δ*pipB2*, Δ*sseJ*, and Δ*sseF* were transformed with their respective plasmid-borne HA-tagged effectors, to yield strains exclusively producing the tagged version of each respective effector in the T3SS2$^+$ mutant background (see Table 3.1 in materials and methods). Strains were grown to stationary phase under SPI-2 inducing conditions and secreted proteins were isolated from the culture supernatant. All the tagged effectors were detected in the culture supernatant (Figure 3.5A); however, some effectors were found at a significantly lower abundance than others. SifA-2HA (from T3SS2$^+$Δ*sifA*-pSifA-2HA) and SopD2-2HA (from T3SS2$^+$Δ*sopD2*-pSopD2-2HA) were only minimally detected in the culture supernatant. The rest of the tagged effectors (PipB2-2HA, SteA-2HA, SseJ-2HA, and SseF-2HA) were readily detected in the culture supernatant in the T3SS2$^+$ complemented single-effector deletion mutants. From these results, we can conclude that the HA-tagged effectors are expressed and secreted under SPI-2 inducing conditions by the T3SS2$^+$ single effector deletion mutants.

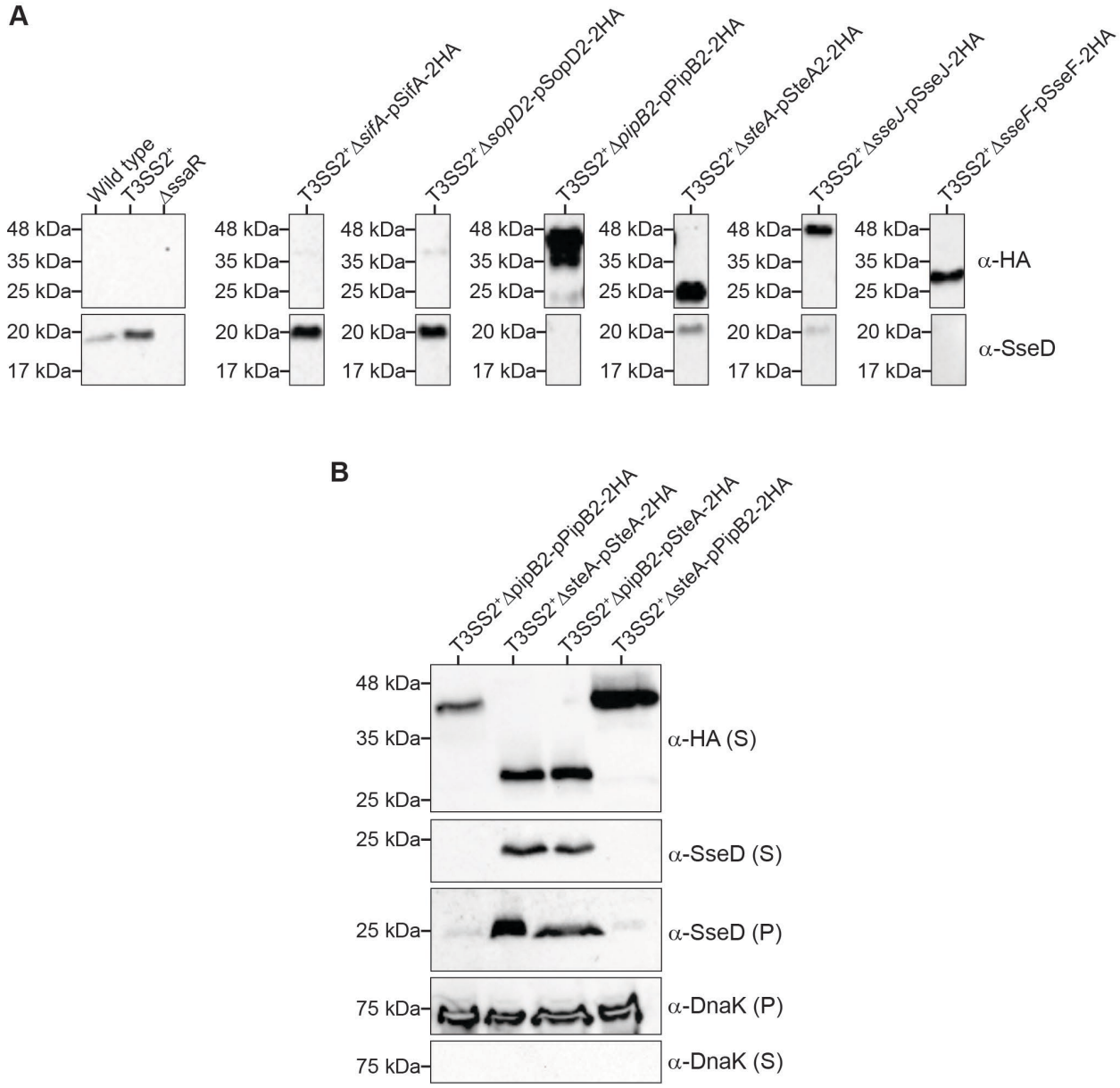

Figure 3.5 - Secretion of tagged effectors by single-effector deletion mutants. All blots are representative of *n*=3 experiments **(A)** Secretion of tagged effectors in single deletion mutants the *ssrB* overexpression (T3SS2$^+$) background complemented with the corresponding tagged effectors. The indicated strains were cultured for 9 hours in a minimal medium optimized for induction of SPI-2 gene expression and subsequent SPI-2 effector secretion. Bacterial cultures were pelleted by centrifugation and the culture supernatant proteins were precipitated using trichloroacetic acid and dissolved in SDS-PAGE sample buffer. Samples were resolved on a 12% SDS-PAGE gel, Western blotted, and probed with α-HA or α-SseD antibodies. **(B)** Translocation of pPipB2-2HA or pSteA-2HA in either the T3SS2$^+$Δ*pipB2* or T3SS2$^+$Δ*steA* backgrounds. Culture supernatant (S) was prepared as in **(A)** while the cell pellet fraction (P) was prepared by boiling the cell pellet in a volume of SDS-PAGE loading buffer normalized to the A_{600} of the original culture. Samples were resolved on a 12% SDS-PAGE gel, Western blotted, and probed with α-HA, α-SseD, or α-DnaK antibodies

Expression and/or secretion of SseD, an indicator of T3SS2-mediated secretion, appears to be reduced for strains carrying the pSseJ-2HA or the pSseF-2HA plasmids. I am confident that the observed reduction of SseD expression/translocation is due to a camera issue when imaging the blot. See Figure A.1 in Appendix A showing normal expression and translocation of SseD in T3SS2^{+} strains transformed with each of pSseJ-2HA and pSseF-2HA.

SseD was found in the culture supernatant of all strains except for strains complemented with the pPipB2-2HA plasmid. While SseD was not found in the culture supernatant of strains carrying the pPipB2-2HA plasmid, PipB2-2HA was readily detected in the culture supernatant suggesting the T3SS2-secretion apparatus may indeed be functional. It seems that either the deletion of PipB2 affects T3SS2-effector secretion, or somehow the expression of the pPipB2-2HA plasmid affects T3SS2-effector protein production or secretion. To test this, pPipB2-2HA was transformed into the T3SS2^{+}Δ*steA* background, and pSteA-2HA was transformed into the T3SS2^{+}Δ*pipB2* background. All four of these strains secreted their respective tagged effectors; however, SseD was not detected in the culture supernatant of either T3SS2^{+}Δ*pipB2* or T3SS2^{+}Δ*steA* strains transformed with pPipB2-2HA (Figure 3.5B) indicating that the pPipB2-2HA plasmid expression may interfere with T3SS2-secretion. However, SseD was found at very low levels in the cell pellet fraction of T3SS2^{+}Δ*pipB2* and T3SS2^{+}Δ*steA* strains with the pPipB2-2HA, suggesting that expression of pPipB2-2HA may decrease either SseD protein production or section, and may therefore impact T3SS2-mediated secretion.

If T3SS2-secretion is decreased, then how is PipB2-2HA found in the culture supernatant? The chaperone protein DnaK should only be found in the pellet fraction unless there is bacterial contamination of the secreted fraction, or cells have lysed releasing DnaK into the culture supernatant. DnaK was not found in the culture supernatant for any of the T3SS2^{+}Δ*pipB2*

and T3SS2^{+}Δ*steA* strains with either pPipB2-2HA or pSteA-2HA plasmids thus ruling out the possibility that PipB2-2HA is found in the culture supernatant as a result of cell lysis. It remains unclear how PipB2-2HA is secreted when SseD is not, but it may be related to altering the hierarchy of effector secretion.

A concern when epitope tagging secreted bacterial effectors is that the tag addition will either cause the tagged protein to misfold or become too large to be secreted by the secretion apparatus. Here, I show that the addition of a tandem double HA-tag to the C-terminus of the effectors of interest (namely PipB2, SteA, SseJ, and SseF) does not hinder effector secretion by the T3SS2.

3.4.5 Translocation of tagged effectors during infection

Thus far I have confirmed that the tagged effectors are expressed and secreted under *in vitro* SPI-2 inducing conditions but not under infection conditions. I infected HeLa cells for 8 hours with the T3SS2^{+} *ssrB* overexpression single effector deletion mutants complemented with their respective tagged effectors to assess expression of tagged effectors during infection. Cell lysate was separated by SDS-PAGE and immunoblotted with an anti-HA antibody (Figure 3.6). Five of the six tagged effectors were readily detected in the HeLa cell lysate without further enrichment for the tagged effectors. SifA-2HA was noticeably absent from the T3SS2^{+}Δ*sifA*-pSifA-2HA strain. The beta tubulin loading control indicates that approximately equal amounts of lysate was loaded for each sample, suggesting that the failure to detect SifA-2HA was not due to an error during lysate preparation. The pSifA-2HA plasmid has successfully been used in our lab in the past. Brumell *et al*. 2002 used this plasmid to discover that SifA is present in the membrane but not the cytosolic fraction of infected HeLa cells [166]. I did not fractionate the lysate, so it is possible that SifA-2HA was expressed and translocated into the host cell but the

amount of SifA-2HA protein concentration was below the limit of detection. In all, this data indicates that the T3SS2^{+} *ssrB* overexpression mutant successfully expresses each of the six HA-tagged effector constructs from within the intracellular environment in HeLa cells.

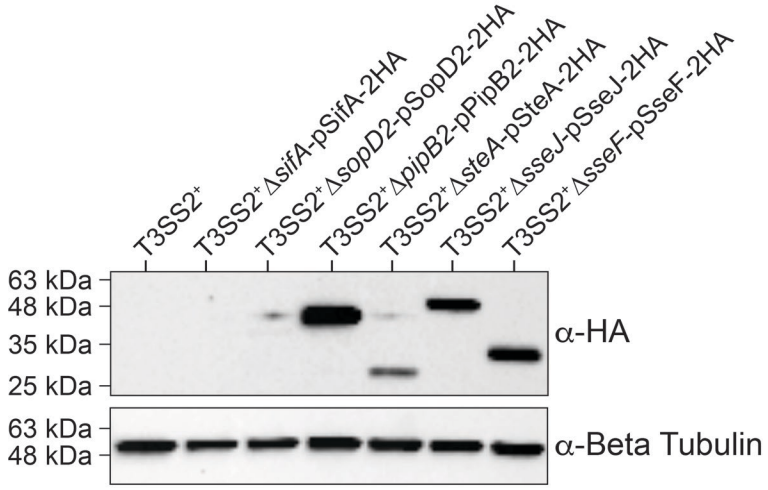

Figure 3.6 – T3SS2^{+} -mutants express tagged effectors during infection of HeLa cells. Blot is representative of *n*=3 experiments. HeLa cells were infected with an MOI of 100 for each strain for 8 hours. Cell lysates were separated on an 12% SDS-PAGE gel and immunoblotted with α-HA and α-Beta Tubulin (loading control) antibodies

3.4.6 Translocated tagged effectors complement the SIF phenotype during infection

Epitope tagging proteins can have unintended effects on the final protein product potentially altering the 3D shape of the protein and rendering it no longer functional or translocatable. I have already demonstrated that the tandem double HA tag at the C-terminal ends of our effectors of interest does not deleteriously impact effector expression or secretion. Whether these tagged effectors can still fulfill their biological role during infection remains a question. Using SIF phenotype complementation as an indicator has previously been used to test functionality of T3SS2-secreted effector fusion proteins [238]. HeLa cells were infected with the

various T3SS2^{+} complemented strains and evaluated for the frequency of SIF formation in infected cells.

Complementation of T3SS2^{+}Δ*sifA* and T3SS2^{+}Δ*steA* with pSifA-2HA and pSteA-2HA, respectively, increased the frequency of SIF biogenesis in infected cells relative to their uncomplemented counterpart strains (Figure 3.7B and E, respectively). The rescue of the SIF phenotype in the complemented T3SS2^{+}Δ*sifA* strain indicates that SifA-2HA is indeed translocated into host cells despite not detecting SifA-2HA in appreciable amounts in infected HeLa cells (Figure 3.6). There was no significant difference in the frequency of SIF formation in infected cells in the complemented T3SS2^{+}Δ*sopD2,* T3SS2^{+}Δ*sseJ,* and T3SS2^{+}Δ*sseF* compared to their respective uncomplemented counterpart strains (Figure 3.7C, F and G, respectively).

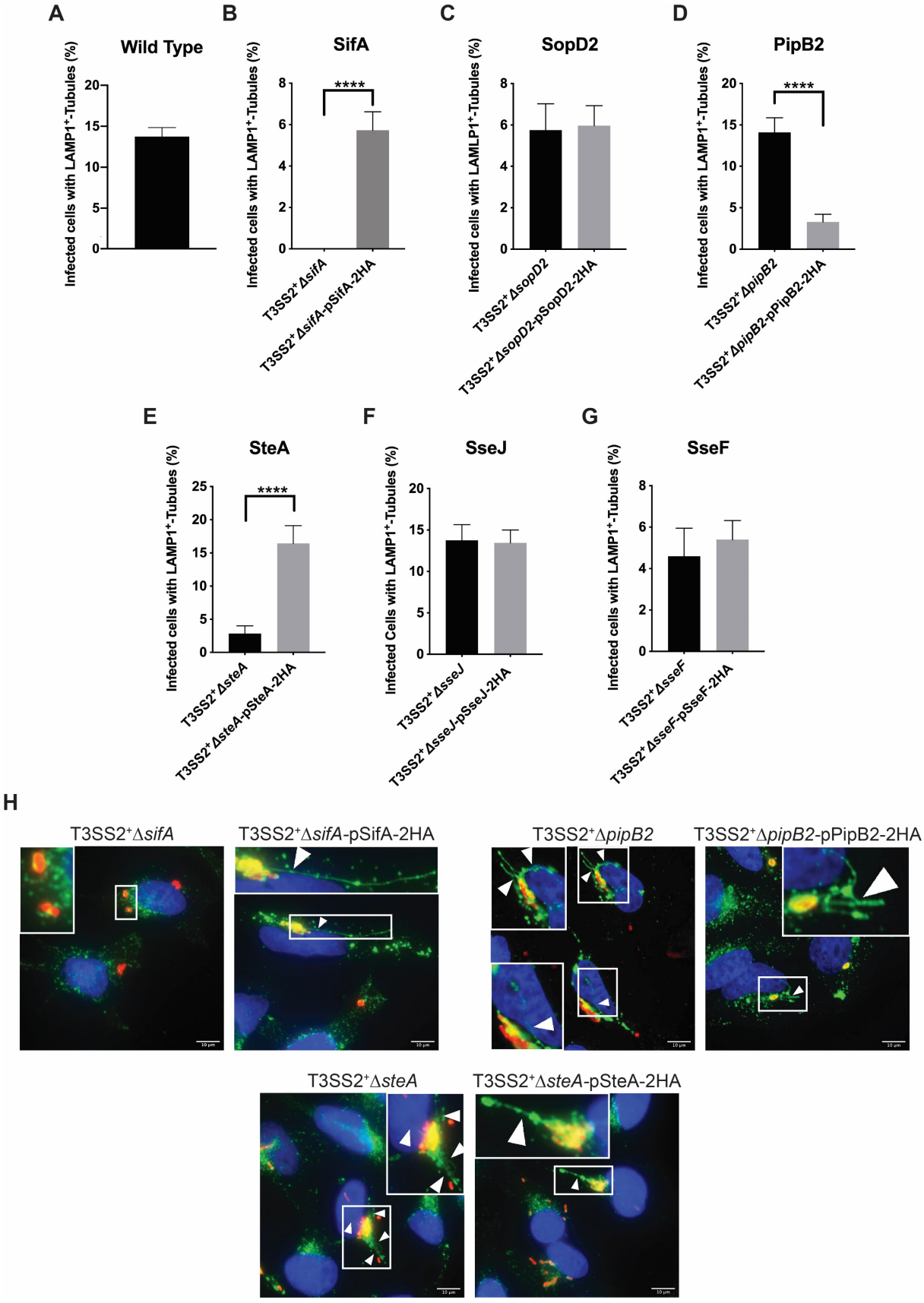
A
Wild Type
Infected cells with LAMP1+-Tubules (%)
B
SifA
****
T3SS2+ΔsifA
T3SS2+ΔsifA-pSifA-2HA
C
SopD2
Infected cells with LAMLP1+-Tubules (%)
T3SS2+ΔsopD2
T3SS2+ΔsopD2-pSopD2-2HA
D
PipB2
T3SS2+ΔpipB2
T3SS2+ΔpipB2-pPipB2-2HA
E
SteA
T3SS2+ΔsteA
T3SS2+ΔsteA-pSteA-2HA
F
SseJ
Infected Cells with LAMP1+-Tubules (%)
T3SS2+ΔsseJ
T3SS2+ΔsseJ-pSseJ-2HA
G
SseF
T3SS2+ΔsseF
T3SS2+ΔsseF-pSseF-2HA
H
T3SS2+ΔsifA
T3SS2+ΔsifA-pSifA-2HA
T3SS2+ΔpipB2
T3SS2+ΔpipB2-pPipB2-2HA
T3SS2+ΔsteA
T3SS2+ΔsteA-pSteA-2HA

Figure 3.7 - Complementation of SIF biogenesis. (A-G) Quantification of LAMP1$^+$-tubule frequency (SIFs) in HeLa cells infected with single effector deletion mutants in the *ssrB* overexpression mutant background (T3SS2$^+$) and their corresponding complemented strains after 8 hours of infection. The average frequency of infected cells with LAMP1$^+$-tubules ± standard error of the mean for three separate experiments is shown (n=3). At least 60 infected cells per strain were blindly analyzed in each experiment. Asterisks indicate significant differences between complemented and the corresponding uncomplemented strain as determined by Mann-Whitney test (****p<0.0001). **(H)** Representative images for select strains. Cells were immunostained for *Salmonella* (red) and LAMP1 (green) and stained with DAPI (blue) for enumeration of the proportion of infected cells with LAMP1$^+$-tubules shown in (A-G). White boxes indicate zoomed-in region in inset. Arrowheads indicate LAMP1$^+$-tubules. Scale Bar = 10 μm.

The difference in SIF frequency between wild type infected cells and Δ*sseJ* infected cells is not significant (Figure 2.2, Figure 3.7A); therefore, complementation of T3SS2$^+$Δ*sseJ* with pSseJ-2HA should have negligible effect on the percentage of infected cells presenting with SIFs—consistent with our findings (Figure 3.7F). The deletion of *sseF* dramatically reduces SIF frequency relative to wild type (Figure 2.2), so complementation of T3SS2$^+$Δ*sseF* with pSseF-2HA should at least partially restore or increase the ability of complemented T3SS2$^+$Δ*sseF* to form SIFs. While I saw small increase in the percentage of infected cells with SIFs in the complemented T3SS2$^+$Δ*sseF* as compared to the uncomplemented strain, the increase was not significant (Figure 3.7G). SseF-2HA was readily detected in infected HeLa cells (Figure 3.6), so failure to increase the frequency of SIF biogenesis is not due to a lack of expression. It remains unclear why the pSseF-2HA plasmid did not complement the SIF phenotype in the T3SS2$^+$Δ*sseF* strain; speculatively, it could be due to interference of the double HA tag with either the final 3D conformation of the protein, or obstruction of effector-host protein binding by the HA-tag.

There was no increase in the frequency of infected cells with SIFs in the complemented T3SS2$^+$Δ*sopD2* strain versus its uncomplemented counterpart (Figure 3.7C) and a decrease in the frequency of infected cells with SIFs in the complemented T3SS2$^+$Δ*pipB2* strain versus its uncomplemented counterpart (Figure 3.7D). Other groups have successfully increased the frequency of SIF in HeLa cells infected with complemented SL1344Δ*sopD2* using the same

pSopD2-2HA plasmid [161,171], so it stands to reason that expression of pSopD2-2HA should increase SIF frequency in the T3SS2^{+}Δ*sopD2* background. Consistent with findings from a previous report, strains complemented with a plasmid-borne copy of PipB2-2HA reduces the frequency of SIF formation in infected cells [239].

In summary, I have constructed complemented *ssrB* overexpression mutants that express their respective functional tagged effectors during infection where they participate in SIF biogenesis. Further investigation is required to determine the effect of *ssrB* overexpression (*i.e.,* the T3SS2^{+} strain) on additional aspects of *S.* Typhimurium infection such as subcellular localization, intramacrophage replication, and virulence/colonization in a mouse model of infection.

3.5 Discussion

Many medically relevant pathogens including *Shigella,* pathogenic *E. coli,* and *Shigella* use type III secretion systems to mediate infection and disease [240]. Translocated bacterial effectors manipulate a variety of host processes to promote colonization and virulence. Due to the complex nature of the bacteria-host interaction and the multifunctional and cooperative nature of T3SS secreted effectors, the specific functions and interactions of these effectors are poorly understood. Indeed, the mechanisms underpinning the ability of *S.* Typhimurium to establish and maintain its intracellular niche remains unclear.

During infection, the T3SS2-secreted effectors are expressed upon entry of *S.* Typhimurium into the cell and establishment of the SCV; consequently, expression levels of T3SS2-secreted effectors pales in comparison to the relative amount of host proteins. Thus, previous attempts to identify molecular targets of T3SS2-secreted effectors have heavily relied

on effector transfection into host cells [71,113,114,121,162,165,171,219]. Transfection-based single effector studies are unable to address effector redundancy cooperation. Furthermore, the nuanced complexities in the specific roles of individual effectors are not captured by single effector studies, and single effector protein function studies lead to oversimplification of the complex host-pathogen interaction. For these reasons, identification of molecular targets of T3SS2-secreted effectors is challenging. To address the above challenges, I aimed to create a *S.* Typhimurium strain that secretes increased amounts of all T3SS2-secreted effectors by overexpressing components of the *ssrA/B* two component system.

In this study, I created a strain that secretes increased amounts of T3SS2-secreted effectors by inserting a chromosomal *ssrB* duplication at a location distant from the SPI-2 locus. An elevated copy number of *ssrB* through expression from a plasmid has previously been shown to increase secretion of T3SS2 effectors [235]. Increased *ssrB* expression has been hypothesized to allow SsrB to self-activate through spontaneous dimerization and self-phosphorylation, a similar process known to occur with other *S.* Typhimurium regulators of two component systems [235,241],

The T3SS2^{+} mutant infected approximately the same proportion of HeLa cells as wild type, but significantly increased the proportion of infected cells with SIF relative to wild type infected cells. It is important to note that the percentage of infected cells with SIFs was counted, not the percentage of intracellular *S.* Typhimurium cells producing SIFs, and not the total number of SIF tubules within each cell. These alternative metrics may provide additional insight into the effect of *ssrB* overexpression on the frequency of SIFs in infected cells. Given the increase in SseD and SseB secretion by the T3SS2^{+} strain and the increased SIF biogenesis in

T3SS2$^+$ infected cells, I am confident that the extra chromosomal copy of *ssrB* is sufficient to upregulate SPI-2 expression and its associated T3SS2-secreted effectors.

I created single effector deletion mutants of each of the six effectors of interest enabling complementation of effector deletion with tagged versions of each effector. The HA-tagged effectors were secreted by the T3SS2$^+$ strain, indicating that effector secretion was not impaired by either the increased SPI-2 expression or the double HA tags. Complementation of the SIF phenotype in the single-effector deletion mutants was met with mixed success. There was not a significant increase in the frequency of infected cells with SIFs when the T3SS2$^+$Δ*sopD2* strain was complemented with a plasmid expressing SopD2-2HA (Figure 3.7C). I have previously demonstrated that deletion of *sopD2* from wild type SL1344 reduces the frequency of SIFs in infected HeLa cells (Figure 2.2), thus successful complementation should at least partially restore/increase the frequency of SIF biogenesis. Other groups have successfully increased the frequency of SIF in HeLa cells infected with complemented SL1344Δ*sopD2* using the same pSopD2-2HA plasmid [161,171]. SopD2-2HA is secreted at high levels by the T3SS2$^+$strain under SPI-2 inducing conditions (Figure 3.4). I observed very little SopD2-2HA secretion with pSopD2-2HA complementation in T3SS2$^+$Δ*sopD2,* yet SseD secretion remains robust indicating that T3SS2-secretion remains unaffected (Figure 3.5). It stands then to reason that the insignificant rescue of the SIF phenotype in the complemented T3SS2$^+$Δ*sopD2* strain (Figure 3.7C) may not be due to a non-functional translocated effector, but rather translocation of a limited amount effector resulting in an imperceptible difference between the complemented and uncomplemented T3SS2$^+$Δ*sopD2* strains.

The T3SS2$^+$Δ*pipB2*-pPipB2-2HA strain exhibited fewer SIFs than its uncomplemented counterpart strain. The reduction of SIFs in a strain complemented with a plasmid-borne copy of

PipB2-2HA has been previously observed [72]. They noted that the plasmid encoding *pipB2*-2HA, while a low copy-number plasmid, has more copies of the genes encoding *pipB2* relative to the single copy of *pipB2* in the chromosome resulting in increased synthesis and translocation of PipB2-2HA [72,242,243]. Consistent with our findings, other groups observed reduced SIF frequency both with deletion of *pipB2* and overexpression of *pipB2* [72,114]. PipB2 functions to reorganize late endosomal and lysosomal compartments within host cells [72]. Expression of *pipB2* at wild type levels promotes SIF extension away from the SCV. However, overexpression of *pipB2* induces accumulation of late endosomal and lysosomal compartments at the cell periphery thereby reducing the pool of membrane components necessary for SIF biogenesis and thus reduces the frequency of SIF biogenesis [72]. The decrease in SIF frequency in the T3SS2$^+$Δ*pipB2*-pPipB2 strain is not likely due to a failure in complementation, but rather a successful complementation resulting in an altered phenotype.

Our results indicate that expression of pPipB2-2HA may decrease T3SS2 expression or secretion as evidenced by the absence of SseD secretion in the complemented T3SS2$^+$Δ*pipB2* strain (T3SS2$^+$Δ*pipB2*-pPipB2-2HA) (Figure 3.5). Despite this, SIFs are observed in HeLa cells infected with complemented T3SS2$^+$Δ*pipB2*. Therefore, the complemented T3SS2$^+$Δ*pipB2* strain must have active T3SS2-secretion and its associated effectors despite having decreased SseD expression and/or secretion. The effect of *pipB2* overexpression in the complemented T3SS2$^+$Δ*pipB2* strain on reducing SIF frequency may therefore be twofold: 1) PipB2-mediated reorganization of the late endosomal and lysosomal compartments reduces membrane components for SIF biogenesis, and 2) decreasing, but not ceasing, T3SS2 expression, by reducing SseD which is a component of the T3SS2 apparatus.

Taken together, I have developed a toolkit comprising a strain with increased expression of SPI-2 and a library of tagged effectors to facilitate further study of the effectors associated with SIF biogenesis, intracellular positioning of the SCV, and SCV membrane dynamics modulation during infection. This toolkit can be used to further investigate the complexities of *S.* Typhimurium infection and to unravel how multiple effectors are required to facilitate establishment of the *S.* Typhimurium intracellular replicative niche.

Chapter 4: The type III secretion system effectors SopD2 and PipB2 interact with host annexin A2

4.1 Synopsis

Intracellular pathogens need to establish an intracellular replicative niche to promote survival and replication within the hostile environment of the host cell. *S.* Typhimurium initiates formation of the unique *Salmonella*-containing vacuole and an extensive network of *Salmonella*-induced tubules in order to survive and thrive within host cells. At least six T3SS2-secreted effectors, namely SifA, SopD2, PipB2, SteA, SseJ, and SseF purportedly manipulate host cell intracellular trafficking and establish the intracellular replicative niche for *S.* Typhimurium. The phenotypes of these effectors are both subtle and complex, complicating elucidation of the mechanism underpinning host cell manipulation by *S.* Typhimurium.

In this work we used stable isotope labeling of amino acids in cell culture (SILAC) and a previously created *ssrB* overexpression mutant (see Chapter 3) to identify cognate effector binding partners during infection. Using this method, we identified the host protein annexin A2 as a binding partner for both SopD2 and PipB2 and confirmed its binding to SopD2 by reciprocal pull-down. This indicates that SopD2 and PipB2 likely both interact with annexin A2 through protein-protein interactions to establish the *S.* Typhimurium intracellular replicative niche. This demonstrates the value of studying effector interactions using proteomic techniques and natural effector delivery during infection rather than transfection.

4.2 Introduction

Understanding the mechanism for formation of the *S.* Typhimurium intracellular replicative niche is imperative to developing new treatment strategies to disrupt infection at the early stages. T3SS2-secreted effectors SifA, SopD2, SteA, PipB2, SseJ, and SseF mediate interactions with the host endomembrane system to facilitate SIF biogenesis, SCV membrane maintenance, and subcellular SCV localization of the throughout infection [80]. We have previously shown that these phenotypes during infection are mediated by multiple effectors; a single effector of our six of interest is not solely responsible for mediating these infection phenotypes (Chapter 2). Characterization of the protein-protein interactions mediating these critical infection stages is key to understanding the significance of T3SS2-secreted effectors during *S.* Typhimurium infection. The overlapping and redundant nature of many T3SS2 effectors hampers efforts to discover novel effector functions. Concerted efforts by several research groups to understand the precise mechanisms permitting these interactions during infection have highlighted the essentiality of these effectors but have stopped short of finding a detailed mechanism.

As we have shown previously in Chapter 2, effector phenotypes during infection are nuanced and complex in ways that are not captured by single effector studies because it is likely that effectors work in concert to mediate multiple aspects of SIF biogenesis or SCV membrane maintenance. Additionally, effectors may interact with multiple host proteins dynamically over the course of infection. Host binding partners for SifA, SopD2, SteA, PipB2, SseJ, and SseF have previously been identified (reviewed in [80]), however these effector-host binding partners were largely identified by single-effector transfection studies. Single effector studies express effectors out the of the context of a native infection, which would not be expected to demonstrate

a phenotype if multiple T3SS2 effectors cooperate to form SIFs or maintain the SCV membrane. The concept of two effectors binding to same host protein was recently illustrated by a study showing that both PipB2 and SifA both form a complex with host kinesin-1 to regulate its activity and promote centrifugal extension of SIFs along microtubules [115]. This result was not captured by transfection-based single effector studies that initially identified the host-binding partners for SifA and PipB2 [110,114].

While a detailed mechanism for SIF biogenesis remains elusive, the purpose of SIFs during infection was recently discovered as providing intravacuolar *S.* Typhimurium with nutrients to promote growth [193,194]. It has been firmly established that the membrane components required for SIF biogenesis come from the host cell. *S.* Typhimurium redirects the host's endosomal system in a T3SS2-dependent manner to form SIFs, gather nutrients from the host, and protect intravacuolar *S.* Typhimurium from host defences [100].

Despite these advances in understanding the *S.* Typhimurium intracellular lifestyle, several questions remain: Which host compartments do membranes for SIF biogenesis come from? What is the mechanism by which T3SS2-secreted effectors mediate integration of host membranes for SIF biogenesis? How do host membranes fuse to either the SCV or SIFs? A detailed mechanism would certainly help to answer these questions.

In order to answer these questions, we set out to identify cognate binding partners of the effectors associated with SIF biogenesis, SCV membrane maintenance, and intracellular positioning of the SCV during infection. We used SILAC (stable isotope labelling with amino acids in cell culture) to identify effector binding partners during infection. SILAC is a quantitative mass spectrometry-based technique that relies on non-radioactive isotopic labelling to detect differences in protein abundance between different samples. This is accomplished by

growing two populations of tissue culture cells in differentially "labelled" media: one population is cultivated in normal growth medium ("light labelled"), while the second is cultivated in growth medium supplemented with stable heavy isotopes of lysine and arginine ("heavy labeled"). The differential labelling of experimental and control cell populations enables direct comparison of the control sample versus the experimental sample. A SILAC ratio greater than 1 occurs when the abundance of a specific protein purified from the experimental sample is significantly higher than the control sample, thus indicating a specific interaction. In contrast, the abundance of non-specific proteins should be comparable in both control and experimental samples resulting in a ratio close to 1 [244]. Thus, SILAC enables distinguishment between non-specific and specific protein-protein interactions. This methodology permits identification and quantification of effector binding partners, whether that be a host protein or a secreted bacterial effector. Our lab previously used the SILAC method to identify protein-protein interactions during *S.* Typhimurium infection by incorporating stable isotope-labelled amino acids into the entire proteome of host cells, followed by effector transfection, immunoprecipitation of effector complexes, and analysis by mass spectrometry [218].

A challenge in immunoprecipitation of T3SS2 effectors during infection is the limitation of low abundance of T3SS2-secreted effectors *in vitro* and within host cells. We previously created a *S.* Typhimurium strain that overexpresses *ssrB* ($T3SS2^{+}$) to increase T3SS2-secretion and tagged each of our six effectors of interest enabling immunoprecipitation of each effector from infected cells (Chapter 3), resulting in expression and translocation of tagged T3SS2 effectors into host cells. In the following study, we presumed that these effector overexpression strains would provide sufficient material to permit identification of effector-effector or effector-host protein interactions.

We hypothesize that the nuanced phenotypes resulting from effector deletion studies arise from effectors targeting the same host protein or forming an effector-effector complex. In this study, we aimed to get the entire picture of T3SS2-secreted effector protein-protein interactions during infection by performing a series of immunoprecipitation experiments in SILAC-labelled host cells infected *ssrB* overexpression mutants secreting HA-tagged T3SS2- effectors. We identified the host protein annexin A2 as potential target of both SopD2 and PipB2 and confirmed the interaction between annexin A2 and SopD2 by a reciprocal pull-down experiment. This indicates annexin A2 may be an important target for *S*. Typhimurium during infection. In addition, these data show that interaction of multiple effectors with host proteins in multi-protein complexes could explain the ambiguous and subtle phenotypes observed in single-effector deletion mutants.

4.3 Materials and Methods

4.3.1 Bacterial strains, culture conditions, and plasmids

All bacterial strains were routinely grown in Luria Bertani (LB) medium at 37˚C with shaking and supplemented with antibiotics when appropriate. Broth cultures were inoculated from single bacterial colonies on LB agar plates containing appropriate antibiotics. Antibiotic concentrations were as follows: streptomycin 50 μg/mL and chloramphenicol 30 μg/mL. A complete list of bacterial strains and plasmids used in this study is described in Table 4.1 and Table 4.2, respectively.

Table 4.1 - Bacterial strains used in this study

Strain Designation	Relevant Characteristics/Genotype	Source/Reference
T3SS2$^+$	chromosomal duplication of *ssrB* in *S.* Typhimurium SL1344 resulting overexpression of SPI-2 and its associated effectors	Section 3.3.1
E. coli DH10B	*F- araDJ39 Δ(ara, leu)7697 ΔlacX74 galU galK rpsL deoR ϕ80dlacZΔM15 endAI nupG recAl mcrA Δ(mrr hsdRMS mcrBC)*	[205]
T3SS2$^+$ Δ*sifA*-pSifA-2HA	*sifA* single deletion mutant in the *ssrB* overexpressing mutant background complemented pSifA-2HA	Section 3.3.1
T3SS2$^+$ Δ*sopD2*-pSopD2-2HA	*sopD2* single deletion mutant in the *ssrB* overexpressing mutant background complemented with pSopD2-2HA	Section 3.3.1
T3SS2$^+$ Δ*pipB2*-pPipB2-2HA	*pipB2* single deletion mutant in the *ssrB* overexpressing mutant background complemented with pPipB2-2HA	Section 3.3.1
T3SS2$^+$ Δ*steA*-pSteA-2HA	*steA* single deletion mutant in the *ssrB* overexpressing mutant background complemented with pSteA-2HA	Section 3.3.1
T3SS2$^+$ Δ*sseJ*-pSseJ-2HA	*sseJ* single deletion mutant in the *ssrB* overexpressing mutant background complemented with pSseJ-2HA	Section 3.3.1
T3SS2$^+$ Δ*sseF*-pSseF-2HA	*sseF* single deletion mutant in the *ssrB* overexpressing mutant background complemented with pSseF-2HA	Section 3.3.1
T3SS2$^+$ pACYC-2HA	*ssrB* overexpressing mutant transformed with pACYC184 containing a 2xHA tag under the control of the native promoter for *pipB2* expression	This study

Table 4.2 - Plasmids used in this study

Plasmid Designation	Relevant Characteristics/Genotype	Source/Reference
pSopD2-2HA	SopD2 with a tandem C-terminal HA tag in pACYC184	[171]
pSifA-2HA	Tandem HA Tag in middle of SifA in pACYC184	[176]
pPipB2-2HA	PipB2 with a tandem C-terminal HA tag in pACYC184	Section 3.3.2
pSteA-2HA	SteA with a tandem C-terminal HA tag in pACYC184	Section 3.3.2
pSseJ-2HA	SseJ with a tandem C-terminal HA tag in pACYC184	Section 3.3.2
pSseF-2HA	SseF with a tandem C-terminal HA tag in pACYC184	Section 3.3.2
pACYC-2HA	Tandem HA Tag under the control of the native *pipB2* promoter in pACYC184	This study

4.3.2 Generation of T3SS2$^+$ pACYC-2HA

Phusion High-Fidelity DNA Polymerase (NEB) was routinely used for PCR. The plasmid pPipB2-2HA was simultaneously amplified and linearized using the following primers: 5'-GTACGCCTCGAGGAGTGAACGCTCCATATATTTTCTCCCAGAGACAG-3' and 5'-CGAATTTTATAGTGAAAATATTCTCGAGTATCCGTATG-3' (XhoI restriction sites). The entire plasmid except for amino acids 6-350 in PipB2 were amplified, leaving the entire backbone of pACYC184, the native promoter for *pipB2,* and first 5 amino acids of PipB2. The

amplified linearized plasmid was digested with XhoI (NEB) and ligated back together using T4 DNA ligase (Invitrogen) resulting in circularized plasmid with truncated *pipB2* fused to the tandem double HA tag under the control of the native promoter for *pipB2* (pACYC-2HA). The resulting plasmid was transformed into *E. coli* DH10B for plasmid propagation and sequencing. Plasmid was sequenced (Genewiz) prior to transformation into the T3SS2^{+} *ssrB* overexpression strain to generate T3SS2^{+}pACYC-2HA.

4.3.3 Cell lines

HeLa cells (ATCC® CCL-2™) were routinely cultured normal growth media: Dulbecco's Modified Essential Medium (DMEM) (Hyclone) containing 10% (v/v) heat-inactivated fetal bovine serum (FBS) (Gibco), 1% (v/v) Glutamax (Gibco), and 1% (v/v) nonessential amino acids (Gibco). Cells were maintained at 37˚C in a 5% CO_2 atmosphere.

4.3.4 SILAC labelling

HeLa cells were split from normal growth media into arginine and lysine-free DMEM (Caisson Laboratories Inc.) supplemented with 10% heat inactivated dialyzed FBS (Gibco) and either 1 mM $^{2}H_4$-lysine and 0.1 mM $^{13}C_6$-arginine (Cambridge Isotope Laboratories) for heavy cells or normal isotopic abundance of L-lysine and K-arginine (Sigma) for light cells. Cells were maintained in labelling media for at least 5 cell divisions to ensure complete labelling as previously described [245].

4.3.5 HeLa infections and analysis

Light and heavy labelled HeLa cells were seeded at a density of approximately 4.5 x 10^6 cells per 15 cm culture plate 16-24 hours prior to infection. For all HeLa cell infections: overnight bacterial cultures were subcultured 1:33 in LB without antibiotic and incubated for 3 hours at 37˚C with shaking. 1 mL of bacterial cultures were pelleted and resuspended in Dulbecco's Phosphate-Buffered Saline (DPBS) (Hyclone), diluted in the appropriate isotope-supplemented DMEM, and added to the HeLa cells at a multiplicity of infection (MOI) of ≈ 100:1. Infections proceeded for 15 minutes at 37˚C in 5% CO_2, after which non-internalized bacteria were removed by three washes in DPBS and cells incubated in growth media containing 100 μg/mL gentamicin until 2 hours post-infection, followed by growth media containing 10 μg/mL gentamicin for the remainder of the experiment. HeLa cells were infected for a total of 8 hours (Figure 4.1)

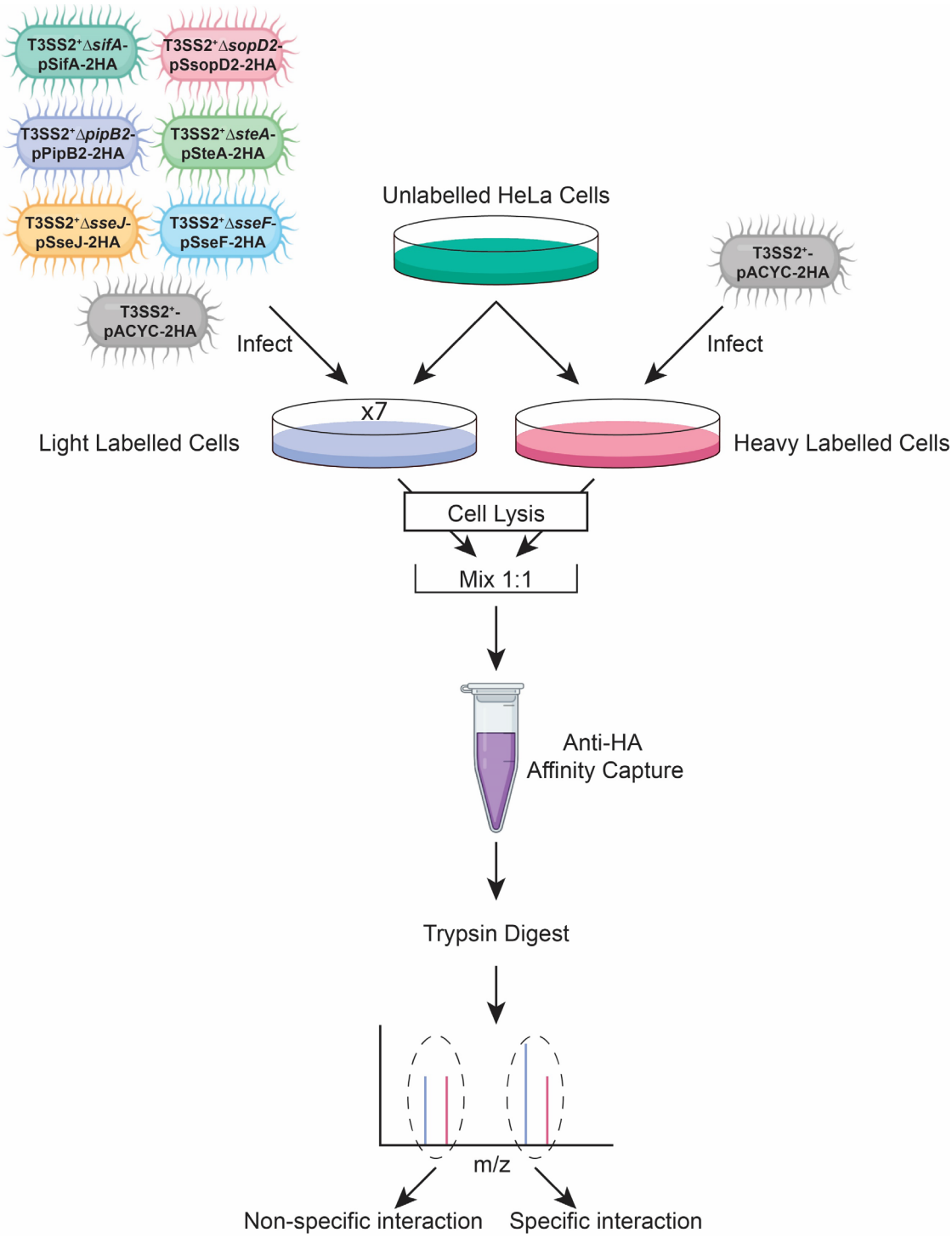

Figure 4.1 - Schematic representation of SILAC methodology and infection experiments. HeLa cells are grown in SILAC medium for at least 5 doublings to ensure complete incorporation of the isotope labels. Cells are infected with the indicated strains (one 15 cm dish for each strain) for 8 hours prior to cell lysis. Lysate from each dish of infected cells is mixed with an equivalent amount of lysate from heavy-labelled cells infected with a T3SS2^{+} strain secreting the control vector. Samples are processed for simultaneous identification and quantification of host and bacterial peptides. Parts of figure created using Biorender.com.

For two of the three replicate experiments, seven 15 cm cell culture plates of light labelled HeLa cells were infected with one of T3SS2$^+$Δ*sifA*-pSifA-2HA, T3SS2$^+$Δ*sopD2*-pSopD2-2HA, T3SS2$^+$Δ*pipB2*-pPipB2-2HA, T3SS2$^+$Δ*steA*-pSteA-2HA, T3SS2$^+$Δ*sseJ*-pSseJ-2HA, T3SS2$^+$Δ*sseF*-pSseF-2HA, or T3SS2$^+$pACYC-2HA (vector control) (Table 4.1), while seven 15 cm cell culture plates of heavy labelled HeLa cells were infected with T3SS2$^+$pACYC-2HA. For the third experimental replicate, we performed a label swap wherein seven 15 cm cell culture plates of light labelled HeLa cells were infected with T3SS2$^+$pACYC-2HA and seven 15 cm cell culture plates of heavy labelled HeLa cells were infected with one of T3SS2$^+$Δ*sifA*-pSifA-2HA, T3SS2$^+$Δ*sopD2*-pSopD2-2HA, T3SS2$^+$Δ*pipB2*-pPipB2-2HA, T3SS2$^+$Δ*steA*-pSteA-2HA, T3SS2$^+$Δ*sseJ*-pSseJ-2HA, T3SS2$^+$Δ*sseF*-pSseF-2HA, or T3SS2$^+$pACYC-2HA. This label swap allowed us to control for interference by the heavy or light isotopes used for SILAC labelling.

Infected light and heavy labelled cells were washed three times in ice cold DPBS and manually detached from the culture dish containing 5 mL ice-cold DPBS and transferred into 15 mL tubes. Cells were spun at 300 x *g* for 10 minutes in a centrifuge set to 4˚C. The supernatant was removed, and cell pellets were resuspended in RIPA buffer (25 mM Tris-HCl pH 7.6, 150 mM NaCl, 1% NP-40, 1% sodium deoxycholate, 0.1% SDS, supplemented with cOmplete protease inhibitor cocktail (Roche)) and incubated on ice for 10 minutes. Cell lysates were centrifuged for 20 minutes in a 4˚C microcentrifuge at max speed to pellet cell debris. Protein concentrations were determined using a Bicinchoninic Acid Assay (BCA) (Sigma). Lysates from cells infected with each of the seven different T3SS2$^+$ strains were then mixed at a 1:1 ratio with lysate from the opposite SILAC labelled HeLa cells infected with the vector control T3SS2$^+$pACYC-2HA. *E.g.,* lysate from light labelled HeLa cells infected with T3SS2$^+$Δ*sifA*-

pSifA-2HA was combined at a 1:1 ratio with lysate from heavy labelled HeLa cells infected with T3SS2^{+}pACYC-2HA. 25μL of anti-HA magnetic beads (Thermo Fisher Scientific) were added to mixed lysates and incubated with end-over-end rotation overnight at 4˚C. Immunoprecipitated proteins were eluted from the magnetic beads using a basic elution protocol according to manufacturer's specifications. Eluted proteins were separated by SDS-PAGE, bands were excised and subjected to in-gel tryptic digestion as described previously [246]. The resulting peptides were analyzed by liquid chromatography-tandem mass spectrometry (LC-MS/MS) using an Bruker Impact II Qtof as described elsewhere [247]. Peptides were searched on MaxQuant version 1.6.7.0 against UniProt sequence database for human and *S.* Typhimurium.

4.3.6 Pull-down assays

Strains T3SS2^{+}Δ*sopD2*-pSopD2-2HA, T3SS2^{+}Δ*pipB2*-pPipB2-2HA, and T3SS2^{+}pACYC-2HA were grown in LB for 9 hours at 37˚C with shaking. SPI-2 expression was induced by washing cell pellets from cultures twice in LPM (low phosphate and low magnesium-containing medium; 5 mM KCl, 7.5 mM $(NH_4)_2SO_4$, 0.5 mM K_2SO_4, 80 mM MES, 38 mM glycerol (0.3% v/v), 0.1% casamino acids, 24 μM $MgCl_2$, 337 μM PO_4^{3-} [230]), prior to inoculation at a 1:50 dilution in 400 mL of LPM at a pH of 5.8. Cells were pelleted by centrifugation and culture supernatant was filter sterilized by passage through a 0.22 μm filter. Sterilized culture supernatant was concentrated by passage through a 10 kDa molecular weight cut-off centrifugal filter unit (Millipore Sigma). Protein concentration of the concentrated culture supernatant was determined by BCA assay. Approximately 20 μg of concentrated culture supernatant was mixed with 5 μg of recombinant human His_6-tagged annexin A2 (Novus Biologicals) and incubated with end-over-end rotation at 4 ˚C overnight. Samples were incubated

with Ni-Sepharose High Performance Beads (Sigma) for two hours at room temperature. Beads were washed four times with TBS-T (20 mM Tris-HCL, 150 mM NaCl, 0.75% Triton X-100), resuspended in 160 μL SDS-PAGE loading buffer, and boiled for 10 minutes prior to Western blot analysis.

4.3.7 Western blotting

Samples were separated on 12% polyacrylamide gels and transferred to Pure Nitrocellulose (Bio-Rad) using a wet transfer cell. Membranes were blocked with blocking buffer (5% w/v skim milk powder in Tris-buffered saline containing 0.1% Tween-20 (TBS-T)) overnight at 4˚C. Membranes were incubated with the following primary antibodies diluted in blocking buffer for one hour at room temperature: α-HA (rat; Roche) diluted 1:2000 and α-Annexin A2 Clone 5 (mouse; BD Biosciences) diluted 1:2000. Membranes were washed three times for five minutes each with TBS-T prior to incubation with the following secondary antibodies diluted in blocking buffer for one hour at room temperature: HRP-conjugated goat α-rat or goat α-mouse (Sigma) diluted 1:5000. Membranes were washed as described above and treated with ClarityTM Western ECL Substrate (Bio-Rad) prior to chemiluminescent developing.

4.3.8 Data analysis

Mass spectrometry data was analyzed in Perseus version 1.6.7.0. Venn diagrams were created in RStudio (https://www.rstudio.com) using the Eulerr package. STRING analysis was performed using the STRING database online tool version 11.0 (https://string-db.org/). Graphs were made using Prism9 (GraphPad)

4.4 Results

4.4.1 Identifying of effector interaction partners

We set out to systematically investigate effector-effector and effector-host protein interactions during *S.* Typhimurium infection through quantitative proteomic analysis of *S.* Typhimurium infected SILAC-labelled HeLa human epithelial cells. Briefly, HeLa cells were infected with the T3SS2^{+} strain harboring plasmid encoded HA-tagged effectors of interest (Chapter 3). Pull-down of HA-tagged effectors and interacting proteins was performed by immunoprecipitation against the tagged effector's HA tag (effector-IP). Immunoprecipitated complexes were then profiled by mass spectrometry. In total, we identified 554 different proteins originating from either the human or *S.* Typhimurium proteome after removal of common contaminants. Proteins were further gated for those with infection/control SILAC ratios of at least 0.66, demonstrating a relative difference in quantity between control and infection, thus demonstrating enrichment of that protein and suggestive of an interaction with the tagged effector. 273 proteins passed this threshold which were then used for subsequent analysis (Figure 4.2A).

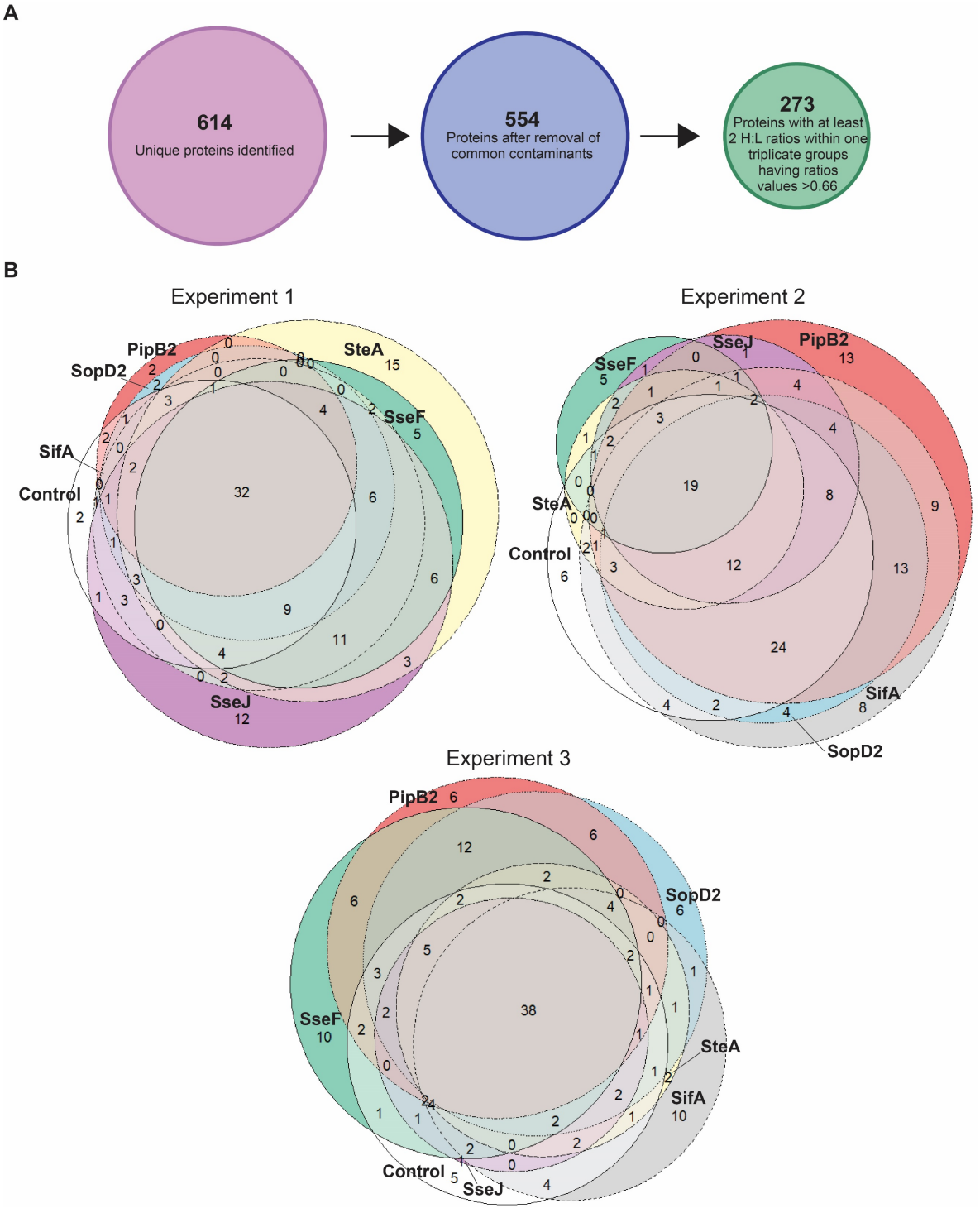

Figure 4.2 - T3SS2-secreted effector-host interactions identified by IP-MS. (A) Visual representation of processing of MS/MS proteins. The number of proteins indicated were from all three replicates. **(B)** Venn diagrams indicating number of unique proteins and common proteins identified by immunoprecipitation and mass spectrometry of each HA-tagged T3SS2 effector as indicated. All proteins with a SILAC ratio of 1 or greater were included in this analysis. Area of overlap is approximately proportional to the number of proteins that fall into that group. Each replicate is shown individually to illustrate inter-replicate variability.

Figure 4.2B illustrates the number of unique and common proteins identified by each immunoprecipitation of and subsequent mass spectrometry (IP-MS) analysis of each HA-tagged effector. There was a large amount of overlap amongst the effector-IPs, both with each other, as well as with the control-IP of SILAC-labelled HeLa cells infected with T3SS2^{+}pACYC-2HA (empty vector) (Figure 4.2B). This may indicate that T3SS2 effectors bind to similar sets of host or *S.* Typhimurium secreted proteins but may also represent non-specific immunoprecipitation. Inter-replicate variability is likely due to multiple factors including weak interactions between tagged effector and binding partner and alterations in stoichiometry within the cell affecting tagged effector binding. Additionally, relative quantitation of low abundance proteins is challenging, *e.g.,* T3SS2 effectors, as their identification peaks may be difficult to distinguish from normal background noise, non-specific interactors, and small changes in protein abundance causing disproportionately large changes in SILAC ratios [184–186]. While many of these proteins may represent background and non-specific binding, several proteins demonstrated consistently high SILAC ratios in multiple replicates across several samples, so we focused on these for further analysis.

4.4.2 SopD2 and PipB2 share common interaction partners

We constructed a list of proteins with SILAC ratios approximately greater than 1.2 to differentiate from non-specific protein interactions (see Table B.1 in Appendix B for full list of proteins). We then performed STRING analysis [248] on these proteins for all effector-IPs to identify trends or common interaction partners or networks amongst the effector-IPs. STRING is a database of known protein-protein interactions including both direct and indirect associations. Direct associations are protein-protein binding events and indirect associations are proteins interacting together on a similar pathway, but not directly binding to each other. The STRING

analysis on the list of proteins with SILAC ratios greater than 1.2 from the SopD2-IPs and PipB2-IPs revealed several identified proteins in common that may interact either directly or indirectly (Figure 4.3). Specifically, the proteins alpha-actinin-4, annexin A2 (AnxA2), vimentin, and plectin appear to form a series of protein-protein interactions. Each of these four proteins were consistently enriched in both the SopD2- and PipB2-IPs, suggesting that a multi-protein complex between SopD2, PipB2, and these host proteins may form.

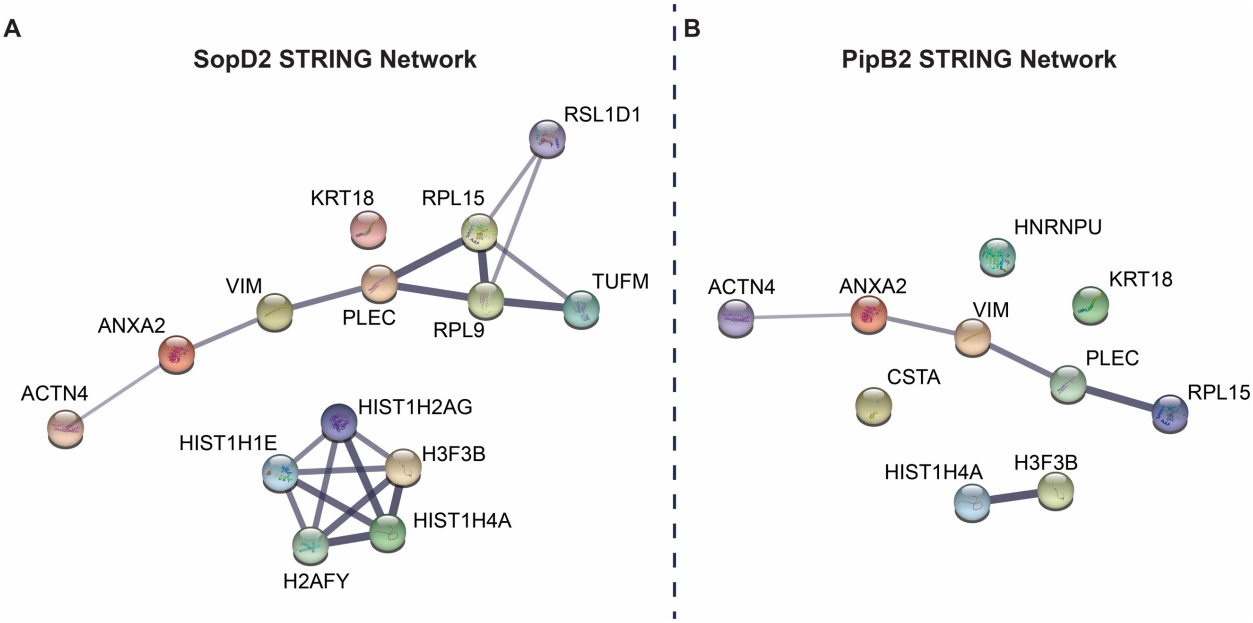

Figure 4.3 - SopD2 and PipB2 immunoprecipitation reveals common proteins that are either directly or indirectly linked. STRING analysis on the top hits from the SopD2-IP **(A)** and PipB2-IP **(B)** as identified by mass spectrometry. The STRING network shows both functional and physical protein associations. Line thickness indicates the strength of data supporting the interaction with a minimum confidence of interaction score of 0.4.

Within our data set, we gated for either host or *S.* Typhimurium proteins found in two or more effector-IPs in two or more experimental replicates. Table 4.3A (SopD2-IP) and Table 4.3B (PipB2 IP) show that in experimental replicates 2 and 3, the host proteins AnxA2, vimentin, alpha-actinin-4, and plectin, are consistently enriched in the *S.* Typhimurium SopD2- and PipB2-IP samples relative to control. Vimentin was found with a median 1.579-fold and 1.530-fold

increase in SopD2 and PipB2 IPs relative to control, respectively. AnxA2 was found with a median 1.213-fold and 1.313-fold increase in SopD2 and PipB2 IPs relative to control, respectively. Alpha-actinin-4 was found with a median 1.225-fold and 1.268-fold increase in SopD2 and PipB2 IPs relative to control, respectively. Finally, plectin was found with a median 1.629-fold and 1.752-fold increase in SopD2 and PipB2 IPs relative to control, respectively. It is important to note that vimentin and alpha-actinin-4 were also found with SILAC ratios slightly less than 1 in $Control_{Heavy}$:$Control_{Light}$ samples (data not shown) suggesting that vimentin and alpha-actinin-4 may be non-specifically binding to the anti-HA coated magnetic beads.

Table 4.3 - SILAC ratios of important hits from SopD2 and PipB2 IPs identified by STRING analysis. Effector:control SILAC ratios for each replicate, as well as the median for the four related hits identified from the **(A)** SopD2-IP and **(B)** PipB2-IP. Negative values represent missing values (*i.e.,* protein was not detected in that replicate) imputed from Perseus version 1.6.7.0.

(A): Proteins identified by SopD2-IP.

Replicates			Median	Protein
1	2	3		
0.634	1.579	1.656	1.579	Vimentin
0.528	1.519	1.213	1.213	Annexin A2
-0.354	1.294	1.225	1.225	Alpha-actinin-4
0.206	1.799	1.629	1.629	Plectin

(B): Proteins identified by PipB2-IP.

Replicates			Median	Protein
1	2	3		
0.712	1.545	1.530	1.530	Vimentin
0.594	1.960	1.313	1.313	Annexin A2
0.789	1.395	1.268	1.268	Alpha-actinin-4
-1.215	2.142	1.752	1.752	Plectin

It is unclear why experimental replicate 1 does not follow the same trend as experimental replicates 2 and 3 for vimentin, AnxA2, alpha-actinin-4, and plectin; however, it is worth noting that these four proteins were all found with low—and sometimes absent as represented by negative values—SILAC ratios in replicate 1, but significantly higher SILAC ratios in replicates

2 and 3. This suggests variation in either sample preparation or host cell culture causing an unknown issue with the SopD2 and PipB2 IPs in replicate 1. Despite this, we are confident in our data given that replicates 2 and 3 have consistently higher SILAC ratios for all four proteins.

4.4.3 Identified proteins common between effector-IPs

The *S.* Typhimurium T3SS1-secreted effector SipC was identified in the SifA-IP (1.487-fold increase), PipB2-IP (1.932-fold increase), SteA-IP (1.453-fold increase), and SseJ-IPs (1.320-fold increase) with consistently high SILAC ratios relative to control (Table B.1 in Appendix B). Given the role of SipC in invasion and translocation of T3SS1-secreted effectors, it seems unlikely that SipC is a specific interaction partner with SopD2 and PipB2 to regulate the host endomembrane system; however, we cannot discount that SipC could play a role in T3SS2-effector processes during infection. During infection, SipC typically functions to nucleate actin, bind F-actin, and participate T3SS1-secreted effector translocation. It is highly expressed both *in vitro* under T3SS1-inducing conditions and *in vivo* [249]. In our hands, SipC is readily detected in the culture supernatant of *S.* Typhimurium grown under SPI-1 inducing conditions (Figure 3.2) hinting that large amounts of SipC are typically translocated into host cells during infection and are thus easily detected as background by SILAC. Furthermore, SipC was also detected in SILAC-labelled cells infected with the T3SS2^{+} strain harboring the control empty vector (Table B.1 in Appendix B), indicating that SipC may indeed be highly secreted into host cells and may be a non-specific interaction partner with SifA-2HA, PipB2-2HA, SteA-2HA, and SseJ-2HA, or more specifically, a non-specific interaction partner with the HA-tags.

The host protein cystatin A was found to have a median ratio between 4.5- and 9.2-fold more in IPs from SifA, PipB2, SteA, and SseJ, with individual experimental SILAC ratio of up to 14.7 for experimental replicate 1 of SteA (Table B.1 in Appendix B). Cystatin A is a member

of the cystatins superfamily which are a group of protein inhibitors of papain-like cysteine proteinases that efficiently inhibit endogenous lysosomal cysteine proteinases. Cystatin A has been shown to interact with, and likely inhibit the activity of, cathepsins B and L1 [250]. *S.* Typhimurium secreted T3SS2-effectors have previously been implicated in blocking cathepsin D recruitment to the SCV, and several cathepsins are associated with the SCV [108]. However, cystatin A was also found at a very high SILAC ratio between the control groups of infected cells. This could mean that cystatin A is naturally expressed at low levels in HeLa cells but has non-specific interactions with the anti-HA coated magnetic beads used for immunoprecipitation. The low expression of cystatin A would result in drastic detection differences when non-specifically pulled down by the anti-HA beads, and subsequently very high SILAC ratios. However, this does not preclude the possibility that cystatin A binds to SifA, PipB2, SteA, or SseJ in a specific manner. Further work is required to determine the potential role of cystatin A during *S.* Typhimurium infection.

4.4.4 SopD2 targets annexin A2 during *S.* Typhimurium *in vitro*

We decided to validate the interaction between AnxA2 and both SopD2 and PipB2 given that *S.* Typhimurium alters host endosomal maturation and host AnxA2 plays an important role in multiple steps of host cell membrane trafficking [139]. To validate the interactions between AnxA2 and the *S.* Typhimurium T3SS2-secreted effectors SopD2 and PipB2 we performed a reciprocal pull-down, using purified His_6-tagged AnxA2 to enrich for SopD2-2HA and PipB2-2HA. Concentrated culture supernatant from T3SS2$^+$Δ*sopD2*-pSopD2-2HA, T3SS2$^+$Δ*pipB2*-pPipB2-2HA, and T3SS2$^+$ pACYC-2HA was grown under SPI-2 inducing conditions, mixed with His_6-tagged AnxA2, AnxA2 complexes pulled-down against the His-tag, and analyzed by

Western blotting. Both SopD2-2HA and PipB2-2HA were successfully pulled-down along with His_6-AnxA2 (Figure 4.4A).

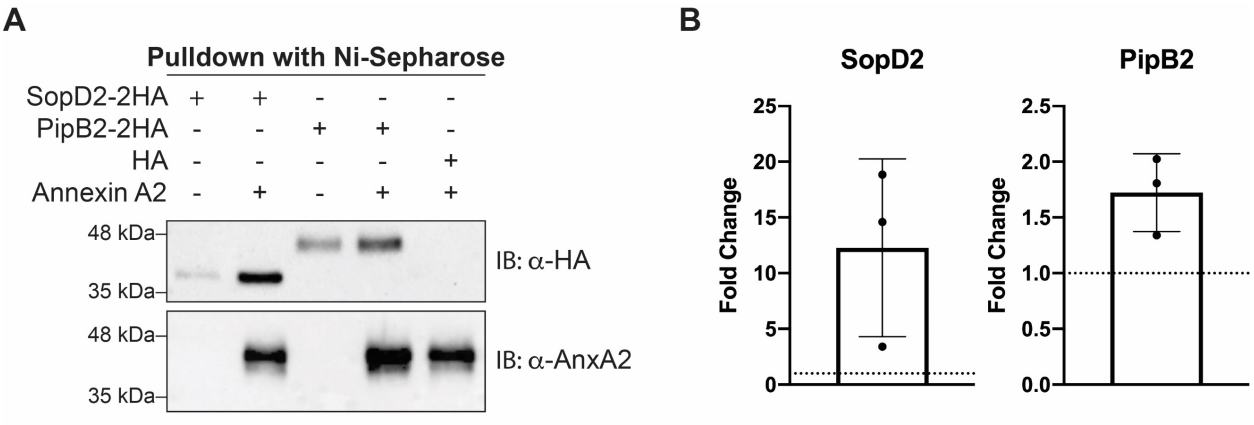

Figure 4.4 - SopD2 targets annexin A2 during infection. Representative blot of reciprocal pull-down of AnxA2 and SopD2 or PipB2. Concentrated culture supernatants of *S.* Typhimurium strains secreting SopD2-2HA, PipB2-2HA, or HA empty vector were mixed with His_6-AnxA2. Pull-downs were analyzed by Western blot using α-HA or α-AnxA2. IB: Immunoblot. Leftmost lane: pull-down of SopD2-2HA in the absence of AnxA2. Lane second from the left: pull-down of SopD2-2HA in the presence of AnxA2. Middle lane: pull-down of PipB2-2HA in the absence of AnxA2. Lane second from the right: pull-down of PipB2-2HA in the presence of AnxA2. Rightmost lane: pull-down of empty vector expressing a HA-tag in the presence of AnxA2. **(B)** Fold change determined by densitometry of 3 Western blots from independent experiments. Mean fold change ± standard deviation is shown. Fold change = (Densitometry of effector + AnxA2)/(Densitometry of effector). Dashed line = 1.

SopD2 was pulled down significantly more in the presence of AnxA2 as compared to the pull-down in the absence of AnxA2. This indicates that while SopD2-2HA can bind to Ni-sepharose without AnxA2, the presence of AnxA2 significantly increases pull down of SopD2. This strongly suggests that SopD2 binds to AnxA2 during *S.* Typhimurium infection.

Increased amounts of PipB2 were also pulled down in the presence of AnxA2. Non-specific binding of PipB2 to the Ni-Sepharose beads makes it difficult to conclude with certainty that PipB2 specifically binds to AnxA2, however in three independent experiments increased amounts of PipB2 was pulled down in the presence of AnxA2 as compared to in the absence of AnxA2 (Figure 4.4B). The non-specific binding of SopD2-2HA and PipB2-2HA in the absence of AnxA2 could be due to exposed histidine residues on the outside surface of SopD2 and PipB2 resulting in effector pulldown by the Ni-Sepharose beads. In all, we can conclude that SopD2

targets AnxA2 during infection and it appears likely from these data that PipB2 also directly interacts with AnxA2.

4.4.5 Annexin A2 in *S.* Typhimurium infection

The process of SIF biogenesis requires the activity of several T3SS2-secreted effectors working in conjunction with each other in order to hijack the host cell's endosomal system [12,194]. To our knowledge, AnxA2 has never been implicated in T3SS2-mediated processes. Given AnxA2's variety of functions within host cell including its involvement in the endocytic pathway, it is conceivable that AnxA2 could play a role in SIF biogenesis. To understand how AnxA2 could play a role in SIF biogenesis, we performed STRING analysis [248] that included the four proteins previously identified by our SILAC screen (AnxA2, vimentin, plectin, and alpha-actinin-4) and other host proteins known to be involved in SIF biogenesis and SCV membrane maintenance identified in previous studies (Figure 4.5).

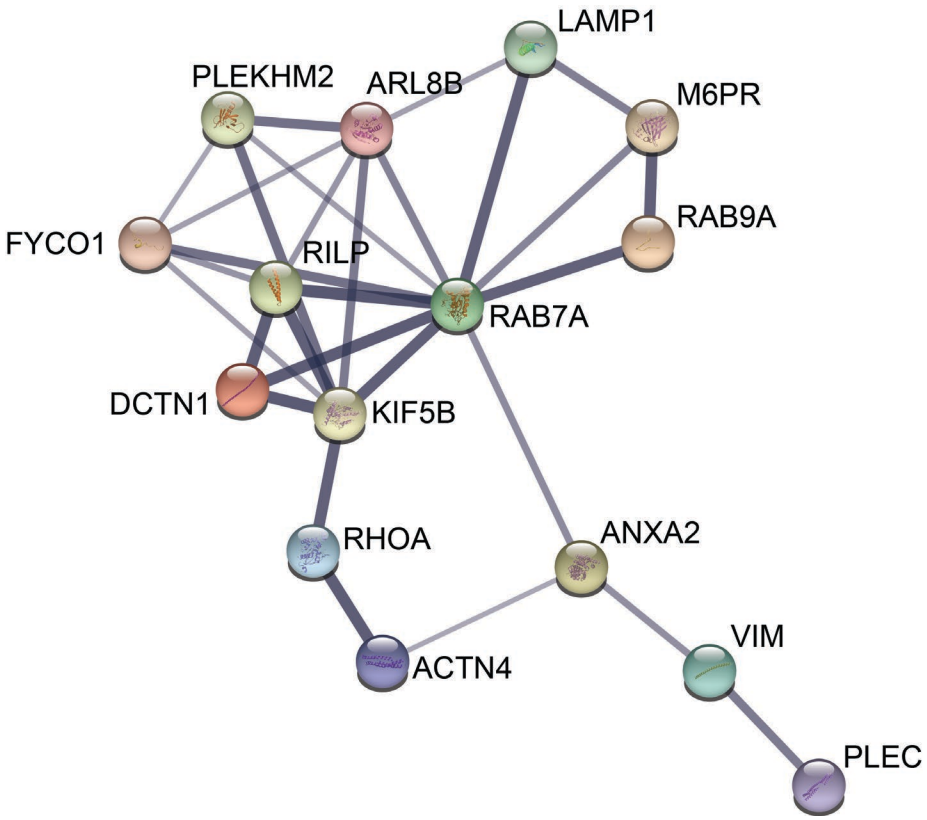

Figure 4.5 - STRING analysis including annexin A2 and host proteins known to interact with T3SS2-secreted effectors to mediate SIF biogenesis. STRING network showing both direct and indirect protein associations between AnxA2 and previously identified host proteins known to be involved in SIF biogenesis. Line thickness indicates the strength of data supporting the interaction with a minimum confidence of interaction score of 0.4.

The STRING analysis shown in Figure 4.5 indicates that AnxA2 associates either directly (*i.e.,* AnxA2 binds Rab7a) or indirectly associates with Rab7a, vimentin, and alpha-actinin-4. The interaction between AnxA2 and both vimentin and alpha-actinin 4, and tangentially plectin, highlights the role of AnxA2 in regulating cytoskeletal rearrangements within the host cell. Identification of vimentin and plectin in association with AnxA2 is likely due to AnxA2's role within the host cell to regulate cytoskeletal rearrangements and may not be directly associated with T3SS2-secreted effectors. However, the association between AnxA2 and alpha-actinin 4, a F-actin crosslinking protein, may be linked to the T3SS2-mediated formation of an actin nest comprised of F-actin around the SCV several hours post invasion. There is also evidence that

AnxA2 interacts either directly or indirectly with Rab7, a known target of SopD2. SopD2 modulates Rab7 activity thereby disrupting endocytic trafficking, and contributing to evasion of lysosomal degradation of intravacuolar *S.* Typhimurium [118]. SopD2 may bind both Rab7 and AnxA2 to alter the host's endocytic maturation programme.

From these data, we theorize that SopD2, and likely PipB2, targets AnxA2 to modulate formation of the actin nest around the SCV or participates in altering the host's endosomal system to promote bacterial replication within the host cell. Further research is required to determine the precise role of AnxA2 during T3SS2-mediated hijacking of the host cell and whether SopD2 and PipB2 bind AnxA2 sequentially or as a SopD2-PipB2 complex.

4.5 Discussion

As an intracellular pathogen, *S.* Typhimurium must enter host cells and establish an intracellular niche permissive of both survival and replication. *S.* Typhimurium relies on secretion of bacterial effectors into host cells to mediate both invasion and creation of its replicative niche. It is widely recognized that the T3SS2-secreted effectors are required to establish and maintain this intracellular niche; however, the precise mechanisms underpinning these processes remain ambiguous. Significant efforts over the years to identify T3SS2-secreted effector binding partners have provided many pieces to the puzzle but understanding how they fit together has proven challenging. Only in recent years have we begun to understand the function of SIFs during infection and small parts of the mechanism underpinning SIF biogenesis, but the mechanism as a whole remains unclear.

Recently, a study compared proximity-dependent biotin labelling (BioID) and immunoprecipitation coupled with mass spectrometry (IP-MS) to investigate T3SS2-secreted

effectors known to manipulate host intracellular trafficking (SifA, SopD2, PipB2, SseF, and SseG) [238]. The authors found that the two methods identified different known interactors suggesting that BioID should be used to compliment, rather than replace, traditional approaches. Furthermore, they suggested that the BioID data set produced by their work represents the molecular environment of the T3SS2 effectors and not necessarily effector binding partners [238]. Thus, we decided traditional techniques such as IP-MS better suits our purposes to identify direct effector binding partners and not proximal interactors.

We demonstrated in a previous study that *S.* Typhimurium requires multiple effectors to establish its replicative niche within host cells (Chapter 2), highlighting the need to study effectors as an ensemble rather than individually. A popular approach to studying T3SS2-effectors—namely SifA, SopD2, PipB2, SteA, SseJ, SseF, and SseG—is to transfect individual effectors into host cells and identify cognate binding partners [109,110,173,186,238,251,113,115,118,121,129,164,170,171]. To our knowledge, no one has attempted to identify multiple T3SS2-effector binding partners during infection and not relied on transfection. We hypothesize that multiple effectors may bind host targets, either cooperating simultaneously or sequentially. Consequently, the absence of any single effector, whether through deletion or transfection of select effectors, may drastically impact identification of host binding partners. For these reasons, we set out to identify T3SS2-secreted effector interactions during infection where all T3SS1 and 2 effectors are present using IP-MS.

The host protein annexin A2 (AnxA2) is a pleiotropic phospholipid and Ca^{2+} binding protein which generally functions to regulate actin-associated processes at dynamic membranes [139]. AnxA2's precise function is regulated by multiple factors including subcellular localization, timing of expression, and formation of either a monomeric or heterotetrameric

complex with p11/S100A10 [133]. AnxA2 influences endosome localization and participates in trafficking specific cargo within the cell in addition to functioning as a platform for actin remodeling near cellular membranes [137,139,252]. AnxA2 is thought to regulate actin associated with both early and late endosomes [150] and may be specifically involved in the maturation of late endosomes [151]. AnxA2 has previously been shown to be involved with T3SS1-mediated invasion [135], but has not been shown to be involved in T3SS2-mediated processes. As *S.* Typhimurium is known to disrupt the maturation of late endosomes and regulation of the conversion from early to late endosomes [100,118,190], and AnxA2 plays a key role within the endosomal system, it would not be surprising if *S.* Typhimurium targets AnxA2 as a means to subvert the host's endocytic and exocytic pathways. AnxA2 could be involved in two distinct T3SS2-mediated processes: 1) redirection of the host endosomal system to promote SIF biogenesis, and 2) linkage between the SCV and the actin nest surrounding in the SCV.

Here, we demonstrate that the T3SS2-secreted effector SopD2, and likely PipB2, targets the host protein AnxA2. To our knowledge, this is the first report of a common binding partner for SopD2 and PipB2. Intriguingly, the single effector deletion mutants of both Δ*sopD2* and Δ*pipB2* exhibit decreased frequency of $LAMP1^{+}$-tubulation (SIFs) in infected cells [72,157]. SopD2 is a guanine nucleotide activating protein whose activity inhibits host endocytic trafficking and promotes SIF biogenesis [80,118,157,171,253]. The N-terminal region of SopD2 directly binds to and inhibits the host GTPase Rab7's ability to exchange nucleotides. This limits Rab7's interaction with host RILP and FYCO1 (kinesin- and dynein- binding effectors) thereby disrupting host-driven regulation of microtubule motors [118]. In uninfected cells, FYCO1 links kinesin-1 to Rab7 localized on the membrane of late endosomes/lysosomes to promote anterograde movement of late endosomes/lysosomes within the cell. Similarly, RILP links

dynein to Rab7 localized on the membrane of late endosomes/lysosomes to promote retrograde movement of late endosomes/lysosomes within the cell [254]. SopD2 inhibition of RILP and FYCO1 accumulation on the SCV membrane may therefore free up host microtubule motors to promote SIF extension [109,118,159,161].

PipB2 contributes to SIF biogenesis by acting as a linker to kinesin-1 to promote centrifugal extension of SIFs along microtubules to the cell periphery [72,114] as evidenced by deletion of *pipB2* significantly reducing the frequency of SIF biogenesis in infected cells. That said, a Δ*pipB2* single effector deletion mutant still forms SIFs, albeit at a lower frequency relative to wild type, indicating a capacity to extend SIFs outwards in even without the PipB2-mediated linkage to kinesin-1.

We theorize that SopD2 and PipB2 both interact with AnxA2 to redirect endosomal trafficking towards the nascent SCV to promote SIF extension outwards from the SCV. In this proposed model, in the events leading up to conversion of late endosomal membrane into SIF membrane SopD2 interacts with Rab7 to indirectly promote SIF extension, and with AnxA2 to regulate late endosomal-associated actin. Binding of PipB2 to AnxA2 may also contribute to these processes. Given that PipB2 acts as a linker between the SCV/SIF membrane and kinesin-1 [114], kinesin-1 indirectly interacts with Rab7 though FYCO1 [254], and the evidence presented here suggesting that PipB2 interacts with AnxA2, we hypothesize that PipB2 interacts with AnxA2 which in turn may interact with Rab7 to indirectly promote SIF extension. In this way binding of SopD2 and PipB2 to AnxA2, either sequentially or concurrently, promotes SIF extension. This hypothesis is supported by evidence presented in Chapter 2 wherein deletion of either Δ*sopD2* or Δ*pipB2* significantly reduces the frequency of SIF extension, suggesting that binding of both SopD2 and PipB2 to AnxA2 may be required to enable maximal SIF extension

frequency (*i.e.,* wild type levels). Since our data suggests both SopD2 and PipB2 likely interact with AnxA2, the deletion of one of Δ*sopD2* or Δ*pipB2* diminishes AnxA2 recruitment, and thereby diminishes, but does not abrogate, SIF extension. It is unclear if a SopD2-PipB2 complex forms prior to binding to AnxA2, or if a SopD2-PipB2-AnxA2 forms. Further work is required demonstrate AnxA2 recruitment to SIFs or the SCV by SopD2 and PipB2 and whether SopD2 and PipB2 binding to AnxA2 occurs sequentially or concurrently.

The single effector deletion mutants Δ*sopD2* and Δ*pipB2* have reduced replication within macrophages and also have altered subcellular localization relative to wild type infected cells [174,216,237]. These altered phenotypes in the Δ*sopD2* and Δ*pipB2* single effector deletion mutants could be explained by altered interactions with the *S.* Typhimurium-induced vacuole-associated actin polymerization (VAP). The VAP plays an important role in SCV membrane integrity and may be involved in regulating the subcellular localization of the SCV during infection [59,128]. AnxA2 functions at sites of actin association with membranes enriched in cholesterol, such as the membrane of the SCV [139,255]. More specifically, AnxA2 is enriched at the junction between vesicles and actin, possibly functioning as a barbed-end capping protein [139]. Given that SopD2 and PipB2 bind AnxA2, we hypothesize that SopD2 and PipB2 recruit AnxA2 to the interface between the SCV and VAP to stabilize the F-actin filaments and link the SCV to the VAP. Deletion of SopD2 would lessen contact, or even completely detach the SCV from VAP, resulting in the observed scattered distribution of SCVs within the host cell cytoplasm as well as the decreased replication in macrophages in the Δ*sopD2* mutant. It is unclear how PipB2 would play into this connection between the SCV, AnxA2, and VAP, as the Δ*pipB2* single effector deletion mutant remains in very close proximity to the Golgi during infection and the Δ*pipB2* mutant only exhibits a mild decrease in intramacrophage replication

relative to wild type [216,237]. Further research is required to determine whether AnxA2 is recruited to the VAP and whether this occurs in a T3SS2-dependant manner. Furthermore, it is unclear if and how binding of AnxA2 to either SopD2 or PipB2 plays into VAP formation.

It was recently shown that the T3SS2-secreted effectors SseL and SseI both interact with annexin A2 during the infection of macrophages [256]. Annexin A2 plays a role in downregulating infection-initiated inflammation in response to invading pathogens as a means to protect the host from excessive inflammatory damage [257]. It is not surprising that AnxA2 interacts with SseL and SseI. SseL prevents accumulation of lipid droplets and induces late macrophage cell death [80], which are both processes that AnxA2 is implicated in. Similarly, SseI is thought to inhibit dentritic cell migration during infection, a process involving rapid actin rearrangements within the cell [80]. Annexin A2 is know to be found at sites of rapid actin rearrangements [150]. Thus, we and another group have described roles for Annexin A2 during the T3SS2-mediated phase of infection.

We were unfortunately unable to identify any known interactors from previous studies in this work. However, it is important to note that our method differed in key ways from previous studies (reviewed in [80]). As previously mentioned, past studies relied heavily on transfection of single effectors into host cells to identify interacting proteins, discounting the possibility that two effectors are required for binding to the same host protein. Here, we infected host cells with *S.* Typhimurium with its entire T3SS2-secreted effector arsenal at its disposal, a strategy with its own advantages and disadvantages over transfection.

The biggest disadvantage to our technique is that the concentration of each effector within the host cell is low as compared to effectors introduced by transfection. Low effector concentration within the host cell makes it difficult to separate specific effector interactions from

the background noise during mass spectrometry. We attempted to mitigate this limitation by using the *ssrB* overexpression strain which increases expression and secretion of T3SS2-secreted effectors (Chapter 3). Nevertheless, the amount of tagged effector within the host cell is likely orders of magnitude less than that of a transfected effector. This may explain why we did not identify known interactors. Protein complex formation is dependent on the stoichiometry of the interacting proteins. High protein concentrations resultant from effector transfection will shift the formation/dissociation equilibrium to one side [258,259], towards strong binding with one protein present at a greater molar ratio than the effector *e.g.*, the known interactors. Given the low concentration of tagged effectors in our study, the formation/dissociation equilibrium is shifted toward what would be natively expected during normal cell infection, allowing for identification of different binding partners.

The advantage of our native infection-based mass spectrometry study is that all effectors are present, permitting both effector-effector interactions and maintaining all effectors at biologically relevant levels, enabling identification of new effector binding partners. Effector transfection may introduce artificially high signal from the more highly expressed host proteins and drown out true effector binding partners. The absence of known binding partners in our study does not indicate a failed experiment, but rather highlights the differences in techniques used to identify host binding partners for T3SS2-secreted effectors.

Collectively, this study highlights the advantages of *S.* Typhimurium native infection in SILAC labelled cells as a valuable strategy to identify T3SS2-secreted effector binding partners. Using this technique, we demonstrate that SopD2 and PipB2 both bind to AnxA2 which may play a role in SIF extension, SCV membrane integrity, and SCV positioning during infection. Further work is required to ascertain the precise role of AnxA2 during infection and the impact

of AnxA2 binding to SopD2 and PipB2. Identification of a host protein potentially involved in these three phenotypes associated with *S.* Typhimurium infection, and two T3SS2-effectors that bind that host protein, potentially explains the nuanced phenotypes observed in the single effector deletion mutants. Our work demonstrates that a global view of T3SS2-secreted effectors during infection is necessary to unravel the complexities of the *S.* Typhimurium intracellular replicative niche.

Chapter 5: Conclusions

5.1 Relevance and contributions to the field

Elucidating the mechanisms underpinning formation and maintenance of the *S.* Typhimurium intracellular replicative niche is challenging for multiple reasons. First, despite significant efforts by several groups, the complete T3SS2-secretome is likely not fully characterized owing to the fact that the genes encoding T3SS2-secreted effectors are dispersed throughout the chromosome [84]. It is therefore possible additional effectors involved in the formation of the intracellular niche are yet to be identified. Second, T3SS2-effectors are secreted from intracellular *S.* Typhimurium into the host cell at a relatively low abundance thus complicating isolation and analysis of effector binding partners. Third, T3SS2-secreted effectors can have multiple host targets, and overlapping and redundant activities [12,80]. In this dissertation, I explore the interplay between T3SS2 effectors and the host endomembrane system taking into account the entire T3SS2-secretome using *in vitro* biochemical techniques, tissue culture analysis, and surrogate host infections.

In Chapter 2 we created a library of multiple T3SS2 effector deletion mutants designed to pinpoint the contribution of a single effector, or group of effectors, on a given intracellular phenotype. Using a systematic approach, we found that multiple effectors are required for: $LAMP1^{+}$-tubule extension, precise subcellular SCV localization, permitting replication in macrophages, and colonization and virulence in mice. This study emphasizes two core concepts: 1) a single effector does not wholly mediate a single process. The intracellular replicative niche requires the activity of multiple effectors working in conjunction with each other. 2) Single effector studies lead to oversimplification of the complex *S.* Typhimurium-host interaction. These findings paint a clear picture that understanding the intracellular replicative niche of *S.*

Typhimurium requires consideration of all potential T3SS2-effector interactions both with each other and cooperatively at host targets. This is a particularly salient point because the majority of effector interaction studies involve transfection of a single effector into a host cell, or single deletion mutants of select effectors [71,113,114,121,162,165,171,173,174,219,260], and therefore do not capture the nuanced complexities of effector-effector interactions.

Using proteomics to identify T3SS2 effector-host interactions is becoming the standard within the field. Often host cells are infected with *S.* Typhimurium single-effector deletion mutants and compared to wild type infected cells. A recent use of this technique found that T3SS2-secreted effectors contribute to nutrition and resistance against antimicrobial host defenses [261]. Another strategy involves transfection of a target T3SS2-secreted effector cloned into a low-copy expression vector into host cells prior to infection with wild type *S.* Typhimurium to study membranes modified during *S.* Typhimurium infection [262,263]. This technique revealed that *S.* Typhimurium redirects endoplasmic reticulum membrane trafficking to its intracellular niche [262], found additional host proteins involved in SCV maturation, and profiled the similarities and differences between *S.* Typhimurium infection HeLa cells and RAW 264.7 cells [263]. These proteomic techniques have provided important insights into the intracellular replicative niche of *S.* Typhimurium but stopped short of providing a mechanism.

In Chapter 3, I designed a toolkit of *S.* Typhimurium strains with increased T3SS2-secretion enabling identification of effector binding partners during infection. In Chapter 4, I identified the host protein AnxA2 as a binding partner for both SopD2 and PipB2 by performing proteomics on SILAC-labelled HeLa cells infected with the toolkit developed in Chapter 3. To our knowledge, this is the first identification of two effectors binding to the same host target in a study involving the entire T3SS2-secretome. Previous studies have shown that effectors can act

on a similar process such as the interaction between SseJ and SifA to promote SIF biogenesis [165], or the cooperation of SifA and PipB2 to recruit and activate kinesin-1 [110,114,167] through their direct interaction with each other [115]. The hypotheses driving these studies were resultant from data from single effector studies.

A new paradigm will exist if indeed both SopD2 and PipB2 interact with AnxA2 to promote either SIF biogenesis or VAP formation as I hypothesized in Chapter 4. This sets the precedent that the involvement of one effector in a process requires another effector to mediate that effect. Thus, those who study the intracellular replicative nice of *S.* Typhimurium must consider the entire T3SS2-secretome. This may be the very hurdle preventing complete mechanism elucidation for SIF biogenesis, SCV membrane maintenance, and subcellular SCV localization.

5.2 Strengths and limitations

Many of the strengths of the research presented in this work have already been discussed in their respective sections. The overarching theme within this dissertation is that T3SS2-secreted effectors must be studied in the context of infection wherein the entire T3SS2-secretome is present in order to tease apart nuanced phenotypes. The biggest advantage to the entirety of this work is that I always respected the natural conditions of effector delivery and avoided "out-of-context" results from overexpression studies. While these overexpression studies have identified stable host targets of secreted effectors, these stable complexes may not necessarily represent the enzymatic target of an effector. To the best of my ability, I specifically avoided overexpression of only one effector, but rather, overexpressed all effectors to overcome the limitations of low effector abundance. By doing so, I identified a new interaction partner for both SopD2 and PipB2 which was not captured in other studies.

There are several limitations to the work presented in this dissertation. One limitation is that I did not have the chance to determine if SopD2 and PipB2 binding to AnxA2 occurs sequentially or concurrently, and if concurrently, whether a SopD2/PipB2 complex forms prior to interacting with AnxA2. I also did not have the chance to determine if binding of either SopD2 or PipB2 to AnxA2 requires prior activity of the other effector. Furthermore, I have not yet tried to demonstrate the biological significance of the SopD2/PipB2 interaction with AnxA2 and which aspect of *S.* Typhimurium infection it mediates. Moreover, it remains unclear what happens to AnxA2 when bound by SopD2 or PipB2. Does it recruit AnxA2 to the SCV? Does it inhibit AnxA2's ability to mediate cytoskeletal reorganizations near the SCV? Does AnxA2 play a role in SIF biogenesis? These questions, and more, have yet to be answered.

A limitation to the SILAC studies was that the majority of SILAC ratios for identified proteins were less than 2 but greater than 1. While these ratios indicate a specific interaction, they make it more difficult to identify possible hits of interest amongst the six effector pull-downs. These ratios are likely the result of the technique used. As mentioned in Chapter 4, overexpression of effectors through transfection can skew protein-protein interactions towards one complex [258,259] resulting in high SILAC ratios, but may not reflect interactions that occur naturally within the cell. Our method relied on potentially the less frequent or strong natural interactions, consequently resulting in lower SILAC ratios. Subcellular fractionation of infected cells can enrich for T3SS2-secreted effectors [171,176,262,263]. To that end, our technique could be improved by fractionation of HeLa cells into cytoplasmic protein, membrane protein, and cytoskeletal protein fractions [264] post infection but prior to immunoprecipitation to concentrate specific interactions resulting in elevated SILAC ratios in comparable fractions.

A broad limitation to the studies presented here is that they were conducted in HeLa cells. HeLa cells have been the standard for *S.* Typhimurium effector studies since the discovery of SIFs nearly 30 years ago [154]. We opted to perform our studies in HeLa cells for two reasons: 1) HeLa cells are easy to infect, view by microscopy using immunofluorescence, and isotopically label, and 2) we wanted something to compare our results to. Since many studies have been conducted in HeLa cells it seemed pertinent to follow suit. The drawback of HeLa cells is severalfold. First, HeLa cells are derived from cervical cancer cells which is not a cell type typically targeted by *S.* Typhimurium. Second, HeLa cells are nonpolarized whereas the epithelial cells of the intestinal mucosa are polarized. Polarization of epithelial cells affects protein localization within cells as well as microtubule motor directionality. The processes of SIF biogenesis, SCV membrane maintenance, and the T3SS2-effectors involved therein, could therefore be altered in polarized epithelial cells.

Another broad limitation to the studies presented in this work is that we examined infection of HeLa cells at 8 hours post infection. While this time point is of particular interest when it comes to stabilization of the SIF network [156,160], it does not address the T3SS2-mediated event of centrifugal movement implicated in cell-to-cell transfer occurring at 24 hours post invasion. Consequently, I have just a snapshot of effectors roles at 8 hours. SifA, SopD2, PipB2, SteA, SseJ and SseF may have additional activities at later time points. Following *S.* Typhimurium infection for longer than 8 hours has allowed discovery that the T3SS2-secreted effector SseG can influence the propensity for cytosolic hyper-replication in epithelial cells [265]. Deeper insights into the *S.* Typhimurium replicative niche mediated by the effectors studied in this dissertation could arise from examining later time points during infection.

5.3 Future directions

We have shown that SopD2 and PipB2 bind AnxA2 during *S.* Typhimurium infection, however, several aspects surrounding this interaction require further investigation as described above. AnxA2 binding to SopD2/PipB2 was demonstrated through mass spectrometry and an *in vitro* binding assay. This interaction could be verified within the cell by confocal microscopy. Future work should focus on identification of the specific molecular mechanisms of action of both effectors on AnxA2 and possibly the specific molecular mechanisms of action of both effectors on each other. The role of AnxA2 during *S.* Typhimurium infection also needs to be elucidated as it remains unclear due to the many roles of AnxA2 in uninfected cells. Techniques such as siRNA knockdown of AnxA2 in cultured cells could clarify the role of AnxA2 in the intracellular replicative niche of *S.* Typhimurium.

There has been an abundance of proteomic profiling of the intracellular environment of *S.* Typhimurium infected cells in recent years [58,261–263] but a dearth of mechanistic studies. Given the number of T3SS2-effectors and host proteins involved in the intracellular replicative niche of *S.* Typhimurium, it is likely that we could endlessly profile the proteomes of infected cells and find new host targets or effector interactions. While such studies would be fruitful, they may still be unable to provide a mechanism. The more modern approach of BioID was used with the intention of identifying effector-host interaction partners, but the promiscuous nature of the biotin ligase used for BioID gave an excellent picture of the molecular environment of the effector, and not necessarily host binding partners. A method was recently described wherein host cells are infected with strains of *S.* Typhimurium whose T3SS2-secreted effectors are fused to self labeling-enzymes. The self-labeling enzymes did not appear to affect effector translocation, localization, or function during infection and permitted effector detection at high

resolution in real-time in live cells [266]. A technique like this could be used to track effectors during infection, aid in mechanism elucidation, and move the field forward.

Our work highlights the need for additional tools and models with which to study effector interactions during *S.* Typhimurium infection. Hopefully, our study will spur new interest in this field and encourage others to consider the effect of multiple effectors during infection. It will take herculean efforts by several groups to uncover the molecular mechanisms underpinning the *S.* Typhimurium intracellular replicative niche

5.4 Concluding remarks

Salmonella Typhimurium infections remain a global burden in countries across the world. New therapeutic strategies will be required with the emergence of the multi-drug resistant strain *S.* Typhimurium ST313 in Africa [8]. As internalization into intestinal epithelial cells is the first step in infection, it is prudent to understand how *S.* Typhimurium survives and thrives there.

In my doctoral dissertation I have taken a systematic approach to dissect effector interactions during *S.* Typhimurium infection. The findings presented here underscore the complexity of the intracellular replicative niche and demonstrate that multiple effectors are required to mediate specific phenotypes during infection. Together, this research establishes a new paradigm for T3SS2-secreted effector research and may inform future work to unravel T3SS2-secreted effector interactions. The ideas presented herein may be applicable to other intracellular pathogens that use T3SSs to secrete effectors into host cells.

References

1. Haraga A, Ohlson MB, Miller SI. Salmonellae interplay with host cells. Nat Rev Microbiol. 2008 Jan;6(1):53–66. https://doi.org/10.1038/nrmicro1788

2. Andino A, Hanning I. *Salmonella enterica* : survival, colonization, and virulence differences among serovars. Sci World J. 2015;2015:1–16. http://dx.doi.org/10.1155/2015/520179

3. Grimont PAD, Weill F-X. Antigenic formulas of the *Salmonella* serovars. Vol. 9, WHO Collaborating Centre For Reference and Research on Salmonella. Institute Pasteur. 2007.

4. Hohmann EL. Nontyphoidal salmonellosis. Clin Infect Dis. 2001 Jan 15;32(2):263–9. doi: 10.1086/318457

5. Keestra-Gounder AM, Tsolis RM, Bäumler AJ. Now you see me, now you don't: the interaction of *Salmonella* with innate immune receptors. Nat Rev Microbiol. 2015;13(4):206–16. http://dx.doi.org/10.1038/nrmicro3428

6. Buckle GC, Walker CLF, Black RE. Typhoid fever and paratyphoid fever: Systematic review to estimate global morbidity and mortality for 2010. J Glob Health. 2012;2(1):10401. doi: 10.7189/jogh.02.010401

7. Majowicz SE, Musto J, Scallan E, Angulo FJ, Kirk M, O'Brien SJ, et al. The global burden of nontyphoidal Salmonella gastroenteritis. Clin Infect Dis. 2010;50(6):882–9. doi: 10.1086/650733

8. Van Puyvelde S, Pickard D, Vandelannoote K, Heinz E, Barbé B, de Block T, et al. An african *Salmonella* Typhimurium ST313 sublineage with extensive drug-resistance and signatures of host adaptation. Nat Commun. 2019;10(1):1–12. http://dx.doi.org/10.1038/s41467-019-11844-z

9. Kohbata S, Yokoyama H. Cytopathogenic Effect of Salmonella typhi GIFU 10007 on M cells of murine ileal Peyer's patches in ligated ileal loops : an ultrastructural study. Microbiol Immunol. 1986;30(12):1225–37. doi: 10.1111/j.1348-0421.1986.tb03055.x.

10. Jones BD, Ghori N, Falkow S. *Salmonella* Typhimurium initiates murine infection by penetrating and destroying the specialized epithelial M cells of the Peyer's patches. J Exp Med. 1994;180(1):15–23. doi: 10.1084/jem.180.1.15.

11. McGhie EJ, Brawn LC, Hume PJ, Humphreys D, Koronakis V. *Salmonella* takes control: effector-driven manipulation of the host. Curr Opin Microbiol. 2009 Feb;12(1):117–24.

https://doi.org/10.1016/j.mib.2008.12.001

12. LaRock DL, Chaudhary A, Miller SI. Salmonellae interactions with host processes. Nat Rev Microbiol. 2015;13(4):191–205. http://dx.doi.org/10.1038/nrmicro3420

13. Hansen-Wester I, Hensel M. *Salmonella* pathogenicity islands encoding type III secretion systems. Microbes Infect. 2001 Jun;3(7):549–59. doi: 10.1016/s1286-4579(01)01411-3

14. Zhou D, Galán J. *Salmonella* entry into host cells: the work in concert of type III secreted effector proteins. Microbes Infect. 2001;3(14–15):1293–8. doi: 10.1016/s1286-4579(01)01489-7

15. Ginocchio CC, Olmsted SB, Wells CL, Galán JE. Contact with epithelial cells induces the formation of surface appendages on *Salmonella* Typhimurium. Cell. 1994;76(4):717–24. doi: 10.1016/0092-8674(94)90510-X

16. Altier C. Genetic and environmental control of *Salmonella* invasion. J Microbiol. 2005;43 Spec No(February):85–92.

17. Bajaj V, Hwang C, Lee CA. hilA is a novel ompR/toxR family member that activates the expression of *Salmonella* Typhimurium invasion genes. Mol Microbiol. 1995;18(4):715–27. doi:10.1111/j.1365-2958.1995.mmi_18040715.x

18. Darwin KH, Miller VL. InvF is required for expression of genes encoding proteins secreted by the SPI1 type III secretion apparatus in *Salmonella* typhimurium. J Bacteriol. 1999;181(16):4949–54. doi:10.1128/jb.181.16.4949-4954.1999

19. Eichelberg K, Galán JE. Differential regulation of *Salmonella* Typhimurium type III secreted proteins by pathogenicity island 1 (SPI-1)-encoded transcriptional activators InvF and HilA. Infect Immun. 1999;67(8):4099–105. doi:10.1128/iai.67.8.4099-4105.1999

20. Lostroh CP, Bajaj V, Lee CA. The cis requirements for transcriptional activation by HilA, a virulence determinant encoded on SPI-1. Mol Microbiol. 2000;37(2):300–15. doi:10.1046/j.1365-2958.2000.01991.x

21. Lostroh CP, Lee CA. The HilA box and sequences outside it determine the magnitude of HilA-dependent activation of PprgH from *Salmonella* pathogenicity island 1. J Bacteriol. 2001;183(16):4876–85. doi:10.1128/JB.183.16.4876-4885.2001

22. Schechter LM, Jain S, Akbar S, Lee CA. The small nucleoid-binding proteins H-NS, HU, and Fis affect hilA expression in *Salmonella enterica* serovar typhimurium. Infect Immun.

2003;71(9):5432–5. doi:10.1128/IAI.71.9.5432-5435.2003

23. Olekhnovich IN, Kadner RJ. Crucial roles of both flanking sequences in silencing of the hilA promoter in *Salmonella enterica* . J Mol Biol. 2006;357(2):373–86. doi:10.1016/j.jmb.2006.01.007

24. Schechter LM, Damrauer SM, Lee CA. Two AraC/XylS family members can independently counteract the effect of repressing sequences upstream of the hilA promoter. Mol Microbiol. 1999;32(3):629–42. doi:10.1046/j.1365-2958.1999.01381.x

25. Schechter LM, Lee CA. AraC/XylS family members, HilC and HilD, directly bind and derepress the *Salmonella* Typhimurium hilA promoter. Mol Microbiol. 2001;40(6):1289–99. doi:10.1046/j.1365-2958.2001.02462.x

26. Ellermeier CD, Ellermeier JR, Slauch JM. HilD, HilC and RtsA constitute a feed forward loop that controls expression of the SPI1 type three secretion system regulator hilA in *Salmonella enterica* serovar Typhimurium. Mol Microbiol. 2005;57(3):691–705. doi:10.1111/j.1365-2958.2005.04737.x

27. Johnston C, Pegues DA, Hueck CJ, Lee CA, Miller SI. Transcriptional activation of *Salmonella* Typhimurium invasion genes by a member of the phosphorylated response-regulator superfamily. Mol Microbiol. 1996;22(4):715–27. doi:10.1046/j.1365-2958.1996.d01-1719.x

28. Teplitski M, Goodier RI, Ahmer BMM. Pathways leading from BarA/SirA to motility and virulence gene expression in *Salmonella*. J Bacteriol. 2003;185(24):7257–65. doi:10.1128/JB.185.24.7257-7265.2003

29. Ahmer BMM, Van Reeuwijk J, Watson PR, Wallis TS, Heffron F. *Salmonella* SirA is a global regulator of genes mediating enteropathogenesis. Mol Microbiol. 1999;31(3):971–82. doi:10.1046/j.1365-2958.1999.01244.x

30. Martínez LC, Yakhnin H, Camacho MI, Georgellis D, Babitzke P, Puente JL, et al. Integration of a complex regulatory cascade involving the SirA/BarA and Csr global regulatory systems that controls expression of the *Salmonella* SPI-1 and SPI-2 virulence regulons through HilD. Mol Microbiol. 2011;80(6):1637–56. doi:10.1111/j.1365-2958.2011.07674.x

31. Baker CS, Morozov I, Suzuki K, Romeo T, Babitzke P. CsrA regulates glycogen biosynthesis by preventing translation of glgC in Escherichia coli. Mol Microbiol. 2002;44(6):1599–610. doi:10.1046/j.1365-2958.2002.02982.x

32. Lucchetti-Miganeh C, Burrowes E, Baysse C, Ermel G. The post-transcriptional regulator CsrA plays a central role in the adaptation of bacterial pathogens to different stages of infection in animal hosts. Microbiology. 2008;154(1):16–29. doi:10.1099/mic.0.2007/012286-0

33. Timmermans J, Van Melderen L. Post-transcriptional global regulation by CsrA in bacteria. Cell Mol Life Sci. 2010;67(17):2897–908. doi:10.1007/s00018-010-0381-z

34. Weilbacher T, Suzuki K, Dubey AK, Wang X, Gudapaty S, Morozov I, et al. A novel sRNA component of the carbon storage regulatory system of *Escherichia coli*. Mol Microbiol. 2003;48(3):657–70. doi:10.1046/j.1365-2958.2003.03459.x

35. Babitzke P, Romeo T. CsrB sRNA family: sequestration of RNA-binding regulatory proteins. Curr Opin Microbiol. 2007;10(2):156–63. doi:10.1016/j.mib.2007.03.007

36. Jones BD, Falkow S. Identification and characterization of a Salmonella Typhimurium oxygen-regulated gene required for bacterial internalization. Infect Immun. 1994;62(9):3745–52. doi:10.1128/iai.62.9.3745-3752.1994

37. Bajaj V, Lucas RL, Hwang C, Lee CA. Co-ordinate regulation of *Salmonella* Typhimurium invasion genes by environmental and regulatory factors is mediated by control of hilA expression. Mol Microbiol. 1996;22(4):703–14. doi:10.1046/j.1365-2958.1996.d01-1718.x

38. Russell DA, Dooley JS, Haylock RW. The steady-state orgA specific mRNA levels in *Salmonella enterica* serovar Typhimurium are repressed by oxygen during logarithmic growth phase but not early-stationary phase. FEMS Microbiol Lett. 2004;236(1):65–72. doi:10.1016/j.femsle.2004.05.025

39. Hardt WD, Chen LM, Schuebel KE, Bustelo XR, Galán JE. S. typhimurium encodes an activator of Rho GTPases that induces membrane ruffling and nuclear responses in host cells. Cell. 1998;93(5):815–26. doi:10.1016/S0092-8674(00)81442-7

40. Stender S, Friebel A, Linder S, Rohde M, Mirold S, Hardt WD. Identification of SopE2 from *Salmonella* typhimurium, a conserved guanine nucleotide exchange factor for Cdc42 of the host cell. Mol Microbiol. 2000;36(6):1206–21. doi: 10.1046/j.1365-2958.2000.01933.x

41. Patel JC, Galán JE. Differential activation and function of Rho GTPases during *Salmonella*-host cell interactions. J Cell Biol. 2006;175(3):453–63. doi: 10.1083/jcb.200605144

42. Burkinshaw BJ, Prehna G, Worrall LJ, Strynadka NCJ. Structure of *Salmonella* effector protein sopB N-terminal domain in complex with host Rho GTPase Cdc42. J Biol Chem. 2012;287(16):13348–55. https://doi.org/10.1074/jbc.M111.331330

43. Chen L, Hobbie S, Galán JE. Requirement of CDC42 for *Salmonella*-induced cytoskeletal and nuclear responses. Science (80-). 1996;274(5295):2115–8. https://doi.org/10.1126/science.274.5295.2115

44. Alemán A, Rodríguez-escudero I, Mallo G V, Cid VJ, Molina M, Rotger R. The amino-terminal non-catalytic region of *Salmonella* Typhimurium SigD affects actin organization in yeast and mammalian cells. Cell Microbiol. 2005;7(10):1432–46. doi: 10.1111/j.1462-5822.2005.00568.x

45. Bakshi CS, Singh VP, Wood MW, Jones PW, Wallis TS, Galyov EE. Identification of SopE2, a *Salmonella* secreted protein which is highly homologous to SopE and involved in bacterial invasion of epithelial cells. J Bacteriol. 2000;182(8):2341–4. doi:10.1128/JB.182.8.2341-2344.2000

46. Zhou D, Chen LM, Hernandez L, Shears SB, Galán JE. A *Salmonella* inositol polyphosphatase acts in conjunction with other bacterial effectors to promote host cell actin cytoskeleton rearrangements and bacterial internalization. Mol Microbiol. 2001 Jan;39(2):248–59. doi: 10.1046/j.1365-2958.2001.02230.x

47. Dai S, Zhang Y, Weimbs T, Yaffe MB, Zhou D. Bacteria-generated PtdIns (3) P Recruits VAMP8 to Facilitate Phagocytosis. Traffic. 2007;8(10):1365–74. doi:10.1111/j.1600-0854.2007.00613.x

48. Hernandez L, Hueffer K, Wenk M, Galán JE. Salmonella modulates vesicular traffic by altering phosphoinositide metabolism. Science (80-). 2004;20(329):946–9. doi: 10.1126/science.1098188

49. Zhou D, Mooseker MS, Galán JE. Role of the S . typhimurium actin-binding protein SipA in bacterial internalization. Science (80-). 1999;283(5410):2092–6. https://doi.org/10.1126/science.283.5410.2092

50. Zhou D, Mooseker MS, Galán JE. An invasion-associated Salmonella protein modulates the actin-bundling activity of plastin. Proc Natl Acad Sci. 1999;96(August):10176–81. https://doi.org/10.1073/pnas.96.18.10176

51. Hayward RD, Koronakis V. Direct nucleation and bundling of actin by the SipC protein of invasive Salmonella. EMBO J. 1999;18(18):4926–34. doi: 10.1093/emboj/18.18.4926

52. Myeni SK, Zhou D. The C terminus of SipC binds and bundles F-actin to promote *Salmonella* invasion □. J Biol Chem. 2010;285(18):13357–63. https://doi.org/doi: 10.1074/jbc.M109.094045

53. Okuda J, Arikawa Y, Takeuchi Y, Mahmoud MM, Suzaki E, Kataoka K, et al. Intracellular replication of Edwardsiella tarda in murine macrophage is dependent on the type III secretion system and induces an up-regulation of anti-apoptotic NF-kB target genes protecting the macrophage from staurosporine-induced apoptosis. Microb Pathog. 2006;41(6):226–40. doi: 10.1016/j.micpath.2006.08.002

54. Santos JC, Enninga J. At the crossroads: communication of bacteria-containing vacuoles with host organelles. Cell Microbiol. 2016;18(3):330–9. doi: 10.1111/cmi.12567

55. Knodler LA, Vallance BA, Celli J, Winfree S, Hansen B, Montero M, et al. Dissemination of invasive Salmonella via bacterial-induced extrusion of mucosal epithelia. Proc Natl Acad Sci U S A. 2010;107(41):17733–8. doi: 10.1073/pnas.1006098107

56. Malik-Kale P, Winfree S, Steele-Mortimer O. The bimodal lifestyle of intracellular Salmonella in epithelial cells: Replication in the cytosol obscures defects in vacuolar replication. PLoS One. 2012;7(6):1–10. doi: 10.1371/journal.pone.0038732

57. Yu HB, Croxen MA, Marchiando AM, Ferreira RBR, Cadwell K, Foster LJ, et al. Autophagy facilitates Salmonella replication in HeLa cells. MBio. 2014;5(2):e00865-14. doi: 10.1128/mBio.00865-14

58. Santos JC, Duchateau M, Fredlund J, Weiner A, Mallet A, Schmitt C, et al. The COPII complex and lysosomal VAMP7 determine intracellular Salmonella localization and growth. Cell Microbiol. 2015;17(12):1699–720. doi: 10.1111/cmi.12475

59. Steele-Mortimer O. The Salmonella-containing vacuole—Moving with the times. Curr Opin Microbiol. 2008;11(1):38–45. doi: 10.1016/j.mib.2008.01.002

60. Mallo G V., Espina M, Smith AC, Terebiznik MR, Alemán A, Finlay BB, et al. SopB promotes phosphatidylinositol 3-phosphate formation on Salmonella vacuoles by recruiting Rab5 and Vps34. J Cell Biol. 2008;182(4):741–52. doi: 10.1083/jcb.200804131

61. Christoforidis S, Miaczynska M, Ashman K, Wilm M, Zhao L, Yip SC, et al. Phosphatidylinositol-3-OH kinases are Rab5 effectors. Nat Cell Biol. 1999;1(4):249–52. doi:10.1038/12075

62. Huotari J, Helenius A. Endosome maturation. EMBO J. 2011;30(17):3481–500. doi:

10.1038/emboj.2011.286

63. Steele-Mortimer O, Meresse S, Gorvel JP, Toh BH, Finlay BB. Biogenesis of *Salmonella* Typhimurium-containing vacuoles in epithelial cells involves interactions with the early endocytic pathway. Cell Microbiol. 1999;1(1):33-49. doi:10.1046/j.1462-5822.1999.00003.x

64. Smith AC, Cirulis JT, Casanova JE, Scidmore MA, Brumell JH. Interaction of the *Salmonella*-containing vacuole with the endocytic recycling system. J Biol Chem. 2005;280(26):24634–41. https://doi.org/10.1074/jbc.M500358200

65. Sheff DR, Daro E a, Hull M, Mellman I. The receptor recycling pathway contains two distinct populations of early endosomes with different sorting functions. J Cell Biol. 1999;145(1):123–39. doi: 10.1083/jcb.145.1.123

66. Sönnichsen B, De Renzis S, Nielsen E, Rietdorf J, Zerial M. Distinct membrane domains on endosomes in the recycling pathway visualized by multicolor imaging of Rab4, Rab5, and Rab11. J Cell Biol. 2000;149(4):901–13. doi: 10.1083/jcb.149.4.901

67. Garcia-del Portillo F, Finlay BB. Targeting of Salmonella typhimurium to vesicles containing lysosomal membrane glycoproteins bypasses compartments with mannose 6-phosphate receptors. J Cell Biol. 1995;129(1):81–97. doi: 10.1083/jcb.129.1.81

68. Méresse S, Steele-Mortimer O, Finlay BB, Gorvel JP. The rab7 GTPase controls the maturation of Salmonella typhimurium-containing vacuoles in HeLa cells. EMBO J. 1999;18(16):4394–403. doi: 10.1093/emboj/18.16.4394

69. Beuzón CR, Méresse S, Unsworth KE, Ruíz-Albert J, Garvis S, Waterman SR, et al. *Salmonella* maintains the integrity of its intracellular vacuole through the action of SifA. EMBO J. 2000;19(13):3235–49. https://doi.org/10.1093/emboj/19.13.3235

70. Drecktrah D, Knodler LA, Howe D, Steele-Mortimer O. *Salmonella* trafficking is defined by continuous dynamic interactions with the endolysosomal system. Traffic. 2007;8(3):212–25. https://doi.org/10.1111/j.1600-0854.2006.00529.x

71. Brumell JH, Tang P, Mills SD, Finlay BB. Characterization of *Salmonella*-induced filaments (Sifs) reveals a delayed interaction between *Salmonella*-containing vacuoles and late endocytic compartments. Traffic. 2001;2(16):643–53. https://doi.org/10.1034/j.1600-0854.2001.20907.x

72. Knodler LA, Steele-Mortimer O. The *Salmonella* effector PipB2 affects late

endosome/lysosome distribution to mediate Sif extension. Mol Biol Cell. 2005;16:4108–23. https://doi.org/10.1091/mbc.E05-04-0367

73. Knuff K, Finlay BB. What the SIF is happening—the role of intracellular Salmonella-induced filaments. Front Cell Infect Microbiol. 2017;7(July):1–8. doi: 10.3389/fcimb.2017.00335

74. Hensel M, Shea JE, Baumler AJ, Gleeson C, Blattner F, Holden DW. Analysis of the boundaries of *Salmonella* pathogenicity island 2 and the corresponding chromosomal region of *Escherichia coli* K-12. 1997;179(4):1105–11. doi: 10.1128/jb.179.4.1105-1111.1997

75. Fass E, Groisman EA. Control of *Salmonella* pathogenicity island-2 gene expression. Curr Opin Microbiol. 2009;2(12):199–204. doi:10.1016/j.mib.2009.01.004

76. Shea JE, Hensel M, Gleeson C, Holden DW. Identification of a virulence locus encoding a second type III secretion system in *Salmonella* typhimurium. Proc Natl Acad Sci U S A. 1996;93(6):2593–7. doi: 10.1073/pnas.93.6.2593

77. Hensel M, Shea JE, Waterman SR, Mundy R, Nikolaus T, Banks G, et al. Genes encoding putative effector proteins of the type III secretion system of *Salmonella* pathogenicity island 2 are required for bacterial virulence and proliferation in macrophages. Mol Microbiol. 1998;30(1):163–74. https://doi.org/10.1046/j.1365-2958.1998.01047.x

78. Waterman SR, Holden DW. Functions and effectors of the *Salmonella* pathogenicity island 2 type III secretion system. Cell Microbiol. 2003 Aug;5(8):501–11. doi: 10.1046/j.1462-5822.2003.00294.x

79. Figueira R, Holden DW. Functions of the *Salmonella* pathogenicity island 2 (SPI-2) type III secretion system effectors. Microbiology. 2012 May;158(5):1147–61. https://doi.org/10.1099/mic.0.058115-0

80. Jennings E, Thurston TLM, Holden DW. *Salmonella* SPI-2 type III secretion system effectors: Molecular mechanisms and physiological consequences. Cell Host Microbe. 2017;22(2):217–31. https://doi.org/10.1016/j.chom.2017.07.009

81. Valdivia RH, Falkow S. Fluorescence-based isolation of bacterial genes expressed within host cells. Science (80-). 1997;277(5334):2007–12. https://doi.org/10.1126/science.277.5334.2007

82. Brown NF, Vallance BA, Coombes BK, Valdez Y, Coburn BA, Finlay BB. *Salmonella*

pathogenicity island 2 is expressed prior to penetrating the intestine. PLoS Pathog. 2005;1(3):0252–8. doi:10.1371/journal.ppat.0010032

83. Walthers D, Carroll RK, Navarre WW, Libby SJ, Fang FC, Kenney LJ. The response regulator SsrB activates expression of diverse *Salmonella* pathogenicity island 2 promoters and counters silencing by the nucleoid-associated protein H-NS. Mol Microbiol. 2007;65(2):477–93. doi: 10.1111/j.1365-2958.2007.05800.x

84. Worley MJ, Ching KHL, Heffron F. Salmonella SsrB activates a global regulon of horizontally acquired genes. Mol Microbiol. 2000;36(3):749–61. doi: 10.1046/j.1365-2958.2000.01902.x

85. Ochman H, Soncini FC, Solomon F, Groisman EA. Identification of a pathogenicity island required for *Salmonella* in host cells. Proc Natl Acad Sci. 1996;93(15):7800–4. https://doi.org/10.1073/pnas.93.15.7800

86. Feng X, Oropeza R, Kenney LJ. Dual regulation by phospho-OmpR of ssrA/B gene expression in Salmonella pathogenicity island 2. Mol Microbiol. 2003;48(4):1131–43. doi: 10.1046/j.1365-2958.2003.03502.x

87. Navarre WW, Porwollik S, Wang Y, Mcclelland M, Rosen H, Libby SJ, et al. Selective silencing of foreign DNA protein in *Salmonella*. Science (80-). 2006;313(July):236–8. doi: 10.1126/science.1128794

88. Navarre WW, McClelland M, Libby SJ, Fang FC. Silencing of xenogeneic DNA by H-NS - Facilitation of lateral gene transfer in bacteria by a defense system that recognizes foreign DNA. Genes Dev. 2007;21(12):1456–71. doi: 10.1101/gad.1543107

89. Lucchini S, Rowley G, Goldberg MD, Hurd D, Harrison M, Hinton JCD. H-NS mediates the silencing of laterally acquired genes in bacteria. PLoS Pathog. 2006;2(8):0746–52. doi: 10.1371/journal.ppat.0020081

90. Stoebel DM, Free A, Dorman CJ. Anti-silencing: Overcoming H-NS-mediated repression of transcription in Gram-negative enteric bacteria. Microbiology. 2008;154(9):2533–45. doi: 10.1099/mic.0.2008/020693-0

91. Bustamante VH, Martínez LC, Santana FJ, Knodler LA, Steele-Mortimer O, Puente JL. HilD-mediated transcriptional cross-talk between SPI-1 and SPI-2. Proc Natl Acad Sci U S A. 2008;105(38):14591–6. doi: 10.1073/pnas.0801205105

92. Feng X, Walthers D, Oropeza R, Kenney LJ. The response regulator SsrB activates

transcription and binds to a region overlapping OmpR binding sites at *Salmonella* pathogenicity island 2. Mol Microbiol. 2004;54(3):823–35. doi: 10.1111/j.1365-2958.2004.04317.x

93. Lee AK, Detweiler CS, Falkow S. OmpR regulates the two-component system SsrA-SsrB in *Salmonella* pathogenicity island 2. J Bacteriol. 2000;182(3):771–81. doi: 10.1128/JB.182.3.771-781.2000

94. Groisman EA. The pleiotropic two-component regulatory system PhoP-PhoQ. J Bacteriol. 2001;183(6):1835–42. doi: 10.1128/JB.183.6.1835

95. Miller SI, Kukral AM, Mekalanos JJ. A two-component regulatory system (phoP phoQ) controls *Salmonella* Typhimurium virulence. Proc Natl Acad Sci U S A. 1989;86(13):5054–8. doi: 10.1073/pnas.86.13.5054

96. Heithoff DM, Conner CP, Hentschel U, Govantes F, Hanna PC, Mahan MJ. Coordinate intracellular expression of *Salmonella* genes induced during infection. J Bacteriol. 1999;181(3):799–807. doi: 10.1128/jb.181.3.799-807.1999

97. Mouslim C, Groisman EA. Control of the *Salmonella* ugd gene by three two-component regulatory systems. Mol Microbiol. 2003;47(2):335–44. doi: 10.1046/j.1365-2958.2003.03318.x

98. Deiwick J, Nikolaus T, Erdogan S, Hensel M. Environmental regulation of Salmonella pathogenicity island 2 gene expression. Mol Microbiol. 1999;31(6):1759–73. doi:10.1046/j.1365-2958.1999.01312.x

99. Bijlsma JJE, Groisman EA. The PhoP/PhoQ system controls the intramacrophage type three secretion system of *Salmonella enterica* . Mol Microbiol. 2005;57(1):85–96. doi:10.1111/j.1365-2958.2005.04668.x

100. McGourty K, Thurston TL, Matthews SA, Pinaud L, Mota LJ, Holden DW. Salmonella inhibits retrograde trafficking of mannose-6-phosphate receptors and lysosome function. Science (80-). 2012;338(6109):963–7. doi: 10.1126/science.1227037

101. Birmingham CL, Brumell JH. Autophagy recognizes intracellular Salmonella enterica serovar Typhimurium in damaged vacuoles. Autophagy. 2006;2(3):156–8. doi:10.4161/auto.2825

102. Miao EA, Mao DP, Yudkovsky N, Bonneau R, Lorang CG, Warren SE, et al. Innate immune detection of the type III secretion apparatus through the NLRC4 inflammasome.

Proc Natl Acad Sci. 2010;107(7):3076–80. doi: 10.1073/pnas.0913087107

103. Vazquez-Torres A, Jones-Carson J, Mastroeni P, Ischiropoulos H, Fang FC. Antimicrobial actions of the NADPH phagocyte oxidase and inducible nitric oxide synthase in experimental salmonellosis . I . Effects on microbial killing by activated peritoneal macrophages in vitro. J Exp Med. 2000;192(2):227–36. https://doi.org/10.1084/jem.192.2.227

104. Eriksson S, Bjo J, Syk A, Pettersson S, Andersson DI, Rhen M. *Salmonella* typhimurium mutants that downregulate phagocyte nitric oxide production. Cell Microbiol. 2000;2(3):239–50. https://doi.org/10.1046/j.1462-5822.2000.00051.x

105. Vazquez-Torres A, Xu Y, Jones-Carson J, Holden DW, Lucia SM, Dinauer MC, et al. *Salmonella* pathogenicity island 2-dependent evasion of the phagocyte NADPH oxidase. Sci (New York, NY). 2000;287(5458):1655–8. doi: 10.1126/science.287.5458.1655

106. Chakravortty D, Hansen-Wester I, Hensel M. Salmonella pathogenicity island 2 mediates protection of intracellular Salmonella from reactive nitrogen intermediates. J Exp Med. 2002;195(9):1155–66. doi:10.1084/jem.20011547

107. Gallois A, Klein JR, Allen LH, Jones BD, Nauseef WM. *Salmonella* pathogenicity island 2-encoded type III secretion system mediates exclusion of NADPH oxidase assembly from the phagosomal membrane. J Immunol. 2001;166:5741–8. https://doi.org/10.4049/jimmunol.166.9.5741

108. Knodler LA, Steele-Mortimer O. Taking possession: biogenesis of the Salmonella-containing vacuole. Traffic. 2003;4(9):587–99. doi: 10.1034/j.1600-0854.2003.00118.x

109. Harrison RE, Brumell JH, Khandani A, Bucci C, Scott CC, Jiang X, et al. *Salmonella* impairs RILP recruitment to Rab7 during maturation of invasion vacuoles. Mol Biol Cell. 2004;15(7):3146–54. https://doi.org/10.1091/mbc.E04-02-0092

110. Boucrot E, Henry T, Borg J-P, Gorvel J-P, Méresse S. The intracellular fate of *Salmonella* depends on the recruitment of kinesin. Sci (New York, NY). 2005;308(5725):1174–8. https://doi.org/10.1126/science.1110225

111. Salcedo SP, Holden DW. SseG, a virulence protein that targets *Salmonella* to the Golgi network. EMBO J. 2003 Oct 1;22(19):5003–14. https://doi.org/10.1093/emboj/cdg517

112. Deiwick J, Salcedo SP, Boucrot E, Gilliland SM, Henry T, Petermann N, et al. The translocated *Salmonella* effector proteins SseF and SseG interact and are required to

establish an intracellular replication niche. Infect Immun. 2006;74(12):6965–72. https://doi.org/10.1128/IAI.00648-06

113. Yu X-J, Liu M, Holden DW. *Salmonella* effectors SseF and SseG interact with mammalian protein ACBD3 (GCP60) to anchor *Salmonella*-containing vacuoles at the Golgi network. MBio. 2016;7(4):e00474-16. https://doi.org/10.1128/mBio.00474-16

114. Henry T, Couillault C, Rockenfeller P, Boucrot E, Dumont A, Schroeder N, et al. The *Salmonella* effector protein PipB2 is a linker for kinesin-1. Proc Natl Acad Sci U S A. 2006 Sep 5;103(36):13497–502. https://doi.org/10.1073/pnas.0605443103

115. Alberdi L, Vergnes A, Manneville JB, Tembo DL, Fang Z, Zhao Y, et al. Regulation of kinesin-1 activity by the Salmonella enterica effectors PipB2 and SifA. J Cell Sci. 2020;133(9). doi:10.1242/jcs.239863

116. Jordens I, Fernandez-Borja M, Marsman M, Dusseljee S, Janssen L, Calafat J, et al. The Rab7 effector protein RILP controls lysosomal transport by inducing the recruitment of dynein-dynactin motors. Curr Biol. 2001;11(21):1680–5. doi: 10.1016/S0960-9822(01)00531-0

117. Pankiv S, Alemu EA, Brech A, Bruun JA, Lamark T, Øvervatn A, et al. FYCO1 is a Rab7 effector that binds to LC3 and PI3P to mediate microtubule plus end-directed vesicle transport. J Cell Biol. 2010;188(2):253–69. doi: 10.1083/jcb.200907015

118. D'Costa VM, Braun V, Landekic M, Shi R, Proteau A, McDonald L, et al. Salmonella disrupts host endocytic trafficking by SopD2-mediated inhibition of Rab7. Cell Rep. 2015;12(9):1508–18. doi:10.1016/j.celrep.2015.07.063

119. Lossi NS, Rolhion N, Magee AI, Boyle C, Holden DW. The Salmonella SPI-2 effector SseJ exhibits eukaryotic activator-dependent phospholipase A and glycerophospholipid:cholesterol acyltransferase activity. Microbiology. 2008;154(9):2680–8. doi: 10.1099/mic.0.2008/019075-0

120. Sprong H, van der Sluijs P, van Meer G. How proteins move lipids and lipids move proteins. Nat Rev Mol Cell Biol. 2001;2(7):504–13. doi: 10.1038/35080071

121. Ruiz-Albert J, Yu X-J, Beuzón CR, Blakey AN, Galyov EE, Holden DW. Complementary activities of SseJ and SifA regulate dynamics of the *Salmonella* typhimurium vacuolar membrane. Mol Microbiol. 2002;44(3):645–61. https://doi.org/10.1046/j.1365-2958.2002.02912.x

122. Fletcher DA, Mullins RD. Cell mechanics and the cytoskeleton. Nature. 2010;463(7280):485–92. doi: 10.1038/nature08908

123. Alberts B, Johnson A, Lewis J, Morgan D, Martin R, Roberts K, et al. The molecular biology of the cell. 6th editio. Vol. 196. New York, New York: Garland Science, Taylor & Francis Group; 2015. 1–1341 p.

124. Wiche G. Role of plectin in cytoskeleton organization and dynamics. J Cell Sci. 1998;111(9):2477–86.

125. Poh J, Odendall C, Spanos A, Boyle C, Liu M, Freemont P, et al. SteC is a Salmonella kinase required for SPI-2-dependent F-actin remodelling. Cell Microbiol. 2008;10(1):20–30. doi: 10.1111/j.1462-5822.2007.01010.x

126. Miao EA, Brittnacher M, Haraga A, Jeng RL, Welch MD, Miller SI. *Salmonella* effectors translocated across the vacuolar membrane interact with the actin cytoskeleton. Mol Microbiol. 2003;48(2):401–15. https://doi.org/10.1046/j.1365-2958.2003.t01-1-03456.x

127. Miao EA, Miller SI. A conserved amino acid sequence directing intracellular type III secretion by Salmonella typhimurium. Proc Natl Acad Sci U S A. 2000;97(13):7539–44. doi: 10.1073/pnas.97.13.7539

128. Méresse S, Unsworth KE, Habermann A, Griffiths G, Fang F, Martínez-Lorenzo MJ, et al. Remodelling of the actin cytoskeleton is essential for replication of intravacuolar *Salmonella*. Cell Microbiol. 2001;3(8):567–77. doi: 10.1046/j.1462-5822.2001.00141.x

129. Krieger V, Liebl D, Zhang Y, Rajashekar R, Chlanda P, Giesker K, et al. Reorganization of the endosomal system in *Salmonella*-infected cells: the ultrastructure of *Salmonella*-induced tubular compartments. PLoS Pathog. 2014;10(9):e1004374. https://doi.org/10.1371/journal.ppat.1004374

130. Liss V, Hensel M. Take the tube: remodeling of the endosomal system by intracellular *Salmonella* enterica. Cell Microbiol. 2015;17(April):639–47. https://doi.org/10.1111/cmi.12441

131. Gerke V, Moss SE. Annexins: From structure to function. Physiol Rev. 2002;82(2):331–71. doi: 10.1152/physrev.00030.2001

132. Hayes MJ, Shao D, Bailly M, Moss SE. Regulation of actin dynamics by annexin 2. EMBO J. 2006;25(9):1816–26. doi: 10.1038/sj.emboj.7601078

133. Gerke V, Creutz CE, Moss SE. Annexins: Linking Ca2+ signalling to membrane dynamics. Nat Rev Mol Cell Biol. 2005;6(6):449–61. doi: 10.1038/nrm1661

134. Rosengarth A, Luecke H. A calcium-driven conformational switch of the N-terminal and core domains of annexin A1. J Mol Biol. 2003;326(5):1317–25. doi: 10.1016/S0022-2836(03)00027-5

135. Jolly C, Winfree S, Hansen B, Steele-Mortimer O. The Annexin A2/p11 complex is required for efficient invasion of *Salmonella* Typhimurium in epithelial cells. Cell Microbiol. 2014;16(1):64–77. doi: 10.1111/cmi.12180

136. Johnsson N, Marriott G, Weber K. P36, the major cytoplasmic substrate of Src tyrosine protein kinase, binds to its p11 regulatory subunit via a short amino-terminal amphiphatic helix. EMBO J. 1988;7(8):2435–42. doi: 10.1002/j.1460-2075.1988.tb03089.x

137. König J, Gerke V. Modes of annexin-membrane interactions analyzed by employing chimeric annexin proteins. Biochim Biophys Acta - Mol Cell Res. 2000;1498(2–3):174–80. doi: 10.1016/S0167-4889(00)00094-X

138. Hayes MJ, Rescher U, Gerke V, Moss SE. Annexin-actin interactions. Traffic. 2004;5(8):571–6. doi: 10.1111/j.1600-0854.2004.00210.x

139. Grieve AG, Moss SE, Hayes MJ. Annexin A2 at the interface of actin and membrane mynamics: A focus on its roles in endocytosis and cell polarization. Ben-Ze'ev A, editor. Int J Cell Biol. 2012;2012:852430. https://doi.org/10.1155/2012/852430

140. Hayes MJ, Shao DM, Grieve A, Levine T, Bailly M, Moss SE. Annexin A2 at the interface between F-actin and membranes enriched in phosphatidylinositol 4,5,-bisphosphate. Biochim Biophys Acta - Mol Cell Res. 2009;1793(6):1086–95. http://dx.doi.org/10.1016/j.bbamcr.2008.10.007

141. Drust DS, Creutz CE. Aggregation of chromaffin granules by calpactin at micromolar levels of calcium. Nature. 1988;331(7):88–91. doi: 10.1038/331088a0

142. Emans N, Gorvel JP, Walter C, Gerke V, Kellner R, Griffiths G, et al. Annexin II is a major component of fusogenic endosomal vesicles. J Cell Biol. 1993;120(6):1357–69. doi: 10.1083/jcb.120.6.1357

143. Jost M, Zeuschner D, Seemann J, Weber K, Gerke V. Identification and characterization of a novel type of annexin-membrane interaction: Ca2+ is not required for the association of annexin II with early endosomes. J Cell Sci. 1997;110(2):221–8.

144. Harder T, Kellner R, Parton RG, Gruenberg J. Specific release of membrane-bound annexin II and cortical cytoskeletal elements by sequestration of membrnae cholesterol. Mol Biol Cell. 1997;8(March):533–45. doi: 10.1091/mbc.8.3.533

145. Mayran N, Parton RG, Gruenberg J. Annexin II regulates multivesicular endosome biogenesis in the degradation pathway of animal cells. EMBO J. 2003;22(13):3242–53. doi: 10.1093/emboj/cdg321

146. Harder T, Gerke V. The subcellular distribution of early endosomes is affected by the annexin II2p112 complex. J Cell Biol. 1993;123(5):1119–32. doi: 10.1083/jcb.123.5.1119

147. Zeuschner D, Stoorvogel W, Gerke V. Association of annexin 2 with recycling endosomes requires either calcium- or cholesterol-stabilized membrane domains. Eur J Cell Biol. 2001;80(8):499–507. doi: 10.1078/0171-9335-00184

148. Soldati T, Schliwa M. Powering membrane traffic in endocytosis and recycling. Nat Rev Mol Cell Biol. 2006;7(7):897–908. doi: 10.1038/nrm1960

149. Durrbach A, Louvard D, Coudrier E. Actin filaments facilitate two steps of endocytosis. J Cell Sci. 1996;109(2):457–65.

150. Morel E, Parton RG, Gruenberg J. Annexin A2-dependent polymerization of actin mediates endosome biogenesis. Dev Cell. 2009;16(3):445–57. http://dx.doi.org/10.1016/j.devcel.2009.01.007

151. Zobiack N, Rescher U, Ludwig C, Zeuschner D, Gerke V. The Annexin 2/S100A10 complex control the distribution of transferrin receptor-containing recycling endosomes. Mol Biol Cell. 2003;14(December):4896–908. doi: 10.1091/mbc.E03

152. Bujny M V, Ewels PA, Humphrey S, Attar N, Jepson MA, Cullen PJ. Sorting nexin-1 defines an early phase of Salmonella-containing vacuole-remodeling during Salmonella infection. J Cell Sci. 2008;121(Pt 12):2027–36. doi:10.1242/jcs.018432

153. Braun V, Wong A, Landekic M, Hong WJ, Grinstein S, Brumell JH. Sorting nexin 3 (SNX3) is a component of a tubular endosomal network induced by Salmonella and involved in maturation of the Salmonella-containing vacuole. Cell Microbiol. 2010;12(9):1352–67. doi:10.1111/j.1462-5822.2010.01476.x

154. Garcia-del Portillo F, Zwick MB, Leung KY, Finlay BB. *Salmonella* induces the formation of filamentous structures containing lysosomal membrane glycoproteins in epithelial cells. Proc Natl Acad Sci U S A. 1993;90(22):10544–8.

http://doi.org/10.1073/pnas.90.22.10544

155. Van Engelenburg SB, Palmer AE. Imaging type-III secretion reveals dynamics and spatial segregation of Salmonella effectors. Nat Methods. 2010;7(4):325–30. doi: 10.1038/nmeth.1437

156. Rajashekar R, Liebl D, Seitz A, Hensel M. Dynamic remodeling of the endosomal system during formation of *Salmonella*-induced filaments by intracellular *Salmonella* enterica. Traffic. 2008;9(12):2100–16. https://doi.org/10.1111/j.1600-0854.2008.00821.x

157. Schroeder N, Henry T, de Chastellier C, Zhao W, Guilhon A-A, Gorvel J-P, et al. The virulence protein SopD2 regulates membrane dynamics of *Salmonella*-containing vacuoles. PLoS Pathog. 2010;6(7):e1001002. https://doi.org/10.1371/journal.ppat.1001002

158. Mota LJ, Ramsden AE, Liu M, Castle JD, Holden DW. SCAMP3 is a component of the Salmonella-induced tubular network and reveals an interaction between bacterial effectors and post-Golgi trafficking. Cell Microbiol. 2009;11(8):1236–53. doi: 10.1111/j.1462-5822.2009.01329.x

159. Schroeder N, Mota LJ, Méresse S. *Salmonella*-induced tubular networks. Trends Microbiol. 2011;19(6):268–77. https://doi.org/10.1016/j.tim.2011.01.006

160. Drecktrah D, Levine-Wilkinson S, Dam T, Winfree S, Knodler L a., Schroer T a., et al. Dynamic behavior of *Salmonella*-induced membrane tubules in epithelial cells. Traffic. 2008;9(12):2117–29. https://doi.org/10.1111/j.1600-0854.2008.00830.x

161. Jiang X, Rossanese OW, Brown NF, Kujat-Choy S, Galán JE, Finlay BB, et al. The related effector proteins SopD and SopD2 from *Salmonella enterica* serovar Typhimurium contribute to virulence during systemic infection of mice. Mol Microbiol. 2004;54(5):1186–98. https://doi.org/10.1111/j.1365-2958.2004.04344.x

162. Kuhle V, Jäckel D, Hensel M. Effector proteins encoded by *Salmonella* pathogenicity island 2 interfere with the microtubule cytoskeleton after translocation into host cells. Traffic. 2004;5(5):356–70. doi: 10.1111/j.1398-9219.2004.00179.x

163. van der Heijden J, Finlay BB. Type III effector-mediated processes in *Salmonella* infection. Future Microbiol. 2012;7(6):1–19.

164. Diacovich L, Dumont A, Lafitte D, Soprano E, Guilhon A-A, Bignon C, et al. Interaction between the SifA virulence factor and its host target SKIP is essential for *Salmonella*

pathogenesis. J Biol Chem. 2009 Nov 27;284(48):33151–60. https://doi.org/10.1074/jbc.M109.034975

165. Ohlson MB, Huang Z, Alto NM, Blanc M-P, Dixon JE, Chai J, et al. Structure and function of *Salmonella* SifA indicate that its interactions with SKIP, SseJ, and RhoA family GTPases induce endosomal tubulation. Cell Host Microbe. 2008 Nov 13;4(5):434–46. https://doi.org/10.1016/j.chom.2008.08.012

166. Brumell JH, Goosney DL, Finlay BB. SifA, a type III secreted effector of *Salmonella* Typhimurium, directs *Salmonella*-induced filament (Sif) formation along microtubules. Traffic. 2002;3(6):407–15. https://doi.org/10.1034/j.1600-0854.2002.30604.x

167. Dumont A, Boucrot E, Drevensek S, Daire V, Gorvel JP, Poüs C, et al. SKIP, the host target of the *Salmonella* virulence factor SifA, promotes kinesin-1-dependent vacuolar membrane exchanges. Traffic. 2010;11(7):899–911. https://doi.org/10.1111/j.1600-0854.2010.01069.x

168. Kolodziejek AM, Miller SI. Salmonella modulation of the phagosome membrane, role of SseJ. Cell Microbiol. 2015;17(February):333–41. doi: 10.1111/cmi.12420

169. Freeman JA, Ohl ME, Miller SI. The *Salmonella enterica* serovar Typhimurium translocated effectors SseJ and SifB are targeted to the *Salmonella*-containing vacuole. Infect Immun. 2003;71(1):418–27. https://doi.org/10.1128/IAI.71.1.418-427.2003

170. LaRock DL, Brzovic PS, Levin I, Blanc MP, Miller SI. A *Salmonella Typhimurium*-translocated glycerophospholipid:cholesterol acyltransferase promotes virulence by binding to the RhoA protein switch regions. J Biol Chem. 2012;287(35):29654–63. https://doi.org/10.1074/jbc.M112.363598

171. Brumell JH, Kujat-Choy S, Brown NF, Vallance BA, Knodler LA, Finlay BB. SopD2 is a novel type III secreted effector of Salmonella typhimurium that targets late endocytic compartments upon delivery into host cells. Traffic. 2003;4(1):36–48. doi:10.1034/j.1600-0854.2003.40106.x

172. Kuhle V, Hensel M. SseF and SseG are translocated effectors of the type III secretion system of *Salmonella* pathogenicity island 2 that modulate aggregation of endosomal compartments. Cell Microbiol. 2002;4(12):813–24. https://doi.org/10.1046/j.1462-5822.2002.00234.x

173. Domingues L, Ismail A, Charro N, Rodríguez-Escudero I, Holden DW, Molina M, et al. The Salmonella effector SteA binds phosphatidylinositol 4-phosphate for subcellular targeting within host cells. Cell Microbiol. 2016;18(7):949–69. doi: 10.1111/cmi.12558

174. Domingues L, Holden DW, Mota LJ. The *Salmonella* effector SteA contributes to the control of membrane dynamics of *Salmonella*-containing vacuoles. Infect Immun. 2014;82(7):2923–34. https://doi.org/10.1128/IAI.01385-13

175. Stein MA, Leung KY, Zwick M, Garcia-del Portillo F, Finlay BB. Identification of a *Salmonella* virulence gene required for formation of filamentous structures containing lysosomal membrane glycoproteins within epithelial cells. Mol Microbiol. 1996;20(1):151–64. https://doi.org/10.1111/j.1365-2958.1996.tb02497.x

176. Brumell JH, Rosenberger CM, Gotto GT, Marcus SL, Finlay BB. SifA permits survival and replication of *Salmonella* typhimurium in murine macrophages. Cell Microbiol. 2001;3(2):75–84. https://doi.org/10.1046/j.1462-5822.2001.00087.x

177. Zhao W, Moest T, Zhao Y, Guilhon A-A, Buffat C, Gorvel J-P, et al. The *Salmonella* effector protein SifA plays a dual role in virulence. Sci Rep. 2015;5:12979. https://doi.org/10.1038/srep12979

178. Christen M, Coye LH, Hontz JS, LaRock DL, Pfuetzner RA, Megha, et al. Activation of a bacterial virulence protein by the GTPase RhoA. Sci Signal. 2009;2(95):ra71–ra71. doi:10.1126/scisignal.2000430

179. Birmingham CL, Jiang X, Ohlson MB, Miller SI, Brumell JH. *Salmonella*-induced filament formation is a dynamic phenotype induced by rapidly replicating *Salmonella enterica* serovar Typhimurium in epithelial cells. Infect Immun. 2005;73(2):1204–8. https://doi.org/10.1128/IAI.73.2.1204-1208.2005

180. Rajashekar R, Liebl D, Chikkaballi D, Liss V, Hensel M. Live cell imaging reveals novel functions of *Salmonella enterica* SPI2-T3SS effector proteins in remodeling of the host cell endosomal system. PLoS One. 2014;9(12):e115423. https://doi.org/10.1371/journal.pone.0115423

181. Rubinsztein DC, Shpilka T, Elazar Z. Mechanisms of autophagosome biogenesis. Curr Biol. 2012;22(1):R29–34. http://dx.doi.org/10.1016/j.cub.2011.11.034

182. Hernandez LD, Pypaert M, Flavell RA, Galán JE. A Salmonella protein causes macrophage cell death by inducing autophagy. J Cell Biol. 2003;163(5):1123–31. doi: 10.1083/jcb.200309161

183. Wild P, Farhan H, McEwan DG, Wagner S, Rogov V V., Brady NR, et al. Phosphorylation of the autophagy receptor optineurin restricts *Salmonella* growth. Science (80-). 2011;333(July):228–33. doi: 10.1126/science.1205405

184. Cemma M, Brumell JH. Interactions of pathogenic bacteria with autophagy systems. Curr Biol. 2012;22(13):R540-5. doi:10.1016/j.cub.2012.06.001

185. Fujita N, Morita E, Itoh T, Tanaka A, Nakaoka M, Osada Y, et al. Recruitment of the autophagic machinery to endosomes during infection is mediated by ubiquitin. J Cell Biol. 2013;203(1):115–28. doi: 10.1083/jcb.201304188

186. Henry T, Gorvel JP, Méresse S. Molecular motors hijacking by intracellular pathogens. Cell Microbiol. 2006;8(1):23–32. https://doi.org/10.1111/j.1462-5822.2005.00649.x

187. Young AM, Minson M, McQuate SE, Palmer AE. Optimized fluorescence complementation platform for visualizing Salmonella effector proteins reveals distinctly different intracellular niches in different cell types. ACS Infect Dis. 2017;acsinfecdis.7b00052. doi: 10.1021/acsinfecdis.7b00052

188. Castle A, Castle D. Ubiquitously expressed secretory carrier membrane proteins (SCAMPs) 1-4 mark different pathways and exhibit limited constitutive trafficking to and from the cell surface. J Cell Sci. 2005;118(Pt 16):3769–80. doi:10.1242/jcs.02503

189. Falguières T, Castle D, Gruenberg J. Regulation of the MVB pathway by SCAMP3. Traffic. 2012;13(1):131–42. doi: 10.1111/j.1600-0854.2011.01291.x

190. Kuhle V, Abrahams GL, Hensel M. Intracellular *Salmonella enterica* redirect exocytic transport processes in a *Salmonella* pathogenicity island 2-dependent manner. Traffic. 2006;7(6):716–30. https://doi.org/10.1111/j.1600-0854.2006.00422.x

191. Perrett C a, Zhou D. Salmonella type III effector SopB modulates host cell exocytosis. Emerg Microbes Infect. 2013;2(5):e32. doi: 10.1038/emi.2013.31

192. Zhang Y, Hensel M. Evaluation of nanoparticles as endocytic tracers in cellular microbiology. Nanoscale. 2013;5:9296–309. doi:10.1039/c3nr01550e

193. Popp J, Noster J, Busch K, Kehl A, zur Hellen G, Hensel M. Role of host cell-derived amino acids in nutrition of intracellular *Salmonella enterica*. Infect Immun. 2015;83(12):4466–75. https://doi.org/10.1128/IAI.00624-15

194. Liss V, Swart AL, Kehl A, Hermanns N, Zhang Y, Chikkaballi D, et al. *Salmonella enterica* remodels the host cell endosomal system for efficient intravacuolar nutrition. Cell Host Microbe. 2017;21(3):390–402. https://doi.org/10.1016/j.chom.2017.02.005

195. Eswarappa SM, Negi VD, Chakraborty S, Chandrasekhar Sagar BK, Chakravortty D.

Division of the *Salmonella*-containing vacuole and depletion of acidic lysosomes in *Salmonella*-infected host cells are novel strategies of Salmonella enterica to avoid lysosomes. Infect Immun. 2010;78(1):68–79. doi.org/10.1128/IAI.00668-09

196. Steele-Mortimer O, Brumell JH, Knodler LA, Méresse S, Lopez A, Finlay BB. The invasion-associated type III secretion system of *Salmonella enterica* serovar Typhimurium is necessary for intracellular proliferation and vacuole biogenesis in epithelial cells. Cell Microbiol. 2002;4(1):43–54. https://doi.org/10.1046/j.1462-5822.2002.00170.x

197. Buchmeier NA, Heffron F. Inhibition of macrophage phagosome-lysosome fusion by Salmonella Typhimurium. Infect Immun. 1991;59(7):2232–8. doi:10.1128/IAI.59.7.2232-2238.1991

198. Garvis SG, Beuzón CR, Holden DW. A role for the PhoP/Q regulon in inhibition of fusion between lysosomes and *Salmonella*-containing vacuoles in macrophages. Cell Microbiol. 2001;3(11):731–44. https://doi.org/10.1046/j.1462-5822.2001.00153.x

199. Hashim S, Mukherjee K, Basu SK, Chem JB, Mukhopadhyay A. Live *Salmonella* modulate expression of Rab proteins to persist in a specialized compartment and escape transport to lysosomes. J Biol Chem. 2000;275(21):16281–8. https://doi.org/10.1074/jbc.275.21.16281

200. Szeto J, Namolovan A, Osborne SE, Coombes BK, Brumell JH. *Salmonella*-containing vacuoles display centrifugal movement associated with cell-to-cell transfer in epithelial cells. Infect Immun. 2009;77(3):996–1007. https://doi.org/10.1128/IAI.01275-08

201. Ramsden AE, Holden DW, Mota LJ. Membrane dynamics and spatial distribution of *Salmonella*-containing vacuoles. Trends Microbiol. 2007;15(11):516–24. http://doi.org/10.1016/j.tim.2007.10.002

202. Buckner MMC, Croxen M, Arena ET, Finlay BB. A comprehensive study of the contribution of *Salmonella enterica* serovar Typhimurium SPI2 effectors to bacterial colonization, survival, and replication in typhoid fever, macrophage, and epithelial cell infection models. Virulence. 2011 May 1;2(3):208–16. https://doi.org/10.4161/viru.2.3.15894

203. Casadaban MJ, Cohen SN. Analysis of gene control signals by DNA fusion and cloning in *Escherichia coli*. J Mol Biol. 1980;138(2):179–207. https://doi.org/10.1016/0022-2836(80)90283-1

204. Ferrieres L, Hemery G, Nham T, Guerout A-M, Mazel D, Beloin C, et al. Silent mischief: Bacteriophage Mu insertions contaminate products of *Escherichia coli* random

mutagenesis performed using suicidal transposon delivery plasmids mobilized by broad-host-range RP4 conjugative machinery. J Bacteriol. 2010;192(24):6418–27. https://doi.org/10.1128/JB.00621-10

205. Grant SGN, Jessee J, Bloom FR, Hanahan D. Differential plasmid rescue from transgenic mouse DNAs into *Escherichia coli* methylation-restriction mutants. Proc Natl Acad Sci U S A. 1990;87(12):4645–9. https://doi.org/10.1073/pnas.87.12.4645

206. Hoiseth SK, Stocker BAD. Aromatic-dependent *Salmonella* typhimurium are non-virulent and effective as live vaccines. [Internet]. Vol. 291, Nature. 1981. p. 238–9. https://doi.org/10.1038/291238a0

207. Pfeifer CG, Marcus SL, Steele-Mortimer O, Knodler LA, Finlay BB. *Salmonella* typhimurium virulence genes are induced upon bacterial invasion into phagocytic and nonphagocytic cells. Infect Immun. 1999;67(11):5690–8. https://doi.org/10.1128/iai.67.11.5690-5698.1999

208. Gibson DG, Young L, Chuang R-Y, Venter JC, Hutchison C a, Smith HO, et al. Enzymatic assembly of DNA molecules up to several hundred kilobases. Nat Methods. 2009;6(5):343–5. https://doi.org/10.1038/nmeth.1318

209. Edwards RA, Keller LH, Schifferli DM. Improved allelic exchange vectors and their use to analyze 987P fimbria gene expression. Gene. 1998 Jan 30;207(2):149–57. https://doi.org/10.1016/S0378-1119(97)00619-7

210. Chang ACY, Cohen SN. Construction and characterization of amplifiable DNA cloning vectors derived from P15A cryptic miniplasmid. J Bacteriol. 1978;134(3):1141-1156.

211. Sekirov I, Tam NM, Jogova M, Robertson ML, Li Y, Lupp C, et al. Antibiotic-induced perturbations of the intestinal microbiota alter host susceptibility to enteric infection. Infect Immun. 2008;76(10):4726–36. https://doi.org/10.1128/IAI.00319-08

212. Leung KY, Finlay BB. Intracellular replication is essential for the virulence of *Salmonella* Typhimurium. Proc Natl Acad Sci U S A. 1991;88(24):11470–4. https://doi.org/10.1073/pnas.88.24.11470

213. Ramsden AE, Mota LJ, Münter S, Shorte SL, Holden DW. The SPI-2 type III secretion system restricts motility of *Salmonella*-containing vacuoles. Cell Microbiol. 2007;9(10):2517–29. https://doi.org/10.1111/j.1462-5822.2007.00977.x

214. Abrahams GL, Müller P, Hensel M. Functional dissection of SseF, a type III effector

protein involved in positioning the *Salmonella*-containing vacuole. Traffic. 2006 Aug;7(8):950–65. https://doi.org/10.1111/j.1600-0854.2006.00454.x

215. Beuzón CR, Salcedo SP, Holden DW. Growth and killing of a *Salmonella enterica* serovar Typhimurium sifA mutant strain in the cytosol of different host cell lines. Microbiology. 2002;148(9):2705–15. https://doi.org/10.1099/00221287-148-9-2705

216. Figueira R, Watson KG, Holden DW, Helaine S. Identification of *Salmonella* pathogenicity island-2 type III secretion system effectors involved in intramacrophage replication of S. enterica serovar Typhimurium: Implications for rational vaccine design. MBio. 2013;4(2):1–10. https://doi.org/10.1128/mBio.00065-13

217. Santos RL, Raffatellu M, Bevins CL, Adams LG, Tükel Ç, Tsolis RM, et al. Life in the inflamed intestine, Salmonella style. Trends Microbiol. 2009;17(11):498–506. https://doi.org/10.1016/j.tim.2009.08.008

218. Auweter SD, Bhavsar AP, de Hoog CL, Li Y, Chan YA, van der Heijden J, et al. Quantitative mass spectrometry catalogues *Salmonella* pathogenicity island-2 effectors and identifies their cognate host binding partners. J Biol Chem. 2011 Jul 8;286(27):24023–35. https://doi.org/10.1074/jbc.M111.224600

219. Brumell JH, Rosenberger CM, Gotto GT, Marcus SL, Finlay BB. SifA permits survival and replication of Salmonella Typhimurium in murine macrophages. Cell Microbiol. 2001;3(2):75–84. doi:10.1046/j.1462-5822.2001.00087.x

220. McEwan DG, Popovic D, Gubas A, Terawaki S, Suzuki H, Stadel D, et al. PLEKHM1 regulates autophagosome-lysosome fusion through HOPS Complex and LC3/GABARAP Proteins. Mol Cell. 2015;57(1):39–54. https://doi.org/10.1016/j.molcel.2014.11.006

221. Moest T, Zhao W, Zhao Y, Schüssler JM, Yan W, Gorvel JP, et al. Contribution of bacterial effectors and host proteins to the composition and function of *Salmonella*-induced tubules. Cell Microbiol. 2018;20(12):1–13. https://doi.org/10.1111/cmi.12951

222. Kaniuk NA, Canadien V, Bagshaw RD, Bakowski M, Braun V, Landekic M, et al. *Salmonella* exploits Arl8B-directed kinesin activity to promote endosome tubulation and cell-to-cell transfer. Cell Microbiol. 2011;13(11):1812–23. https://doi.org/10.1111/j.1462-5822.2011.01663.x

223. Marsman M, Jordens I, Kuijl C, Janssen L, Neefjes J. Dynein-mediated vesicle transport controls intracellular *Salmonella* replication. Mol Biol Cell. 2004;15(June):2954–64. https://doi.org/10.1091/mbc.e03-08-0614

224. Wasylnka JA, Bakowski MA, Szeto J, Ohlson MB, Trimble WS, Miller SI, et al. Role for myosin II in regulating positioning of *Salmonella*-containing vacuoles and intracellular replication. Infect Immun. 2008;76(6):2722–35. https://doi.org/10.1128/IAI.00152-08

225. Reinicke AT, Hutchinson JL, Magee AI, Mastroeni P, Trowsdale J, Kelly AP. A *Salmonella* typhimurium effector protein SifA is modified by host cell prenylation and S-acylation machinery. J Biol Chem. 2005;280(15):14620–7. https://doi.org/10.1074/jbc.M500076200

226. Rosa-Ferreira C, Munro S. Arl8 and SKIP act together to link lysosomes to kinesin-1. Dev Cell. 2011 Dec 13;21(6):1171–8. https://doi.org/10.1016/j.devcel.2011.10.007

227. Fierer J, Okamoto S, Banerjee A, Guineya DG. Diarrhea and colitis in mice require the *Salmonella* pathogenicity island 2-encoded secretion function but not SifA or Spv effectors. Infect Immun. 2012;80(10):3360–70. https://doi.org/10.1128/IAI.00404-12

228. Matsuda S, Haneda T, Saito H, Miki T, Okada N. *Salmonella enterica* effectors SifA, SpvB, SseF, SseJ, and SteA contribute to type III secretion system 1-independent inflammation in a streptomycin-pretreated mouse model of colitis. Infection and Immunity. 2019;e00872-18. https://doi.org/10.1128/IAI%0A.00872-18

229. Hensel M, Shea JE, Gleeson C, Jones MD, Dalton E, Holden DW. Simultaneous identification of bacterial virulence genes by negative selection. Science (80-). 1995;269(5222):400–3. doi: 0.1126/science.7618105

230. Coombes BK, Brown NF, Valdez Y, Brumell JH, Finlay BB. Expression and secretion of *Salmonella* pathogenicity island-2 virulence genes in response to acidification exhibit differential requirements of a functional type III secretion apparatus and SsaL. J Biol Chem. 2004;279(48):49804–15. doi:10.1074/jbc.M404299200

231. Geddes K, Worley M, Niemann G, Heffron F. Identification of New Secreted Effectors in *Salmonella enterica* Serovar Typhimurium. Infect Immun. 2005;73(10):6260–71.

232. Dai S, Zhou D. Secretion and function of *Salmonella* SPI-2 fffector SseF require its chaperone , SscB. J Bacteriol. 2004;186(15):5078–86. https://doi.org/10.1128/JB.186.15.5078-5086.2004

233. Pegues DA, Hantman MJ, Behlau I, Miller SI. PhoP/PhoQ transcriptional repression of *Salmonella* Typhimurium invasion genes: evidence for a role in protein secretion. Mol Microbiol. 1995;17(1):169–81. doi: 10.1111/j.1365-2958.1995.mmi_17010169.x

234. Mizusaki H, Takaya A, Yamamoto T, Aizawa SI. Signal pathway in salt-activated expression of the Salmonella pathogenicity island 1 type III secretion system in Salmonella enterica serovar typhimurium. J Bacteriol. 2008;190(13):4624–31. doi: 10.1128/JB.01957-07

235. Niemann GS, Brown RN, Gustin JK, Stufkens A, Shaikh-Kidwai AS, Li J, et al. Discovery of novel secreted virulence factors from *Salmonella enterica* serovar Typhimurium by proteomic analysis of culture supernatants. Infect Immun. 2011 Jan;79(1):33–43. https://doi.org/10.1128/IAI.00771-10

236. Kubori T, Sukhan A, Aizawa SI, Galán JE. Molecular characterization and assembly of the needle complex of the Salmonella typhimurium type III protein secretion system. Proc Natl Acad Sci U S A. 2000;97(18):10225–30. doi: 10.1073/pnas.170128997

237. Knuff-Janzen K, Tupin A, Yurist-Doutsch S, Rowland JL, Finlay BB. Multiple *Salmonella*-pathogenicity island 2 effectors are required to facilitate bacterial establishment of its intracellular niche and virulence. PLoS One. 2020;15(6 June):1–25. http://dx.doi.org/10.1371/journal.pone.0235020

238. D'Costa VM, Coyaud E, Boddy KC, Laurent EMN, St-Germain J, Li T, et al. BioID screen of Salmonella type 3 secreted effectors reveals host factors involved in vacuole positioning and stability during infection. Nat Microbiol. 2019; doi:10.1038/s41564-019-0580-9

239. Knodler LA, Vallance BA, Hensel M, Jäckel D, Finlay BB, Steele-Mortimer O. *Salmonella* type III effectors PipB and PipB2 are targeted to detergent-resistant microdomains on internal host cell membranes. Mol Microbiol. 2003;49(3):685–704.

240. Coburn B, Sekirov I, Finlay BB. Type III Secretion Systems and Disease. Clin Microbiol Rev. 2007;20(4):535–49. doi:10.1128/CMR.00013-07

241. Lejona S, Castelli ME, Cabeza ML, Kenney LJ, García Véscovi E, Soncini FC. PhoP can activate its target genes in a PhoQ-independent manner. J Bacteriol. 2004;186(8):2476–80. doi: 10.1128/JB.186.8.2476-2480.2004

242. Drecktrah D, Knodler LA, Galbraith K, Steele-Mortimer O. The Salmonella SPI1 effector SopB stimulates nitric oxide production long after invasion. Cell Microbiol. 2005;7(1):105–13.

243. Cain RJ, Hayward RD, Koronakis V. The target cell plasma membrane is a critical interface for *Salmonella* cell entry effector-host interplay. Mol Microbiol. 2004;54(4):887–904. doi:10.1111/j.1365-2958.2004.04336.x

244. Chen X, Wei S, Ji Y, Guo X, Yang F. Quantitative proteomics using SILAC: Principles, applications, and developments. Proteomics. 2015;15(18):3175–92. doi:10.1002/pmic.201500108

245. Ong S-E, Blagoev B, Kratchmarova I, Dan Bach Kristensen§, Steen H, Pandey A, et al. Stable isotope labeling by amino acids in cell culture, SILAC, as a simple and accurate approach to expression proteomics. Mol Cell Proteomics. 2002;1.5:376–86. doi: 10.1074/mcp.M200025-MCP200

246. Shevchenko A, Wilm M, Vorm O, Mann M. Mass spectrometric sequencing of proteins from silver-stained polyacrylamide gels. Anal Chem. 1996;68(5):850–8.

247. Rogers LD, Kristensen AR, Boyle EC, Robinson DP, Ly RT, Finlay BB, et al. Identification of cognate host targets and specific ubiquitylation sites on the *Salmonella* SPI-1 effector SopB/SigD. J Proteomics. 2008;71(1):97–108. doi: 10.1016/j.jprot.2008.01.011

248. Szklarczyk D, Franceschini A, Wyder S, Forslund K, Heller D, Huerta-Cepas J, et al. STRING v10: Protein-protein interaction networks, integrated over the tree of life. Nucleic Acids Res. 2015;43(D1):D447–52. doi: 10.1093/nar/gku1003

249. Gong H, Vu GP, Bai Y, Yang E, Liu F, Lu S. Differential expression of *Salmonella* type III secretion system factors InvJ, PrgJ, SipC, SipD, SopA and SopB in cultures and in mice. Microbiology. 2010;156(1):116–27. doi: 10.1099/mic.0.032318-0

250. Pavlova A, Björk I. Grafting of features of cystatins C or B into the N-terminal region or second binding loop of cystatin A (stefin A) substantially enhances inhibition of cysteine proteinases. Biochemistry. 2003;42(38):11326–33. doi: 10.1021/bi030119v

251. McEwan DG, Richter B, Claudi B, Wigge C, Wild P, Farhan H, et al. PLEKHM1 Regulates *Salmonella*-Containing Vacuole Biogenesis and Infection. Cell Host Microbe. 2015;17(1):58–71. doi: 10.1016/j.chom.2014.11.011

252. Babiychuk EB, Draeger A. Annexins in cell membrane dynamics: Ca2+-regulated association of lipid microdomains. J Cell Biol. 2000;150(5):1113–23. doi:10.1083/jcb.150.5.1113

253. Spanò S, Gao X, Hannemann S, Lara-Tejero M, Galán JE. A bacterial pathogen targets a host Rab-family GTPase defense pathway with a GAP. Cell Host Microbe. 2016;19(2):216–26. doi: 10.1016/j.chom.2016.01.004

254. Pu J, Guardia CM, Keren-Kaplan T, Bonifacino JS. Mechanisms and functions of lysosome positioning. J Cell Sci. 2016;129(23):4329–39. doi: 10.1242/jcs.196287

255. Nawabi P, Catron DM, Haldar K. Esterification of cholesterol by a type III secretion effector during intracellular Salmonella infection. Mol Microbiol. 2008;68(1):173–85. doi: 10.1111/j.1365-2958.2008.06142.x

256. Walch PDK, Selkrig J, Knodler LA, Rettel M, Stein F, Fernandez K, et al. Global mapping of Salmonella enterica-host protein-protein interactions during infection. bioRxiv. 2020;1–59.

257. Zhang S, Yu M, Guo Q, Li R, Li G, Tan S, et al. Annexin A2 binds to endosomes and negatively regulates TLR4-triggered inflammatory responses via the TRAM-TRIF pathway. Sci Rep. 2015;5(May):1–15.

258. Heck AJR. Native mass spectrometry: A bridge between interactomics and structural biology. Nat Methods. 2008;5(11):927–33. doi: 10.1038/nmeth.1265

259. Schmidt C, Lenz C, Grote M, Lührmann R, Urlaub H. Determination of protein stoichiometry within protein complexes using absolute quantification and multiple reaction monitoring. Anal Chem. 2010;82(7):2784–96. doi: 10.1021/ac902710k

260. Tannous BA. Gaussia luciferase reporter assay for monitoring biological processes in culture and in vivo. Nat Protoc. 2009;4(4):582–91. doi: 10.1038/nprot.2009.28

261. Noster J, Chao T, Id NS, Id MS, Id TR, Hansmeier N, et al. Proteomics of intracellular Salmonella enterica reveals roles of *Salmonella* pathogenicity island 2 in metabolism and antioxidant defense. PLoS Pathog. 2019;15(4):e1007741. doi: 10.1371/journal.ppat.1007741

262. Vorwerk S, Krieger V, Deiwick J, Hensel M, Hansmeier N. Proteomes of host cell membranes modified by intracellular activities of Salmonella enterica. Mol Cell Proteomics. 2015;14(1):81–92. doi: 10.1074/mcp.M114.041145

263. Reuter T, Vorwerk S, Liss V, Chao TC, Hensel M, Hansmeier N. Proteomic analysis of *Salmonella*-modified membranes reveals adaptations to macrophage hosts. Mol Cell Proteomics. 2020;19(5):900–12. doi: 10.1074/mcp.RA119.001841

264. Hagen J Von, Michelsen U. Cellular fractionation - Mammalian cells [Internet]. 1st ed. Vol. 533, Methods in Enzymology. Elsevier Inc.; 2013. 25–30 p. http://dx.doi.org/10.1016/B978-0-12-420067-8.00003-9

265. McQuate SE, Young AM, Silva-Herzog E, Bunker E, Hernandez M, de Chaumont F, et al. Long-term live-cell imaging reveals new roles for Salmonella effector proteins SseG and SteA. Cell Microbiol. 2017;19(1). doi: 10.1111/cmi.12641

266. Göser V, Kommnick C, Liss V, Hensel M. Self-labeling enzyme tags for analyses of translocation of type III secretion system effector proteins. MBio. 2019;10(3):1–18. doi: 10.1128/mBio.00769-19

Appendix A

Supplementary Western blot

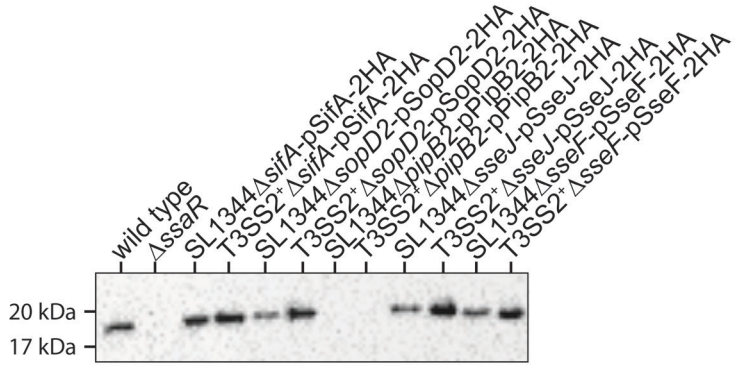

Figure A.1 – SseB is secreted by most *S.* Typhimurium SL1344 and T3SS2$^+$ strains. Blot is representative of *n*=3 experiments. Secretion of SseB into culture supernatant by complemented T3SS2$^+$ strains. The indicated strains were cultured for 9 hours in a minimal medium optimized for induction of SPI-2 expression effector secretion. Bacterial cultures were pelleted by centrifugation and the culture supernatant proteins were precipitated using trichloroacetic acid and dissolved in SDS-PAGE sample buffer. Samples were resolved on a 12% SDS-PAGE gel, Western blotted, and probed with anti-SseB antibodies.

Appendix B

Table B.1 - Significant hits from SILAC experiment for all IPs. Effector-IP:Control-IP SILAC ratios for each replicate, as well as the median for all hits above the SILAC ratio threshold of 1.2 Negative values represent missing values (*i.e.,* protein was not detected in that replicate) imputed from Perseus version 1.6.7.0.

Effector IP	Significant Hits	Median	Replicates		
			1	2	3
SifA	Cystatin-A;Cystatin-A, N-terminally processed	4.5922	7.6581	4.5922	0.1470
	SifA	4.4423	7.7471	4.4423	2.9004
	SipC (Salmonella)	1.4872	1.2569	1.4872	4.2392
	Y-box-binding protein 3	1.2719	1.2719	1.3092	0.8679
	Ribosomal protein L15;60S ribosomal protein L15	1.2504	1.2504	1.1372	1.5466
	Ribosomal L1 domain-containing protein 1	1.2391	1.1766	1.2391	1.3878
	Ribosome biogenesis protein BRX1 homolog	1.2361	1.2361	1.4469	0.3553
	60S ribosomal protein L9	1.2357	1.1922	1.2357	1.9837
	60S ribosomal protein L21	1.2320	1.2320	1.3507	0.2619
	High mobility group protein HMG-I/HMG-Y	1.2028	1.2028	1.7110	0.3731
	SipA (Salmonella)	1.1980	1.1728	1.1980	2.3701
	40S ribosomal protein S6	1.1904	1.0826	1.1904	1.6036
SopD2	Plectin	1.6290	0.2060	1.7994	1.6290
	Vimentin	1.5789	0.6340	1.5789	1.6564
	Keratin, type I cytoskeletal 18	1.4901	0.7066	1.4901	1.6830
	Histone H3;Histone H3.2;Histone H3.1t;Histone H3.3;Histone H3.1;Histone H3.3C	1.4438	0.0535	1.4438	1.6517
	Histone H4	1.3329	0.2881	1.3329	1.6687
	Ribosomal L1 domain-containing protein 1	1.2828	1.1381	1.2828	1.6827
	Ribosomal protein L15;60S ribosomal protein L15	1.2701	1.2701	1.1803	1.9736
	Core histone macro-H2A.1;Histone H2A	1.2687	0.3415	1.3240	1.2687
	Histone H1.4	1.2494	1.2494	1.4738	0.9057
	60S ribosomal protein L9	1.2272	1.2310	1.2272	0.7656
	α-actinin-4	1.2246	-0.3535	1.2943	1.2246
	Annexin A2;Annexin;Putative annexin A2-like protein	1.2130	0.5279	1.5192	1.2130
	Elongation factor Tu, mitochondrial	1.2069	-0.0313	1.2215	1.2069
PipB2	PipB2	8.3928	18.235	8.3928	0.8260
	Cystatin-A;Cystatin-A, N-terminally processed	5.8748	12.319	5.8748	0.6492
	SipC (Salmonella)	1.9320	-1.6419	1.9320	2.2516
	Plectin	1.7519	-1.2153	2.1421	1.7519
	Vimentin	1.5296	0.7116	1.5454	1.5296
	Keratin, type I cytoskeletal 18	1.4766	0.7513	1.4766	1.6689
	Histone H3;Histone H3.2;Histone H3.1t;Histone H3.3;Histone H3.1;Histone H3.3C	1.3757	0.3671	1.3757	1.8784
	Histone H4	1.3387	0.3553	1.3387	1.8443
	Annexin A2;Annexin;Putative annexin A2-like protein	1.3132	0.5940	1.9596	1.3132
	α-actinin-4	1.2682	0.7892	1.3954	1.2682
	Heterogeneous nuclear ribonucleoprotein U	1.2314	1.0271	1.2348	1.2314
	Ribosomal protein L15;60S ribosomal protein L15	1.2310	1.2310	1.0842	1.7727

Table continued on next page

SteA	SteA	14.8089	23.658	14.808	2.3689
	Cystatin-A;Cystatin-A, N-terminally processed	9.1617	14.705	9.1617	0.5293
	SipC (Salmonella)	1.4537	0.6905	1.4537	1.6978
	Ribosomal protein L15;60S ribosomal protein L15	1.3471	1.3471	1.0235	1.3869
	60S ribosomal protein L7	1.2091	1.2091	1.0023	1.2718
	60S ribosomal protein L4	1.2086	1.2630	1.0077	1.2086
	60S ribosomal protein L6	1.2014	1.2014	0.9850	1.2212
	60S ribosomal protein L9	1.1922	1.1922	1.0325	1.4968
SseJ	SseJ	18.1061	34.750	18.106	4.8939
	Cystatin-A;Cystatin-A, N-terminally processed	6.4140	11.120	6.4140	0.4202
	Histone H3;Histone H3.2;Histone H3.1t;Histone H3.3;Histone H3.1;Histone H3.3C	1.3802	0.3974	1.5504	1.3802
	SipC (Salmonella)	1.3201	1.3201	1.8198	1.1187
	Histone H4	1.2841	0.3920	1.4489	1.2841
	40S ribosomal protein S24	1.2337	1.0565	1.2337	1.5387
	60S ribosomal protein L28	1.2231	1.2231	1.0453	1.3018
	60S ribosomal protein L4	1.2150	1.2150	1.0193	1.5427
	Keratin, type I cytoskeletal 18	1.2131	0.9315	1.3080	1.2131
	Ribosomal protein L15;60S ribosomal protein L15	1.2082	1.2082	1.0656	1.6432
	Polyadenylate-binding protein;Polyadenylate-binding protein 4	1.2071	-2.8559	1.2090	1.2071
	Polyadenylate-binding protein 1;Polyadenylate-binding protein;Polyadenylate-binding protein 3	1.2019	1.2471	1.1703	1.2019
SseF	60S ribosomal protein L4	1.3808	1.3808	0.9841	1.6076
	Ribosomal protein L15;60S ribosomal protein L15	1.3453	1.3453	1.0054	1.7629
	Polyadenylate-binding protein 1;Polyadenylate-binding protein;Polyadenylate-binding protein 3	1.3202	1.3417	1.1528	1.3202
	60S ribosomal protein L9	1.2978	1.2978	0.9967	1.8130
	Vimentin	1.2932	0.8377	1.2932	1.3727
	60S ribosomal protein L7	1.2719	1.2719	0.9683	1.5322
	60S ribosomal protein L28	1.2672	1.2672	1.0345	1.3506
	Y-box-binding protein 3	1.2555	1.2763	1.2555	0.8532
	60S ribosomal protein L18	1.2496	1.2496	0.9706	1.3344
	Ribosomal L1 domain-containing protein 1	1.2495	1.2495	0.9943	1.4574
	60S ribosomal protein L6	1.2452	1.2452	0.9902	1.3936
	Keratin, type I cytoskeletal 18	1.2338	0.8294	1.2338	1.4238
	40S ribosomal protein S6	1.2165	1.2165	0.9871	1.6680
	39S ribosomal protein L4, mitochondrial	1.2163	0.6515	1.2163	1.2512
Control	Cystatin-A;Cystatin-A, N-terminally processed	6.4696	9.1946	0.1317	6.4696
	Ig kappa chain C region	5.3076	4.7456	0.6510	4.7456
	SipC (Salmonella)	1.0782	2.6516	1.7569	1.7569
	Ribosomal protein L15;60S ribosomal protein L15	1.3922	1.1009	1.9823	1.3922
	40S ribosomal protein S24	1.2700	1.1483	1.5442	1.2700
	60S ribosomal protein L9	1.1806	1.2638	2.0076	1.2638
	60S ribosomal protein L4	1.2627	1.0125	1.8799	1.2627
	SipA (Salmonella)	0.9029	1.2421	1.3341	1.2421
	40S ribosomal protein S6	1.0700	1.2056	1.5497	1.2056
	60S ribosomal protein L13a	1.2047	1.0208	1.7743	1.2047